MICROWAVE ELECTRONICALLY TUNABLE FILTERS

by

IAN CHARLES HUNTER B.Sc

A Thesis presented for the degree of
Doctor of Philosophy, in the
Department of Electrical and Electronic Engineering
at the University of Leeds

May 1981

ACKNOWLEDGEMENTS

The author wishes to thank Professor J.D. Rhodes for his expert advice and supervision throughout the period of this research. The author would also like to thank Professor P.J. Lawrenson for permission to undertake the research in the Department of Electrical and Electronic Engineering at the University of Leeds and for the use of the departmental facilities. Finally, the author wishes to thank Filtronic Components Ltd., Ferranti Ltd. and the Science Research Council for technical and financial support.

ABSTRACT

Design procedures are presented for varactor tuned microwave bandpass and bandstop filters constructed in Microwave Integrated Circuit form. The tunable bandpass filters were based on a combline filter incorporating novel input and output coupling networks which compensate for the frequency dependence of the coupling between the resonators. Using this filter, tuning over an octave band with an acceptable response and approximately constant passband bandwidth is possible. The tunable bandstop filters consisted of a uniform impedance main line with capacitively decoupled resonators located at intervals along it. A novel design technique is presented for evaluating the correct phase shifts between the resonators of this filter in order to obtain the optimum symmetrical frequency response. Detailed computer analysis of the filters, including both varactor and integrated circuit loss, and the effects of tuning is presented. The measured performances of several practical devices, constructed in Suspended Substrate Stripline, and operating in the frequency range 2-10 GHz are presented, these agree closely with computed performances.

MICROWAVE ELECTRONICALLY TUNABLE FILTERS

Contents

1 INTRODUCTION

1.1 Applications of Electronically Tunable Microwave Filters

There is a large and growing demand for frequency agile microwave filters for application in Electronic Support Measure (E.S.M) systems. For example, a tunable bandpass filter can be used in a crystal video receiver [1.1] to provide frequency discrimination of unknown signals [Fig. 1.1.1]. Tunable bandstop filters have wide application in similar systems for the purpose of rejecting unknown interference signals.

E.S.M systems typically operate over multi-octave frequency bands and thus the first requirement for tunable microwave filters is that of broadband tuning. In addition, in order that relatively fine frequency discrimination can be achieved, the filter passband (stopband) must be narrow.

1.2 YIG Tuned Filters

At present, most E.S.M system requirements are met only by using YIG filters [1.2]. The YIG filter is composed of Yittrium iron garnet spheres located between the poles of a dc magnet. The YIG spheres resonate in the microwave spectrum and variation in the magnetic field changes their resonant frequency.

YIG filters can be tuned over greater than octave bands and the resonator Q factors are in excess of 10000. Unfortunately their inherant magnetic hysteresis effects result in low tuning speeds, typically of the order of one microsecond per Megahertz.

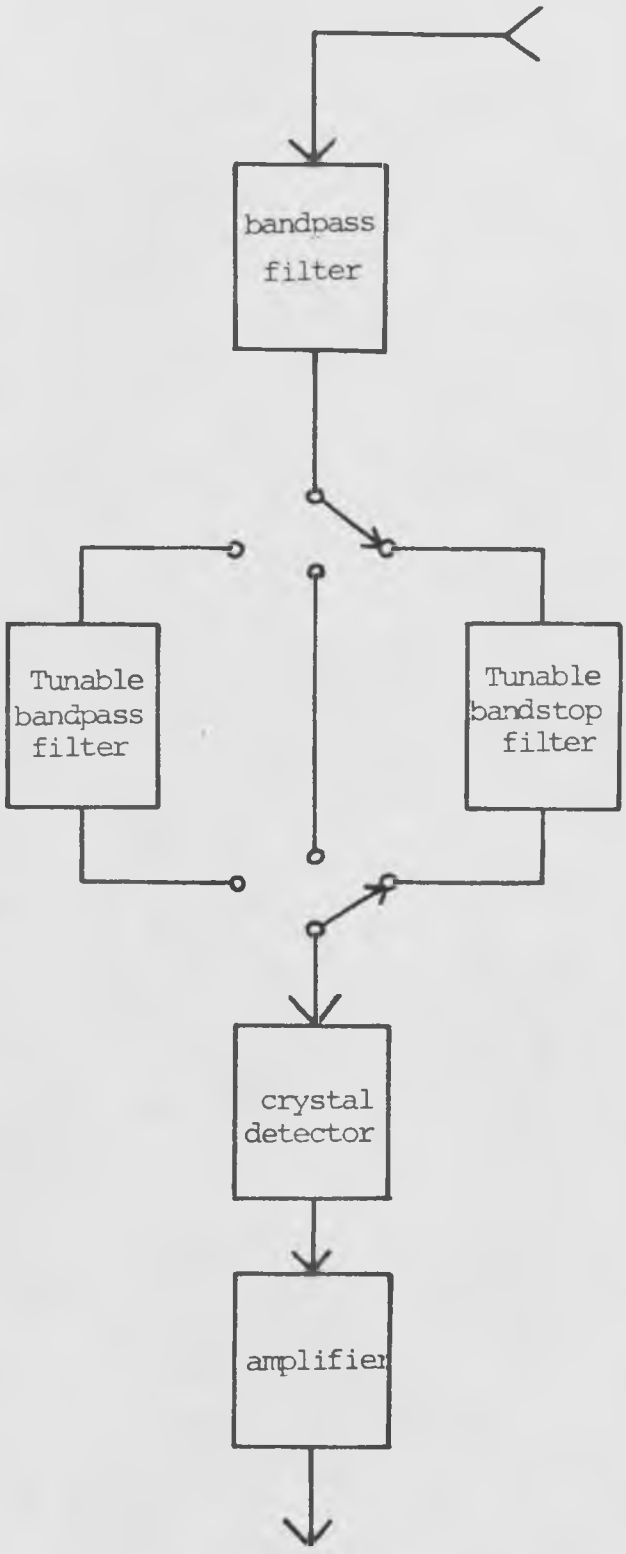

Fig. 1.1.1 A Tunable Video Crystal Receiver

1.3 Varactor Tuned Filters

1.3.1 Fundamentals of Varactor Diodes

For certain E.S.M systems operating in a dense pulse environment it is desirable to have filters with the capability to tune across broad bandwidths at speeds in excess of one microsecond per Gigahertz. The use of filters without this capability would result in a degradation of the receivers probability of intercept.

To achieve such high tuning speeds, or slew rates, it is necessary to use varactor diodes as the tuning elements for microwave resonators. Varactors essentially consist of P.N. junctions operated in reverse bias. A variation in the reverse bias voltage will alter the width of the junction depletion region, thus changing the diode capacitance. The response time of a typical microwave varactor to a step change in bias voltage is of the order of one picosecond. Thus by suitable design of the varactor bias circuit, it is possible to achieve the required high speed tuning.

The details of the physical analysis and construction of varactor diodes are beyond the scope of this thesis, only their relevant properties are presented here. For further information the reader is referred to ref. 1.3.

The most commonly used form of tuning varactor is the abrupt junction varactor. This consists of a $P^{+}N^{-}$ junction diode with an abrupt change in doping density at the junction surface. The doping density of the N^{-} epitaxial layer region is constant throughout its width and depletion occurs mainly

in this region [Fig. 1.3.1]. The voltage dependence of the diode capacitance is given by

$$Cj(v) = \frac{Co}{(1 + v/\psi)^{\frac{1}{2}}} \qquad (1.3.1)$$

where:

$$Co = A\left(\frac{\varepsilon e Nd}{\psi}\right)^{\frac{1}{2}} \qquad (1.3.2)$$

A = Area of the diode

ε = Dielectric constant of the epitaxial layer material

e = The electronic charge

Nd = Epitaxial layer doping density

V = Reverse bias voltage

ψ = Built in junction potential

The maximum capacitance variation is limited by the diode breakdown voltage which can be up to sixty volts. Thus an 8:1 capacitance variation is possible from a varactor chip.

With the voltage capacitance variation given by 1.3.1 the voltage frequency relationship of the resonance of an LC circuit using a varactor as the capacitor is given by

$$Fo \quad \alpha \ (1 + v/\psi)^{\frac{1}{4}} \qquad (1.3.3)$$

This highly non-linear tuning characteristic can be compensated for by using varactors with other doping profiles, e.g. the hyper-abrupt junction varactor [1.4]. Unfortunately these diodes suffer from lower Q factors than abrupt junction varactors and consequently were not used in the work described in this thesis.

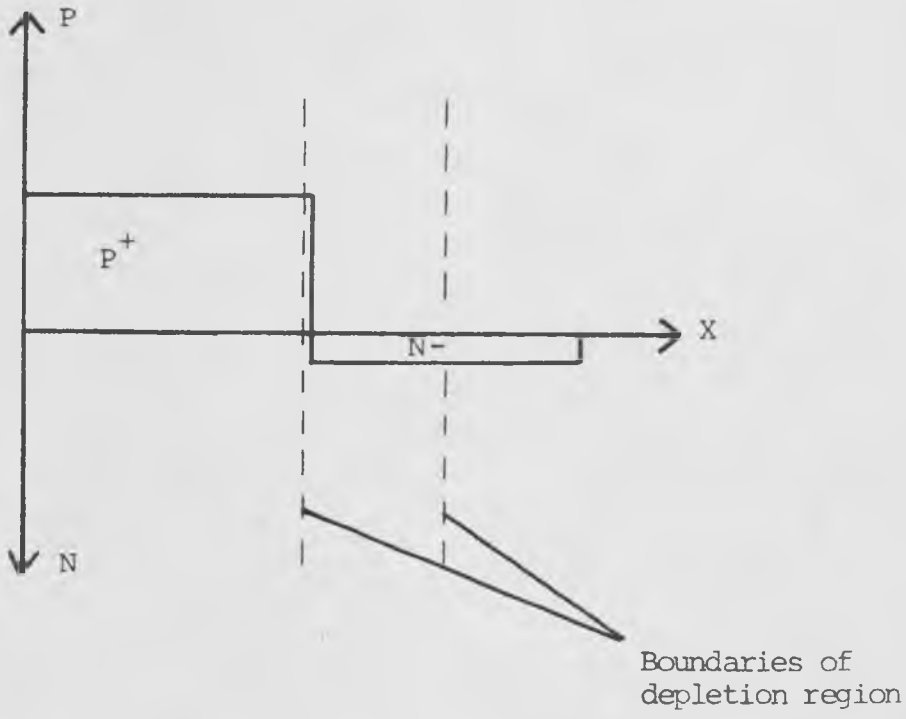

Fig. 1.3.1 Doping profile of abrupt P.N junction

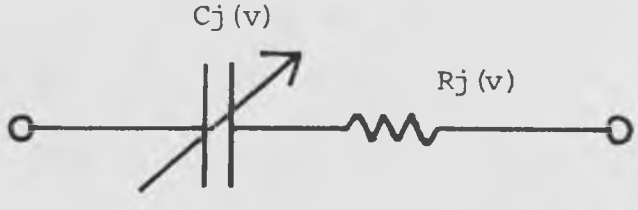

Fig. 1.3.2 Small signal reverse bias model of a varactor

1.3.2 A Simple Circuit Model for a Varactor

Assuming that the diode is unpackaged and that the depletion region is completely depleted of carriers, then the diode can be represented by the small signal reverse bias circuit model shown in Fig. 1.3.2. Since the P^+ region in the diode is very heavily doped, the resistance Rj(v) in the circuit model is dominantly controlled by the resistance of the undepleted region of the epilayer.

The Q factor of the diode can be shown to be given by the following expression [1.5]

$$Q = \frac{1}{2\pi F\, Cj(v) Rj(v)} \qquad (1.3.4)$$

where F is the frequency of operation.

It is obvious that for high frequency operation the varactor epilayer resistance must be minimised. This could be achieved by increasing the area of the diode, however that would increase the junction capacitance and the doping density would then have to be reduced, which in turn would increase the resistance. To achieve this objective varactors are now constructed from Gallium Arsenide [GaAs]. This material has the advantage over Silicon of an approximately seven times greater electron mobility for a given doping density. Since the dielectric constants of the two materials are very similar, Rj(v) will be seven times lower when using GaAs, as opposed to Silicon varactors of the same capacitance.

1.3.3 Performance of Available Varactor Tuned Filters

Varactor tuned filters are not available for operating frequencies above 2GHz and a typical specification of a commercially available U.H.F tunable bandpass filter manufactured in the U.S.A [1.6] is shown in Fig. 1.3.3.

If the assumption is made that the midband dissipation loss of this filter were due only to the varactors, it is possible to evaluate the loss of filters operating at higher frequencies. For example, a filter with the same percentage bandwidth and number of resonators as that described in Fig. 1.3.3, but designed to tune from 4GHz to 8GHz, would have a minimum passband loss of approximately 30dB. This figure would be unacceptable for most applications. The filter described, was however, constructed using Silicon varactors and it was anticipated that by using GaAs devices, broadband tunable low loss filters would be feasible for use at frequencies up to 10GHz.

1.4 Choice of a Suitable Construction Medium for Varactor Tuned Microwave Filters

Initial work at Ferranti Ltd. [1.7] concentrated on the development of X band tunable waveguide bandpass filters. The tuning bandwidths of these filters were limited to less than 10%. This was caused by the swamping of the varactor diodes by the parasitic reactances associated with waveguide discontinuities. Another disadvantage of these filters was their relatively complex mechanical construction.

Tuning range	540-1026 MHz
3dB Passband bandwidth	5%
Number of resonators	2
Passband loss	7 dB Maximum
Passband V.S.W.R	2.5:1 Maximum
Tuning signal	0-60V D.C.
Intercept point (2nd ordered)	5 dBm minimum

Fig. 1.3.3 A typical specification for a commercially available varactor tuned bandpass filter

For the above reasons, waveguide filters were abandoned, as were coaxial filters. It was thus envisaged that a printed circuit realisation was the best alternative. Initially, microstrip was investigated, but this medium was abandoned because of its low Q factor and its inability to operate over broad bandwidths because of spurious mode propogation. conventional stripline was also ruled out because of its high dielectric loss.

Previous work on broadband filters and multiplexers [1.8] suggested that Suspended Substrate Stripline (S.S.S) was an excellent medium for the realisation of high performance microwave filters. The S.S.S structure consists of a thin copper clad dielectric substrate suspended midway between the ground planes of an aluminium housing [Fig. 1.4.1]. Because the dielectric is thin, (normally 0.005" or 0.01") propogation is mainly in air and a loss performance similar to coaxial circuits of the same volume can be achieved. Spurious modes can easily be supressed in this structure and thus broadband operation is possible. The vibrational requirements for many applications can be met using S.S.S because, with the substrate located midway between the ground planes, the first ordered sensitivity of the circuit elements to vibration is zero. Although this structure is printed, it is possible to fine tune filters using capacitive tuning screws located through the main housing.

In conclusion, S.S.S possesses most of the advantages of the coaxial and microstrip structures, but few of their disadvantages.

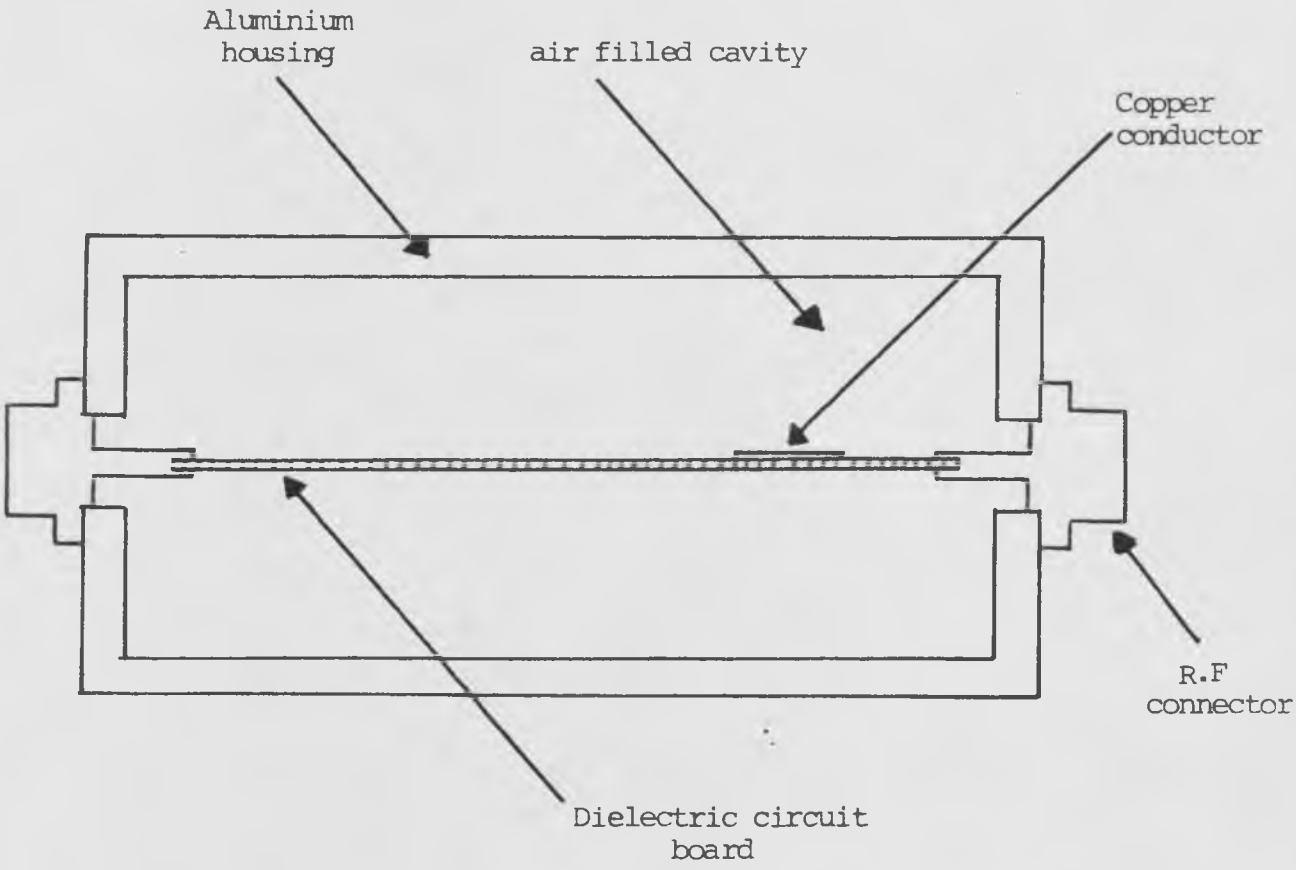

Fig. 1.4.1 The Suspended Substrate Stripline structure

1.5 Development of S.S.S Microwave Filters Suitable for Varactor Tuning

1.5.1 Tunable Bandstop Filters

The S.S.S realisation of the tunable bandstop filter is shown in Fig. 1.5.1. This filter is composed of a uniform impedance main line with resonant capacitively coupled stubs located at intervals along the line. Varactors can be connected to the ends of the stubs to provide electronic tuning. This filter has the advantages of maintaining a good passband from d.c to approximately twice the stopband centre frequency, and the capability of producing very narrow stopbands with high rejection.

In chapter two it is shown that coupling the bandstop resonators via the standard quarter wave impedance inverting lengths of line results in a non optimum assymetric frequency response. This is caused by a fundamental property of the resonators which each have transmission poles at frequencies very close to their transmission zeros. In chapter three a technique is constructed for evaluating the correct phase shift between the resonators to compensate for the assymetric frequency response.

Several bandstop filters have been designed and constructed and the measured performances of three are presented. These include two fixed frequency and one varactor tuned filter. The fixed frequency filters were both 7 cavity devices operating at 4GHz with respective 40dB stopbands of 1% and 10%. The varactor tuned filter was a 3 cavity device with a 1% 20dB

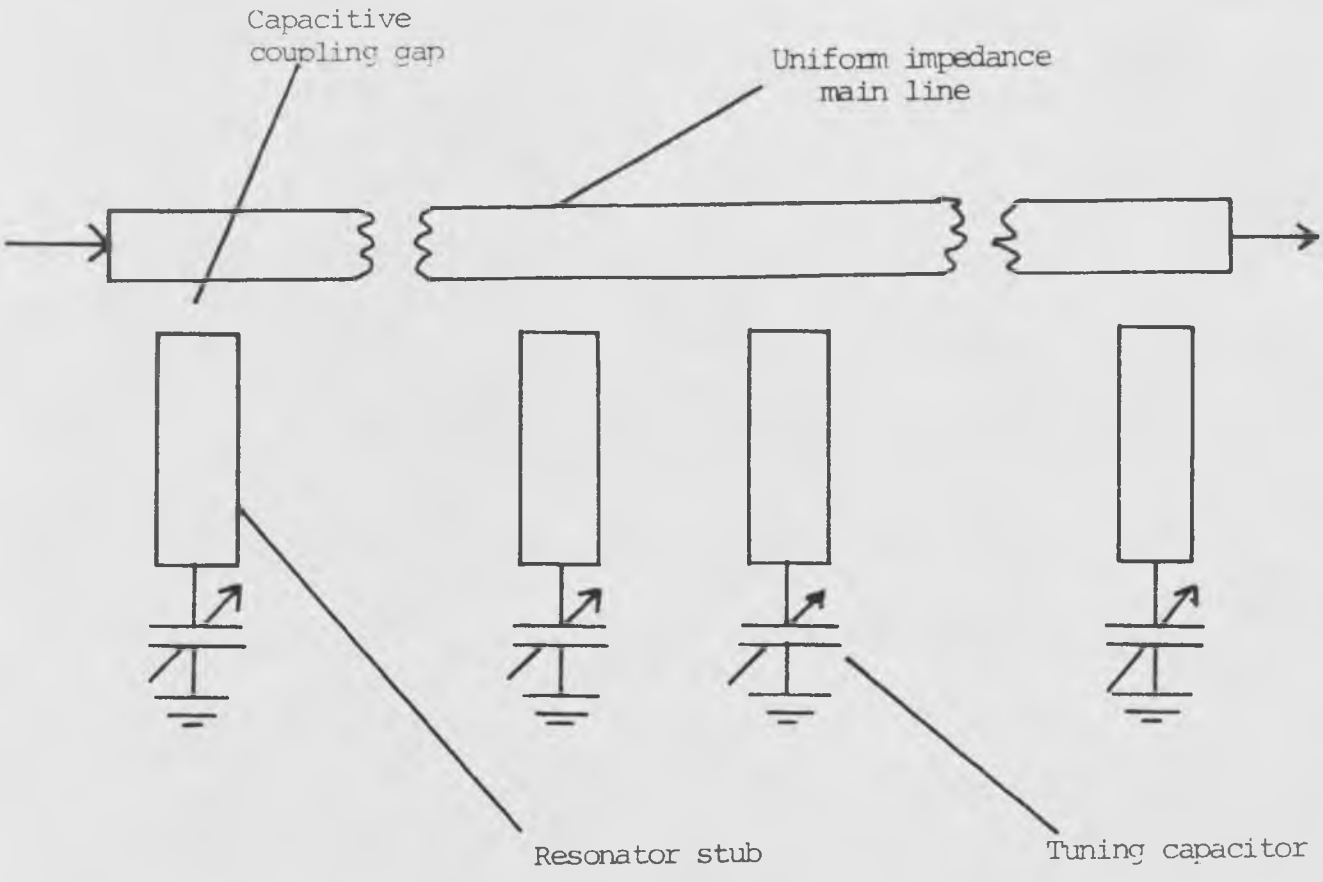

Fig. 1.5.1 The Suspended Substrate Stripline realisation of a tunable microwave bandstop filter

stopband bandwidth at 4GHz. This filter was designed to tune from 3.5GHz to 4.5GHz.

All three devices worked well and the measured performances were in excellent agreement with computer analysis.

1.5.2 Tunable Bandpass Filters

It is shown in chapter two that in order to produce a tunable bandpass filter with a good response over a broad tuning bandwidth it is necessary to choose a circuit in which the coupling between the resonators is not strongly dependent on frequency. If this were not the case, then the filter response would only be correct at one frequency and it would deteriorate rapidly with tuning.

In chapter four, a design technique is presented for tunable combline filters in which the redundant transformer elements are used to approximately compensate for the frequency variation of the coupling between the resonators. Using this technique it is possible to tune over an octave band with only a small deterioration in the filter response. This type of filter also possesses the additional important property of maintaining approximately constant passband bandwidth independant of tuned frequency.

The theory of tunable combline filters is extended to the design of combline filters with open circuited resonators. These filters have a higher Q factor than the normal varactor tuned combline filter when designed for the same degree and passband bandwidth and they also avoid the problem of lossy

short circuits which becomes noticable when very narrow bandwidths are required. The disadvantage of the open circuited varactor tuned combline filter is a reduced tuning bandwidth as compared to the normal combline filter.

The design and measured performances are presented for two varactor tuned bandpass filters. These include a 2 resonator combline filter designed to tune from 3GHz to 5GHz with a 5% passband bandwidth, and a 3 resonator open circuited combline filter tunable from 3.5GHz to 4.5GHz with a 3% passband bandwidth. Measured performances are in close agreement with computer anlaysis.

Finally, the design process for a fixed frequency S.S.S bandpass filter is presented. This filter, which is suitable for passband bandwidths of less than 30% is a modification of the tunable combline filter such that it requires no lumped capacitors. Two of these filters have been designed and constructed. The filters were both 3 resonator devices operating at 4GHz with respective passband bandwidths of 1% and 5%. The measured performances of these devices are similar to those using coaxial circuits.

References

1.1 'Wideband E.S.M. receiving systems part 1'
C.B. Hofmann and A.R. Baron
Microwave Journal Vol. 23 No 9 Sept 1980

1.2 'YIG filters aid wide open receivers'
W.J. Keane
Microwaves Sept. 1978 Vol 17 no 8

1.3 'Variable Impedance Devices' Chapter 1
Edited by M.J. Howes and D.V. Morgan.
Wiley

1.4 'Circuit theory' Vol 1 pp 144-150
J.O. Scanlan and R. Levy
Oliver and Boyd

1.5 'Hyperabrupt varactors from Vapor Phase epitaxial Gallium Arsenide'
J.L. Heaton and R.E. Walline
New Product release. Microwave Associates Ltd.
Burlington, Mass.

1.6 'Voltage Tuned Filters'
Microwaves Magazine January 1976

1.7 Technical Report on Varactor tuned filters
Scott Wilson
Ferranti Ltd. Dundee

1.8 'M.I.C. Broadband filters and Contiguous Multiplexers'
J.E. Dean and J.D. Rhodes
Proceedings of the 9th European Microwave Conference.
Brighton 1979

2 INITIAL INVESTIGATIONS OF VARACTOR TUNED MICROWAVE FILTERS

2.1 Tunable Microwave Bandstop Resonators

2.1.1 Choice of a Suitable Resonator

The main requirements for a tunable bandstop resonator were that a good passband could be maintained over a broad bandwidth, that narrow stopbands could be achieved and that varactor diodes could easily be incorporated into the circuit. These requirements necessitated the use of a straight through line to achieve a good passband performance, and also a means of decoupling the resonator from the main line to achieve the required narrow stopband bandwidths. These conditions can be satisfied by the use of many types of coupled line circuits but the final choice of resonator was the relatively simple structure shown in Fig. 2.1.1. This resonator consists of a transmission line terminated in a variable capacitor at one end with the other end capacitively coupled to a main line. The variable capacitor can be either a varactor, or a tuning screw located through the S.S.S. housing. One very important advantage of using this resonator is that when multisection filters are constructed, consisting of resonators coupled at intervals along a main line then the resonators can all have the same physical length. This is because large variations in the resonator bandwidth can be achieved by varying the capacitive gap from the resonator to the main line, with only a small change in the resonant frequency.

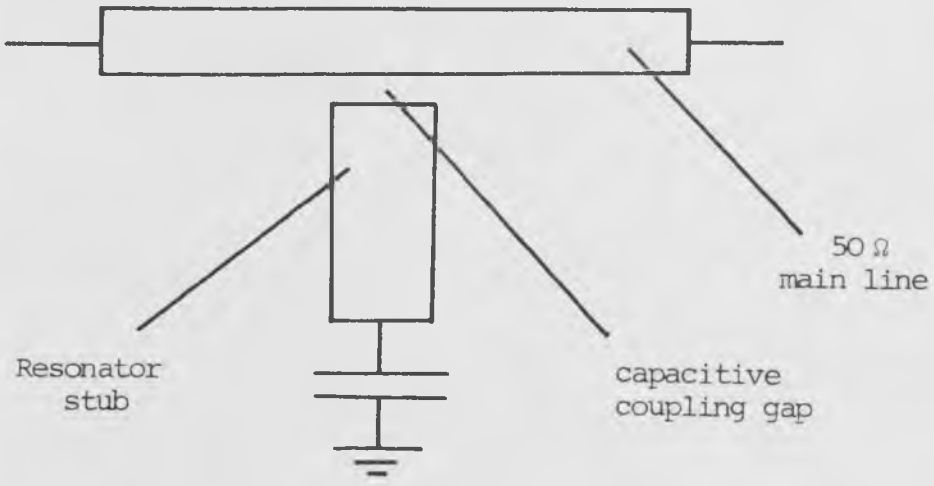

Fig. 2.1.1 The S.S.S structure of a tunable bandstop resonator

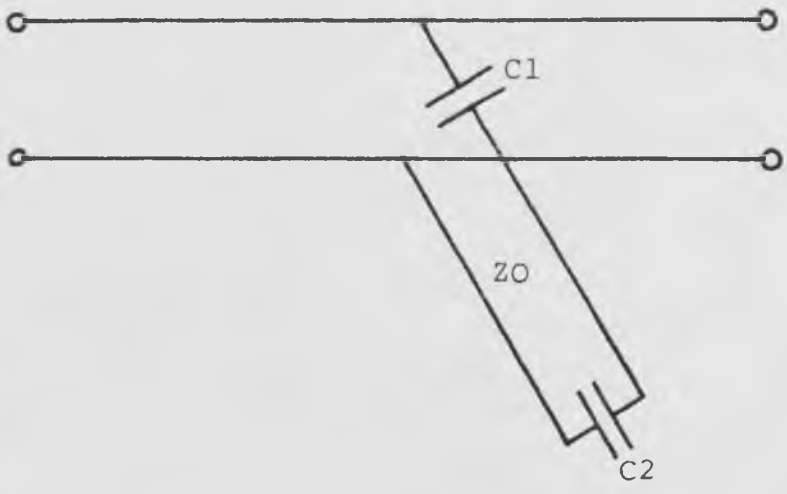

Fig. 2.1.2 The equivalent circuit of the bandstop resonator

2.1.2 Design of the Bandstop Resonators

Several bandstop resonators were constructed firstly in order to obtain information about the effects of the finite S.S.S. Q factor on narrowband filter performance, and secondly to determine the exact equivalent circuit of the resonators. In order to minimise the number of S.S.S housings needed, the resonators were all to have the same length but would have different coupling gaps to the main line. The resonators were to operate at approximately 5 GHz, this being the approximate frequency at which the varactor tuned filters were eventually to be constructed.

Design of resonator lengths

The equivalent circuit of the bandstop resonator is shown in Fig. 2.1.2. The input impedance of this resonator can easily be shown to be (with $C_2 = 0$)

$$Zin(jw) = \frac{-j[wCZo + \tan(aw)]}{wC \tan(aw)} \qquad (2.1.1)$$

Where 'a' is the propogation constant of the resonator stub. At the stopband resonant frequency w_o we have

$$a = \frac{L}{C} = \frac{1}{w_o} \tan^{-1}[-w_o C Z_o] \qquad (2.1.2)$$

where

L = Length of the resonator

C = Velocity of light in air.

To design for a specific resonant frequency it is strictly necessary to be able to relate the value of C_1 to the dimensions of the coupling gap to the main line. However for narrow bandwidths C_1 will be small, as C_1 tends to zero we have

$$a = \frac{\pi}{w_o}$$

Thus for narrow bandwidths the resonator phase length will approach 180^o. In fact the resonator phase lengths were chosen to be 170^o at 5GHz which corresponds to a physical length of approximately 1.1".

Design of widths of S.S.S. transmission lines

The characteristic impedance of an isolated S.S.S. transmission line is related to its static capacitance 'C' per unit length to ground by the following expression.

$$\sqrt{\varepsilon r}\, Zo = \eta/C/\varepsilon \qquad (2.1.3)$$

where

η = Characteristic impedance of free space 377 Ω

ε = Dielectric constant of the S.S.S structure

= εo

The relationship between the dimensions of an isolated strip transmission line [Fig. 2.1.3] and its static capacitance per unit length is

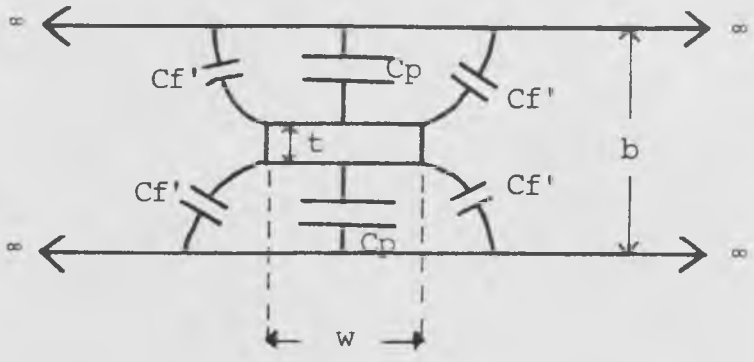

Fig. 2.1.3 An isolated rectangular bar between infinite parallel ground planes

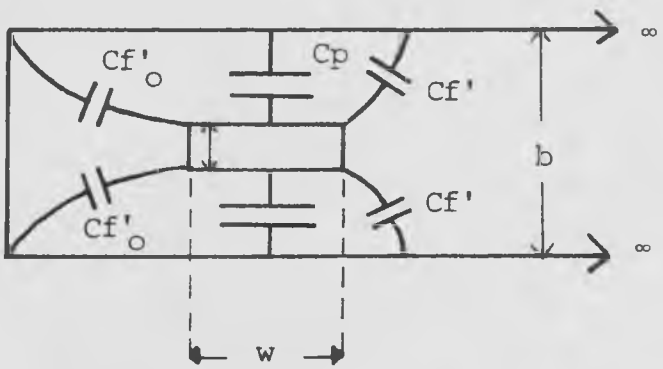

Fig. 2.1.4 A rectangular bar between parallel ground planes and in proximity to a side wall

$$\frac{C}{\varepsilon} = 2Cp + \frac{4Cf'}{\varepsilon} \qquad (2.1.4)$$

where Cp is the parallel plate capacitance to ground from each side of the stripline bar and Cf' is the fringing capacitance from one corner and half the associated side wall of the bar to ground. Getsinger [2.1] has evaluated Cf' as a function of bar thickness, this is shown graphically in Appendix 2.1.

Examining Fig. 2.1.3 we see that

$$Cp = \frac{2w}{b} \qquad (2.1.5)$$

From 2.1.4 and 2.1.5 we obtain

$$\frac{w}{b} = 0.25\left[\frac{C}{\varepsilon} - \frac{4Cf'}{\varepsilon}\right] \qquad (2.1.6)$$

Substituting 2.1.3 into 2.1.6 we obtain

$$\frac{w}{b} = 0.25\left[\frac{377}{Zo} - \frac{4Cf'}{\varepsilon}\right] \qquad (2.1.7)$$

The width of bar required to realise any desired impedance transmission line can be calculated using 2.1.7.

Both the main line and the resonator were designed to have 50 Ω impedance. The ground plane spacing 'b' was chosen to be 0.15", this would give an unloaded resonator Q factor of approximately 300 at 5 GHz [2.2].

The conductor thickness 't' of the S.S.S circuit board was 0.00085", thus

$$\frac{t}{b} = 0.00566$$

Using this value of t/b we obtain from Appendix 2.1 that

$$\frac{Cf'}{\varepsilon} = 0.46$$

From 2.1.7 the resonator and main line widths w1 and w2 can be obtained, these are

$$w1 = w2 = 0.213"$$

The possibility of propogation of unwanted modes

The overall width of the interior of the S.S.S housing must be at least equal to the width of the main line plus the length of the resonator, i.e. the width will be greater than 1.3". With this width of cavity the cut off and resonant frequencies of the lowest possible TE_{101} mode passing through the cavity will be 4.5 GHz and 9.06 GHz. [2.3] It is thus impossible to stop the propogation of the TE_{101} mode at the designed frequency of 5 GHz, however, the method of launching onto the stripline circuit is dissimilar to that used in waveguides, also the characteristic impedance of the S.S.S cavity presented to the TE_{101} mode will be relatively high. These two factors combined, ensure that no box effects will be noticed below the resonant frequency.

In order to minimise the width of the S.S.S cavity, the side wall was to be located at a distance of 0.05" from

the main line. The width of the main line must thus be recalculated to compensate for the increased fringing capacitance to the side wall. The capacitance to ground per unit length from the main line is now

$$\frac{C}{\varepsilon} = \frac{4w2}{b} + \frac{2Cf'}{\varepsilon} + \frac{2Cf'o}{\varepsilon} \qquad (2.1.8)$$

Where, Cf'o is the odd mode fringing capacitance from one corner and half the associated side wall. This situation is shown in Fig. 2.1.4.

The odd mode fringing capacitance from a pair of coupled bars to ground is defined as the fringing capacitance to ground from each bar when a short circuit is placed midway between the bars. Calculation of the odd mode fringing capacitance of one bar near a side wall is equivalent to that for coupled bars except that the distance between the coupled bars is twice that of the single bar to the side wall. Cf'o is shown graphically in Appendix 2.1 as a function of bar separation and bar thickness.

With the main line at a distance of 0.05" from the side wall we have

$$s = 0.1" \quad \text{and}$$

$$\frac{s}{b} = 0.666$$

From appendix 2.1 we obtain

$$\frac{Cf'o}{\varepsilon} = 0.52$$

Thus, from 2.1.8 the main line width is

$$w2 = 0.209"$$

Choice of Resonator coupling gap

No information was yet available for relating the dimensions of the coupling gap between the resonator and the main line to its lumped capacitance. Consequently five circuit boards were constructed with coupling gaps of between 0.004" and 0.020". Although these values seem somewhat arbitrary, it was expected that they would realise relatively narrow band resonances. The layout of one of the circuit boards is shown in Fig. 2.1.5

Design of S.S.S housing and feed terminals

The S.S.S. housing was a relatively simple structure, built in two halves, with milling in each half to the depth of one half of the ground plane spacing. In addition, a 0.05" wide 0.005" deep grove was milled around the edge of the cavity in the lower housing to clamp the circuit board into its correct location [Fig. 2.1.6]

In order to produce a low V.S.W.R transition from the coaxial connector to the stripline medium, the feed terminals must possess an impedance of 50 Ω. The situation as the feed terminals enter the cavity via circular holes is shown in Fig. 2.1.7. Inside the cavity, the feed terminal of diameter 'd' is placed at a distance b/2 from the side wall. The characteristic impedance of the terminal is then given by

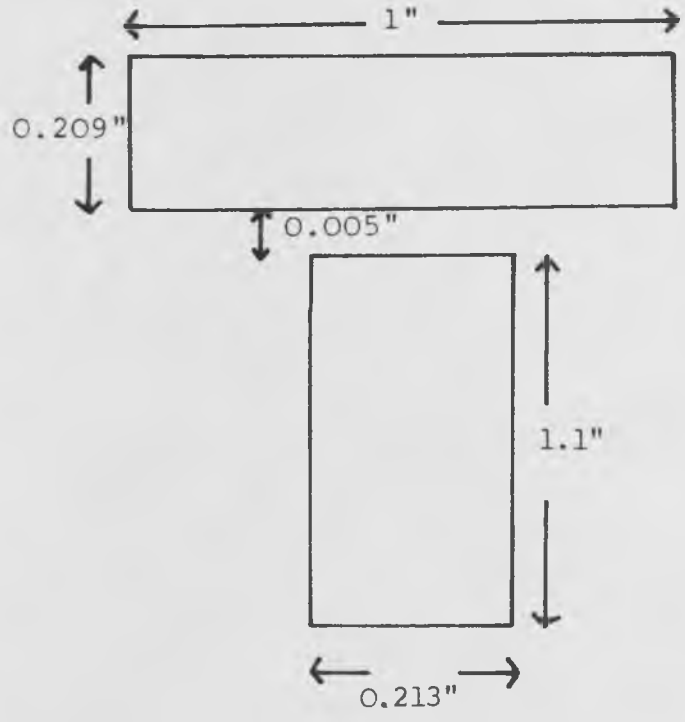

Fig. 2.1.5 Dimensions of a typical bandstop resonator

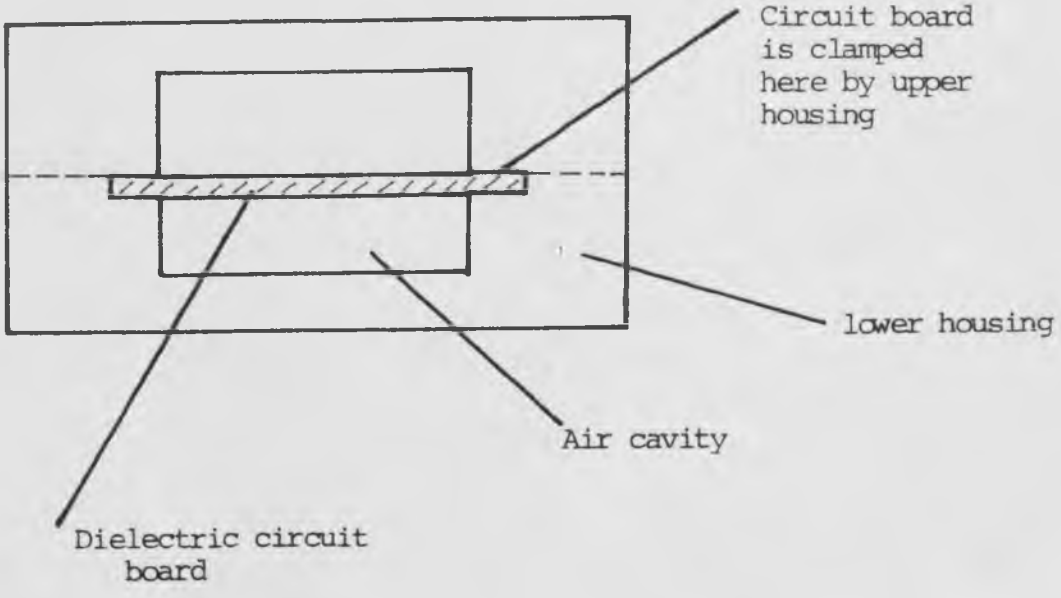

Fig. 2.1.6 The method of suspension of the circuit board in the S.S.S housing

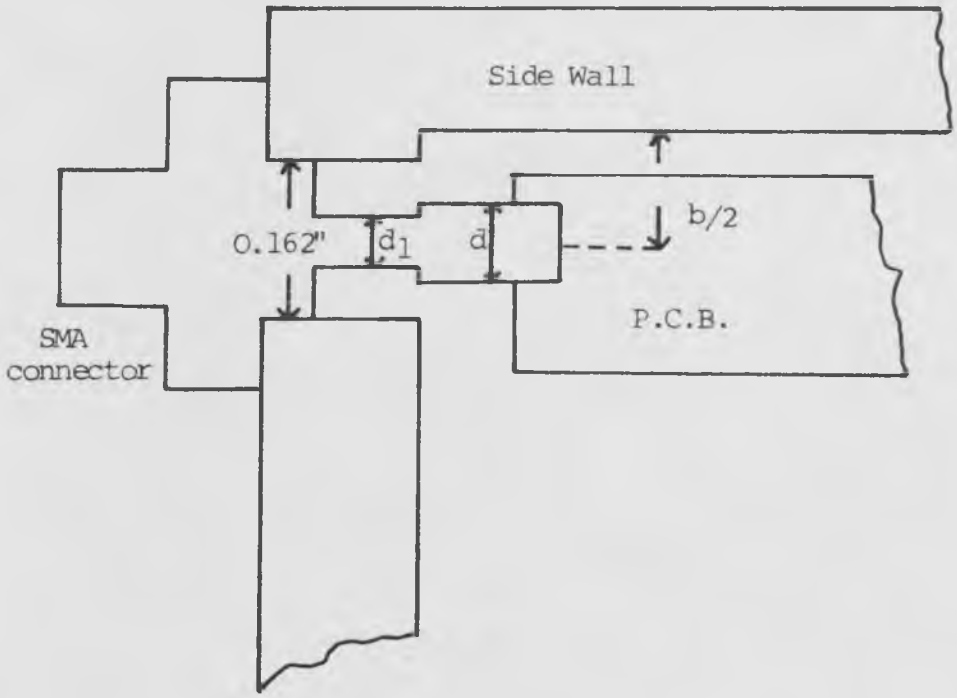

Fig. 2.1.7 The method of launching onto the S.S.S circuit board

the following expression

$$Z = \frac{138}{\sqrt{\varepsilon r}} \text{Log}_{10}[1.17\ b/d] \qquad (2.1.9)$$

For $Z = 50\ \Omega$ with $b = 0.15"$ and $\varepsilon r = 1$

then

$$d = 0.076"$$

The characteristic impedance of the transmission line formed by the centre feed conductor and the hole in the wall of the housing is given by

$$Z = \frac{138}{\sqrt{\varepsilon r}} \text{Log}_{10}\ [c/d1] \qquad (2.1.10)$$

The diameter of the dielectric plug on the S.M.A connector was 0.162". Thus with $c = 0.162"$, $\varepsilon r = 1$ and $Zo = 50\ \Omega$ we obtain

$$d1 = 0.07"$$

2.1.3 Measured Performances of the Bandstop Resonators

The resonant frequency, 3 dB bandwidth and stopband insertion loss of five bandstop resonators were measured using a Hewlett Packard swept amplitude analyser system. The measured performances are shown in Fig. 2.1.8. The results showed that deep notches with 3 dB bandwidths of a little as 0.25% of the centre frequency are possible. All the resonators

Coupling gap $x\ 10^{-3}$	Resonant Frequency GHz	3dB Bandwidth MHz	Notch Insertion loss dB's
4.1	4.7	51	23
10	4.81	30	17.5
14.7	4.89	23	15.5
20.6	4.93	15	12.5
26	4.98	13	11

Fig. 2.1.8 Measured performance of untuned bandstop resonators

Coupling Gap $x10^{-3}$	Resonant Frequency GHz	3dB Bandwidth MHz	Notch Insertion Loss dB's
4.1	4	37	19
10	4	22	17
14.7	4	10	14
20.6	4	11	10.5
26	4	8.5	8

Fig. 2.1.9 Measured performance of bandstop resonators after tuning to 4 GHz

exhibited a passband return loss of at least 15 dB from 2GHz to 7GHz. Attempts to tune the resonators using capacitive tuning screws located through the housing proved successful but tuning down to 4GHz reduced the 3dB bandwidth of the resonators by approximately 35%. Measured results for all five resonators after tuning to 4GHz are shown in Fig. 2.1.9.

2.1.4 The Equivalent Circuit of the Bandstop Resonator

By using the results presented in Fig. 2.1.8 it is possible to evaluate the relationship between the resonator coupling gap 'u' and its associated lumped capacitance. First, it is necessary to obtain the reference plane locations of the resonator in order to accurately determine its length. The reference plane location in the region of the coupling gap was assumed to be similar to that of a stripline T junction [2.4]. That is, the resonator was assumed to extend into the main line to a distance of one quarter of the width of the main line [Fig. 2.1.10]. At the open circuited end of the resonator, fringing capacitance increases the effective length of the resonator. To a good approximation, this situation can be treated as a two dimensional problem with the fringing at the end of the resonator being equivalent to that from the edges of an isolated stripline bar [Fig. 2.1.11]. From Fig. 2.1.11 we obtain the total capacitance per unit width of the resonator, which is

$$\frac{C}{\varepsilon} = \frac{4L}{b} + \frac{2Cf'}{\varepsilon} = \frac{4L'}{b} \qquad (2.1.11)$$

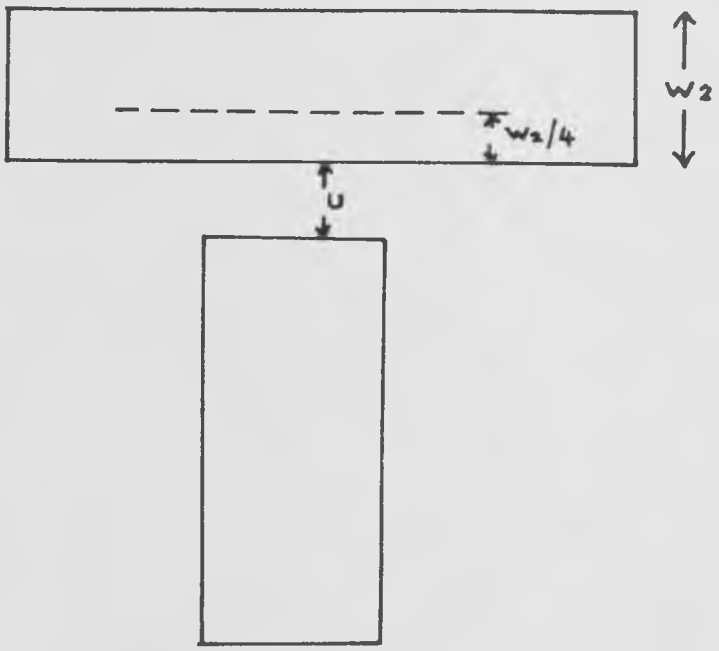

Fig. 2.1.10 Reference plane location of the bandstop resonator in the region of the coupling gap

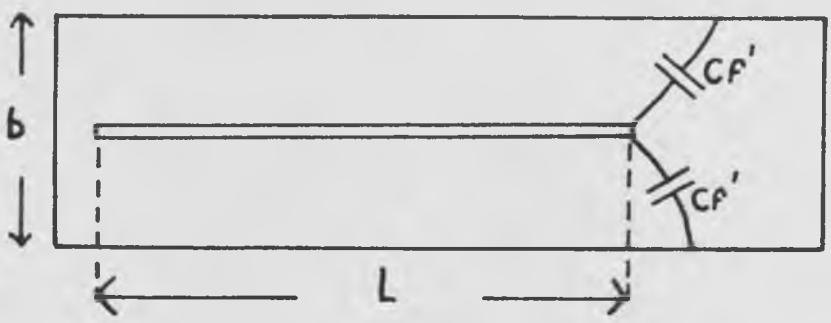

Fig. 2.1.11 Fringing capacitance off the end of a resonator

Where l' is the effective length of the resonator including fringing effects. Thus

$$L' = L + \frac{bCf'}{2\varepsilon} \qquad (2.1.12)$$

For thin strips we have

$$\frac{Cf'}{\varepsilon} = 0.46$$

And

$$L' = L + 0.23b \qquad (2.1.13)$$

Thus the total effective length, including both end effects of the resonator is

$$L' = L + 0.23\,b + \frac{W2}{4} + U \qquad (2.1.14)$$

By analysing the equivalent circuit of the resonator with the modified electrical length it was then possible to deduce the capacitance of the various coupling gaps. This was achieved simply by varying the coupling capacitance C until the computed 3dB bandwidth of the resonator agreed with a measured value, the value of C then corresponded to the capacitance of the coupling gap. The relationship between C and the coupling gap, normalised to 1" wide resonators and a 1" ground plane spacing is shown in Fig. 2.1.12.

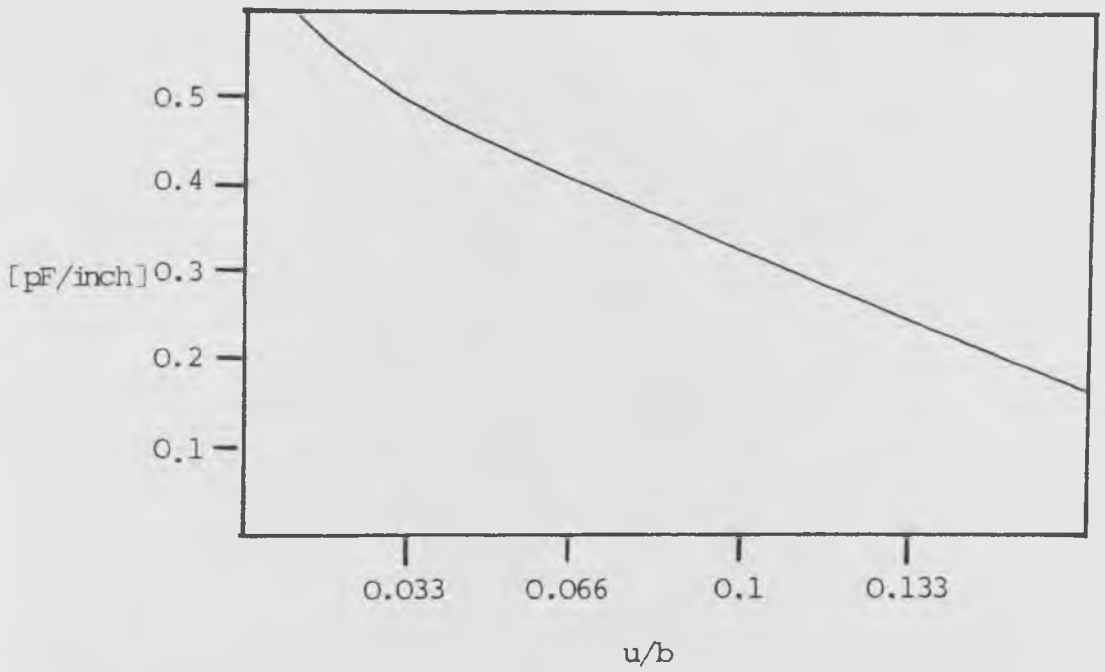

Fig. 2.1.12 The relationship between the dimensions of the resonator coupling gap and its associated lumped capacitance. The capacitance is normalised to 1" wide resonators

2.2 Varactor Tuned Bandstop Filters

2.2.1 Choice of Varactor Diode

As discussed in chapter 1 it was necessary to use GaAs varactors to achieve the highest possible Q factors. It was also necessary to use the lowest possible capacitance values available in order to obtain realisable resonator element values and also to avoid the possibility of the varactors series resonating with their parasitic package inductance.

Although varactor diode chips are available with 8:1 capacitance ratios, this value will be considerably reduced when the varactor is enclosed in a suitable microwave package. For example, a typical microwave package will have approximately 0.2pF capacitance, and this will appear in parallel with the varactor chip capacitance. Thus a varactor with a zero bias capacitance of 1pF and an 8:1 capacitance ratio will only exhibit an external capacitance ratio of 4:1 when enclosed in such a package.

Initially the DC4373B varactor, manufactured by AEI Semiconductors Ltd. was chosen. This device has a zero bias capacitance of 0.8pF, a chip capacitance ratio of 6.5:1 and a claimed zero bias Q factor of 6 at 10GHz. This varactor is enclosed in a LID package which is eminently suitable for S.S.S circuits because of its small size [Fig. 2.2.1], in addition the capacitance of this package is only 0.11pF.

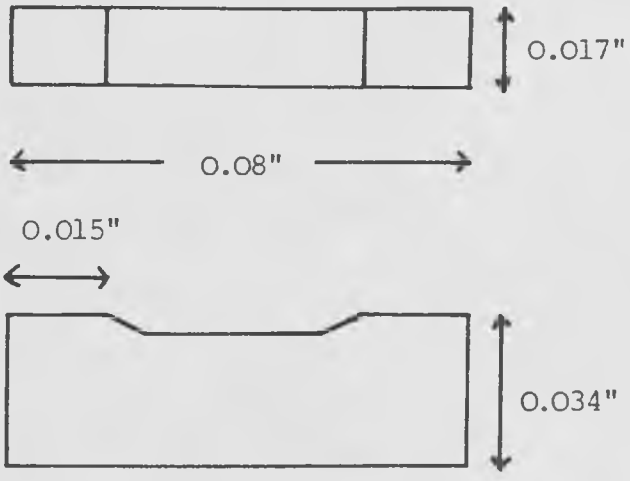

Fig. 2.2.1 The LID varactor package

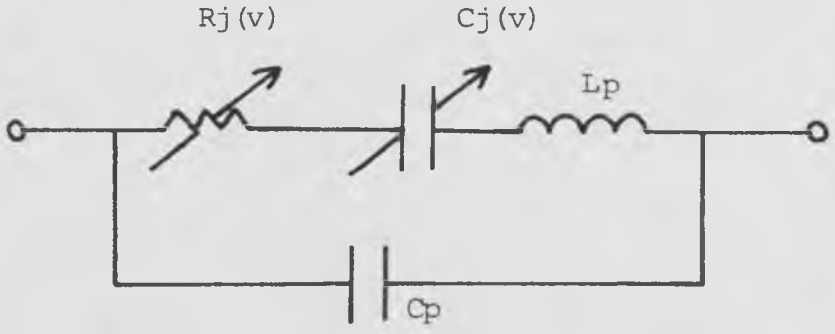

Fig. 2.2.2 Equivalent circuit of packaged varactor

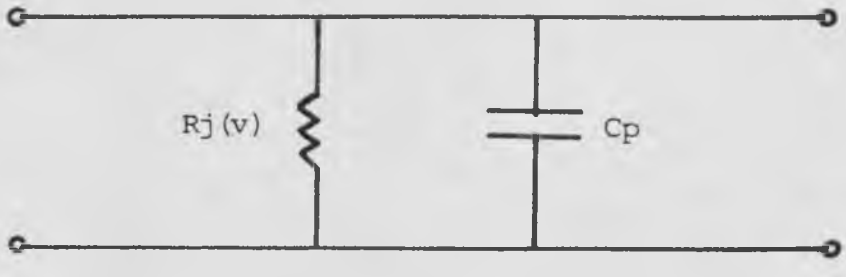

Fig. 2.2.3 Equivalent circuit model of a shunt connected varactor at its series resonant frequency

2.2.2 Measurements of Varactor Diodes

Measurements of the DC4373B varactor at 1MHz using a capacitance bridge confirmed the manufacturers claims with regard to capacitance ratio and zero bias capacitance. Dyer [2.5] has shown experimentally that 1 MHz capacitance measurements of varactors are accurate up to 18GHz.

In order to verify the manufacturers claims with regard to the varactor Q factor it was necessary to measure the varactor's small signal zero bias resistance. To achieve this the diode was forward biased to 1 Volt. At this voltage the depletion region width was zero and the resistance of the diode is then the resistance of the undepleted epilayer plus the substrate and contact resistances. It was then possible to derive the zero bias resistance of the varactor by including the effect of a finite epilayer thickness. This method yielded a zero bias resistance of 4.6 Ω. This result contradicted the manufacturers claim of approximately 3 Ω. However the method of forward biasing the varactor produced a large dc current through the diode which would heat it, thus producing an increase in the epilayer resistance.

To achieve more accurate measurements of the varactor it was necessary to perform measurements at microwave frequencies. The equivalent circuit of the packaged device is shown in Fig. 2.2.2 where Lp is the inductance of the bondwire connecting the chip to the package and Cp is the package capacitance. If the diode were shunt connected to ground from a transmission line, then at its series resonant frequency it

would appear as in Fig. 2.2.3. The package capacitance will possess a much higher impedance than the diode resistance at microwave frequencies and thus the diode can be approximated as a shunt resistor. The resistance can then be obtained by insertion loss measurements at the resonant frequency. The insertion loss for a shunt resistor in a 50 Ω system can be expressed by

$$LA = 20 \text{ Log}_{10}[1 + \frac{25}{R}] \qquad (2.2.1)$$

A diode test unit was constructed in S.S.S for the purpose of this measurement. The circuit layout shown in Fig. 2.2.4 consisted of a 50 Ω line with the diode connected from the line to a grounded conductor. Grounding was achieved by clamping the conductor between the side walls of the S.S.S housing. In addition a four section stepped impedance transmission line filter was used to provide R.f isolation between the varactor and the D.C power supply. The design of bias filters is discussed in more detail later in this chapter.

The varactor resistance was obtained from the insertion loss measurements and was 2.9 Ω at zero bias and 2.5 Ω at minus 20 volts bias.

The series resonant frequency at which the insertion loss measurement was performed was 5.9 GHz at zero bias. The value of the bondwire inductance was obtained from

$$Lp = 1/w_o^2 Cj(o) \qquad (2.2.2)$$

Thus $Lp \approx 900$ pH

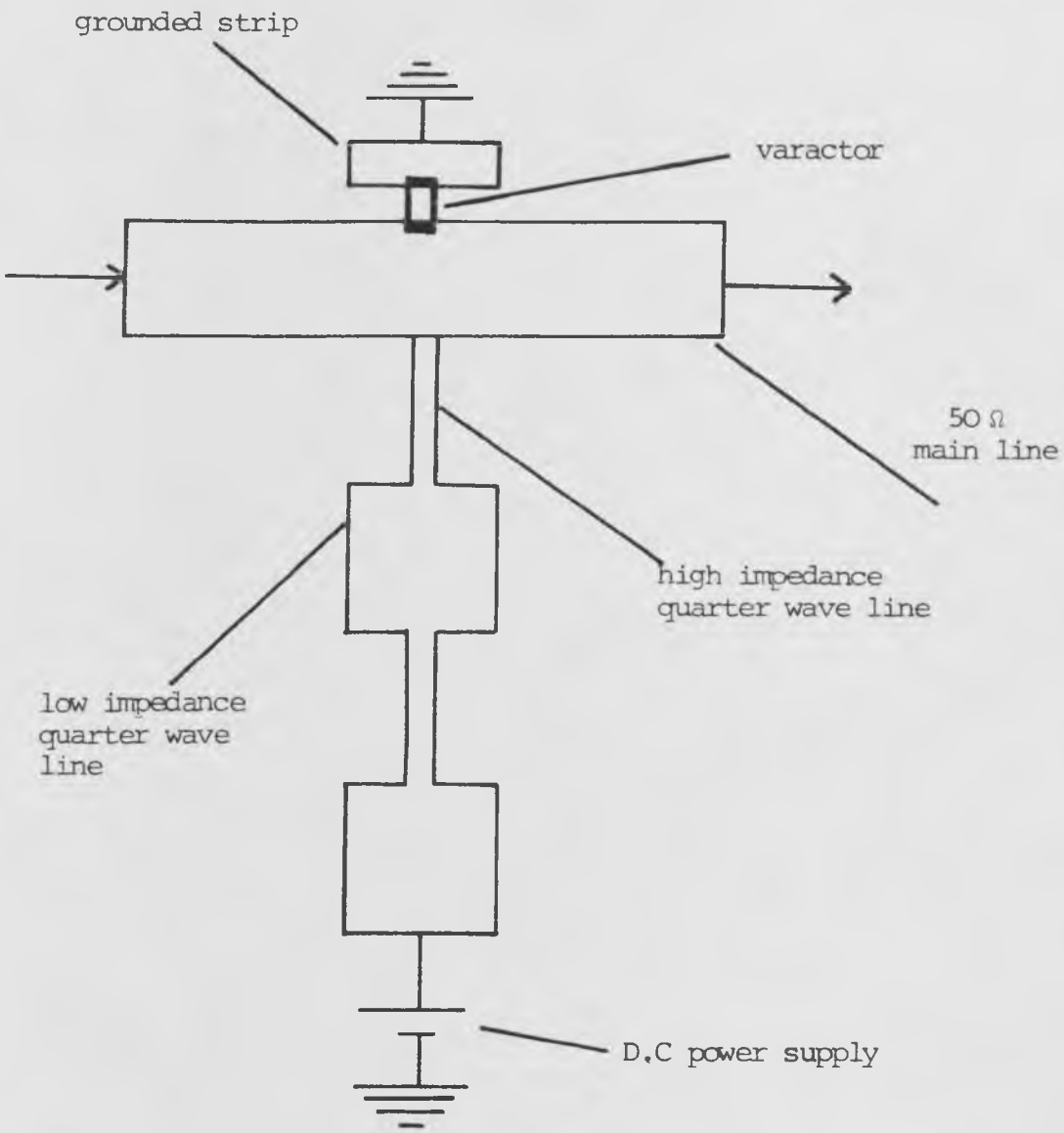

Fig. 2.2.4 Test unit for measuring the equivalent circuit parameters of a varactor

The measured parameters of the varactor circuit model are used extensively in later chapters for the purpose of computer analysis of varactor tuned filters.

2.2.3 Varactor Tuned Bandstop Resonators

By terminating the bandstop resonator discussed in section 2.1 in a varactor diode it is possible to tune the resonator. In order to isolate the varactor from the dc power supply a bias filter or choke must be used. A three section quarter wave stepped impedance transmission line filter was constructed in S.S.S in order to ensure that the bias filter would be adequate. The filter was designed to have a quarter wave (stopband centre) frequency of 6.5 GHz and the line impedances were 15 Ω, 150 Ω and 15 Ω. The low impedance 15 Ω impedance lines required considerable capacitance to ground, thus a low ground plane spacing was necessary, in fact a 0.04" ground plane spacing was used. This would not produce very high Q transmission lines but since the filter was a broadband device this was not considered a problem.

The transfer matrix of this filter normalised to a 1 Ω system is

$$\begin{bmatrix} \cos(\theta) & j0.3\sin(\theta) \\ j3.33\sin(\theta) & \cos(\theta) \end{bmatrix} \begin{bmatrix} \cos(\theta) & j3\sin(\theta) \\ j0.33\sin(\theta) & \cos(\theta) \end{bmatrix} \begin{bmatrix} \cos(\theta) & j0.3\sin(\theta) \\ j3.33\sin(\theta) & \cos(\theta) \end{bmatrix} \qquad (2.2.3)$$

At the stopband centre frequency $\theta = 90^{o}$ and the matrix reduces to

$$\begin{bmatrix} 0 & j0.3 \\ j3.33 & 0 \end{bmatrix} \begin{bmatrix} 0 & j3 \\ j0.33 & 0 \end{bmatrix} \begin{bmatrix} 0 & j0.3 \\ j3.33 & 0 \end{bmatrix} \qquad (2.2.4)$$

$$= \begin{bmatrix} 0 & -j0.33 \\ -j33.3 & 0 \end{bmatrix} \qquad (2.2.5)$$

Using the insertion loss formula of a network for the A,B,C,D parameters we have

$$LA = 10 \text{ Log}_{10} [1 + 0.25(33.3 - 0.33)^{2}] \qquad (2.2.6)$$

$$= 25 \text{ dB}$$

That is the midstopband insertion loss of this filter will be 25 dB. The actual measured performance of this filter, shown in Fig. 2.2.5 exhibited greater than 20 dB loss from 4GHz to 8GHz, the maximum rejection was not 25 dB but 23 dB, the discrepancy probably being caused by the discontinuities at the junctions between the quarter wave sections of transmission line. This value was however sufficient for a varactor tuned filter since less than 1% of the R.f power incident upon the varactor could escape into the bias supply.

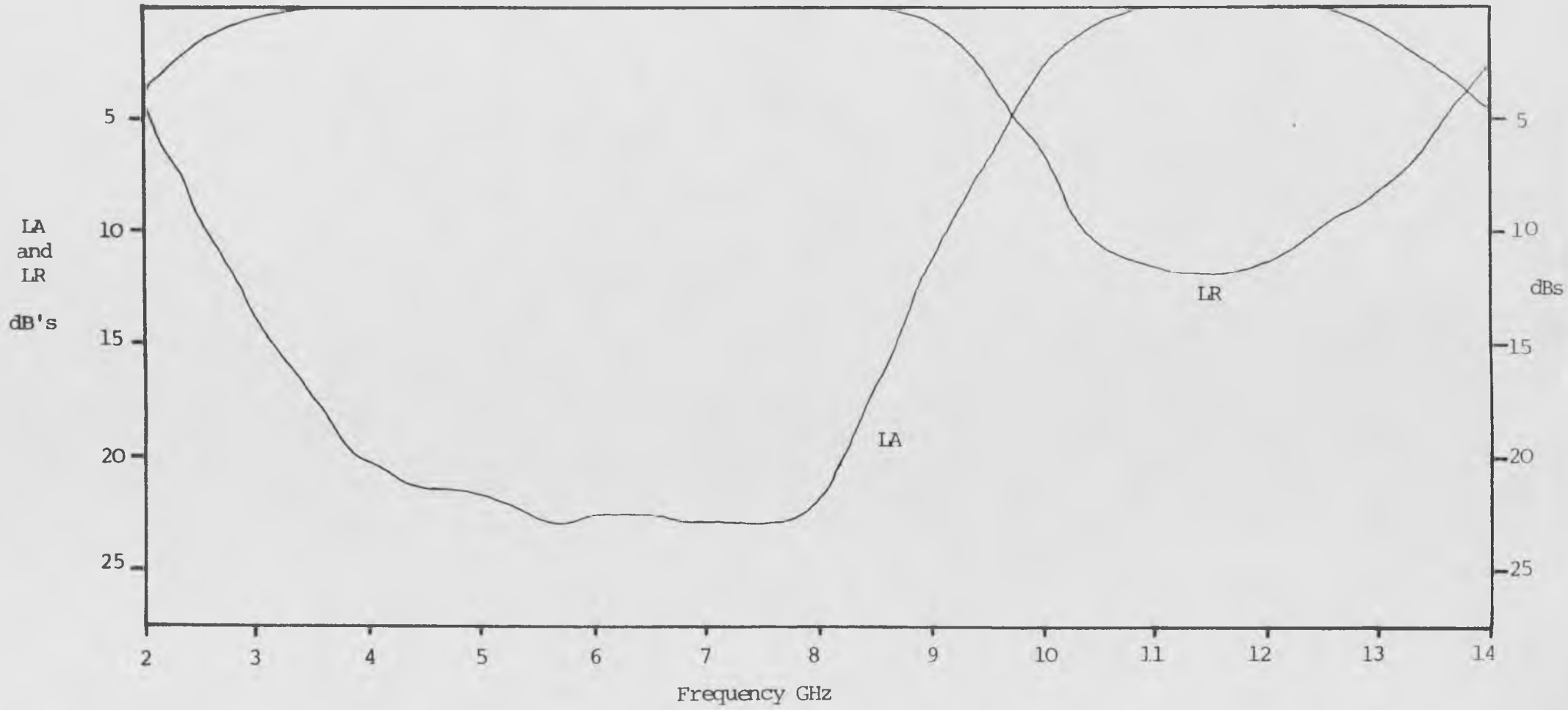

Fig. 2.2.5 Frequency response of stepped impedance transmission line filter

Two varactor tuned bandstop resonators were constructed using the resonators described previously and the bias filters described above. The coupling gaps between the resonators and the main line were 0.005" and 0.008" corresponding to percentage 3 dB bandwidths of 06% and 1% at 4GHz. The bias filters were 2 section quarter wave filters with the low impedance lines being realised by a sandwich structure of dielectric circuit board and conductor clamped between the side walls of the S.S.S housing [Fig. 2.2.6]

The measured performances of these resonators are shown as a function of varactor bias voltage in Fig. 2.2.7. These results show that a tuning bandwidth of approximately 25% of the upper tuned frequency is possible. Unfortunately the Q factor of these resonators was insufficient to produce an acceptable response, the worst case stopband insertion loss was only 1.4 dB.

There are two methods to overcome the problem of low resonator Q factor, the most obvious is to increase the bandwidth of the resonator. Of more interest is the method of decoupling the varactor from the resonator by connecting it in series with a lossless capacitor. For example, consider a 1 pF varactor with a 4:1 capacitance ratio connected in series with a 1 pF lossless capacitor. At zero bias the effective terminal capacitor is 0.5 pF and at maximum bias it is 0.2 pF. Thus the Q factor at zero bias has been doubled albeit the capacitance ratio has been reduced from 4:1 to 2.5:1. This technique would therefore seem to be of some value.

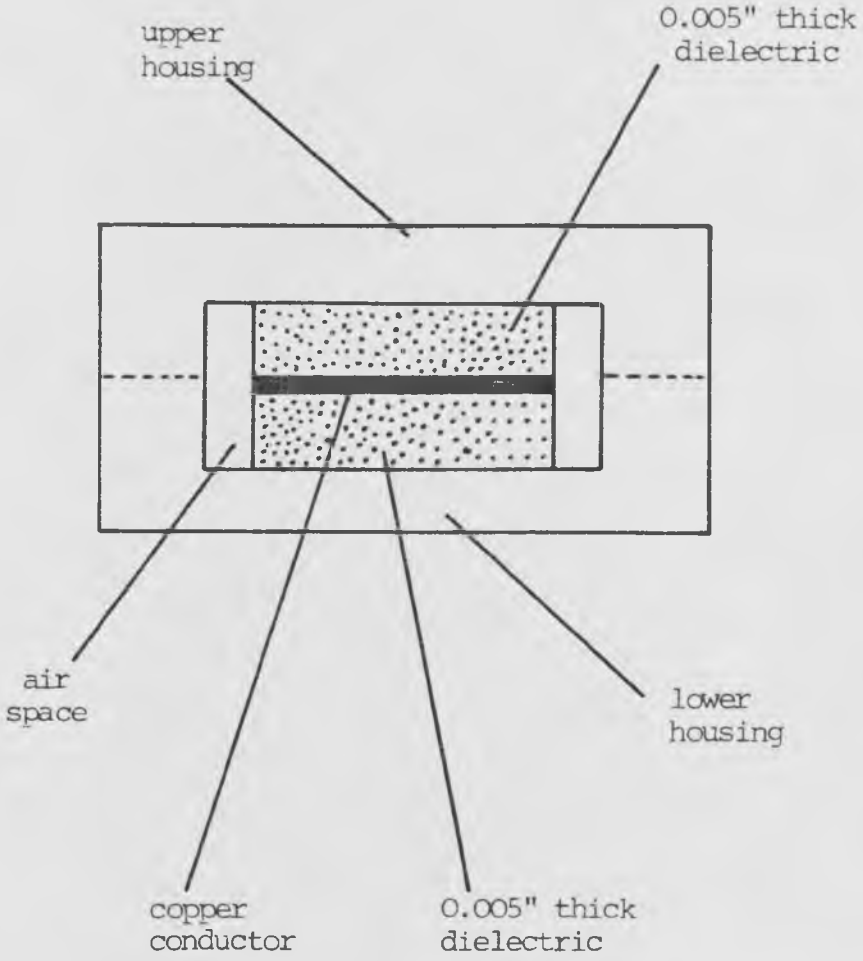

Fig. 2.2.6 Realisation of bias choke with a sandwich structure

Bias -V	0	1	2	3	4	5	10	15	20	30
Stopband insertion loss dB's	1.9	2.5	3.5	4	4.5	4.9	6.5	7	7.5	8.9
Centre frequency GHz	3.04	3.34	3.45	3.53	3.64	3.68	3.78	3.85	3.89	3.95
3 dB stopband bandwidth MHz						74	74	74	75	77

a) Coupling gap = 0.005"

Bias -V	0	1	2	3	4	5	10	15	20	30
stopband insertion loss dB's	1.4	1.8	2.1	2.8	3.3	3.5	4.5	5.2	5.5	6.5
centre frequency GHz	3.06	3.36	3.5	3.59	3.66	3.72	3.83	3.91	3.97	3.99
3 dB stopband bandwidth MHz							42	43	44	46

b) Coupling gap = 0.008"

Fig. 2.2.7 Measured performances of varactor tuned bandstop resonators

Several bandstop resonators have been constructed using this technique. The resonators were again 1.1" long and the coupling gaps varied between 0.003" and 0.025". Two values of series decoupling capacitors were used, these were approximately 1 pF and 0.5 pF and were realised by overlapping conductors on opposite sides of the S.S.S circuit board. The overlapping capacitors were designed as if they were simple parallel plate capacitors with a fringing capacitance of 30% of the parallel plate capacitance.

The measured performances of these varactor tuned resonators are shown in Fig. 2.2.8. The results show that with the varactors decoupled via the 1 pF capacitor, tuning bandwidths of approximately 12% are achieved with acceptable responses for resonator 3 dB bandwidths of greater than 2%. With the lower value of decoupling capacitor tuning bandwidths of 7% are possible and insertion loss levels of greater than 7 dB are maintained for resonators with 3 dB bandwidths of greater than 1%. In conclusion it can be seen that useful varactor tuned resonators with low dissipation loss are achieved with tuning bandwidths of approximately seven times their 3 dB bandwidth.

2.2.4 Varactor Tuned Multi-Resonator Bandstop Filters

Several two section bandstop varactor tuned filters were constructed in order to investigate the effects of tuning on filter performance. The filters were constructed using the resonators discussed in section 2.2.3 which were separated by

Bias	Centre frequency GHz	3 dB bandwidth MHz	Stopband insertion loss dB	Stopband return loss dB
0 V	3.54	36	4.5	6.5
-30V	3.88	45	11.5	2.4

(i) Strong varactor coupling

Bias	Centre frequency GHz	3 dB bandwidth MHz	Stopband insertion loss dB	Stopband return loss dB
0 V	3.65	46	9	3.8
-30 V	3.82	49	13	2

(ii) Weak varactor coupling

Fig. 2.2.8 b) Measured performance of a varactor tuned resonator with a coupling gap of 0.01"

Bias	Centre frequency GHz	3 dB bandwidth MHz	Stopband insertion loss dB	Stopband return loss dB
OV	3.5	30	4.5	8.5
-30V	3.84	40	10.5	3

(i) Strong varactor coupling

Bias	Centre frequency GHz	3 dB bandwidth MHz	Stopband insertion loss dB	Stopband return loss dB
OV	3.55	34	8	4.5
-30V	3.73	40	13	2

(ii) Weak varactor coupling

Fig. 2.2.8c Measured performance of a varactor tuned resonator with a coupling gap of 0.018"

Bias	Centre frequency GHz	3dB bandwidth MHz	stopband insertion loss dB	stopband return loss dB
OV	3.53	15	3.5	14
-30V	3.94	30	7.5	4.5

(i) Strong varactor coupling

Bias	Centre frequency GHz	3 dB bandwidth MHz	stopband insertion loss dB	stopband return loss dB
OV	3.81	25	5	7
-30V	3.93	30	10	4

(ii) Weak varactor coupling

Fig. 2.2.8 d Measured performance of a varactor tuned resonator with a coupling gap of 0.025"

a 50 Ω transmission line with 90° phase length at 3.3GHz. The reference planes of the transmission line were assumed to be at the exact centre of the resonators as shown in Fig. 2.2.9. The measured performances of six filters are shown in Figs. 2.2.10 - 2.2.15, these include designs for three different bandwidths and two different values of varactor decoupling capacitor. The measured results show that the filters exhibit an increase in selectivity over that of the single resonators, and an increase in stopband insertion loss. However, as in the case of the single resonators, good responses were only achieved for tuning bandwidths of 10% or less. In every case the filters could be tuned with a single power supply provided that some initial tuning using tuning screws was performed. It can be seen that the frequency response of each filter varies as a function of tuned frequency. This is partly due to the change in varactor Q factor with bias voltage and also due to the change in phase shift between the resonators.

In order to construct high performance bandstop filters it is necessary to have accurate knowledge of the location of the reference planes of the main transmission line between the resonators. These were measured using a Hewlett-Packard network analyser and are shown in Fig. 2.2.16. Using these reference plane locations a 4 resonator bandstop filter was designed for operation at 10GHz. The phase lengths between the resonators were exactly 90° at 10GHz. The design of the resonators was somewhat intuitive, these being all the same length and the coupling gaps between the outer resonators and the main line were 2.5 times larger than the inner resonator coupling gaps.

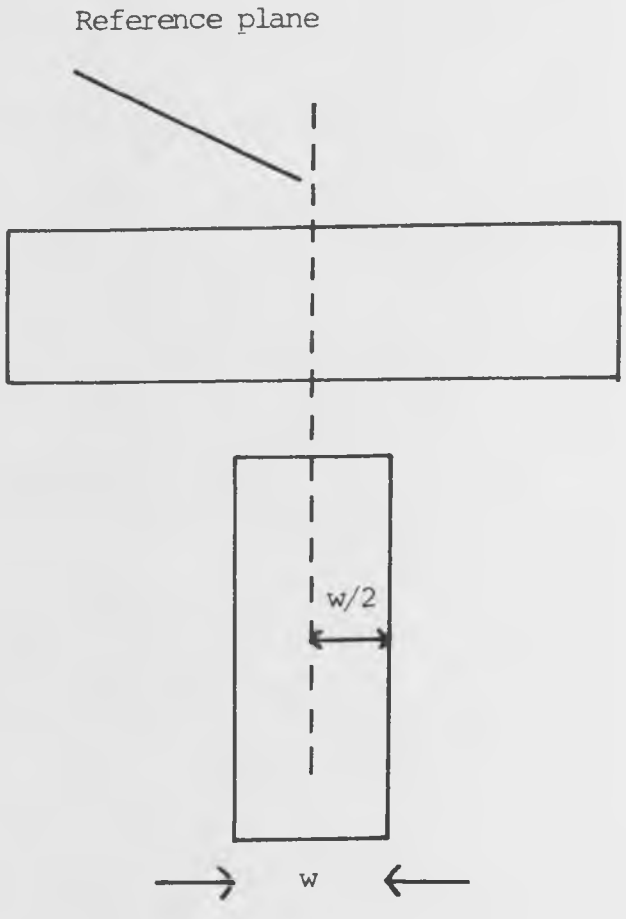

Fig. 2.2.9 The assumed reference plane locations of the resonators for the varactor tuned bandstop filters

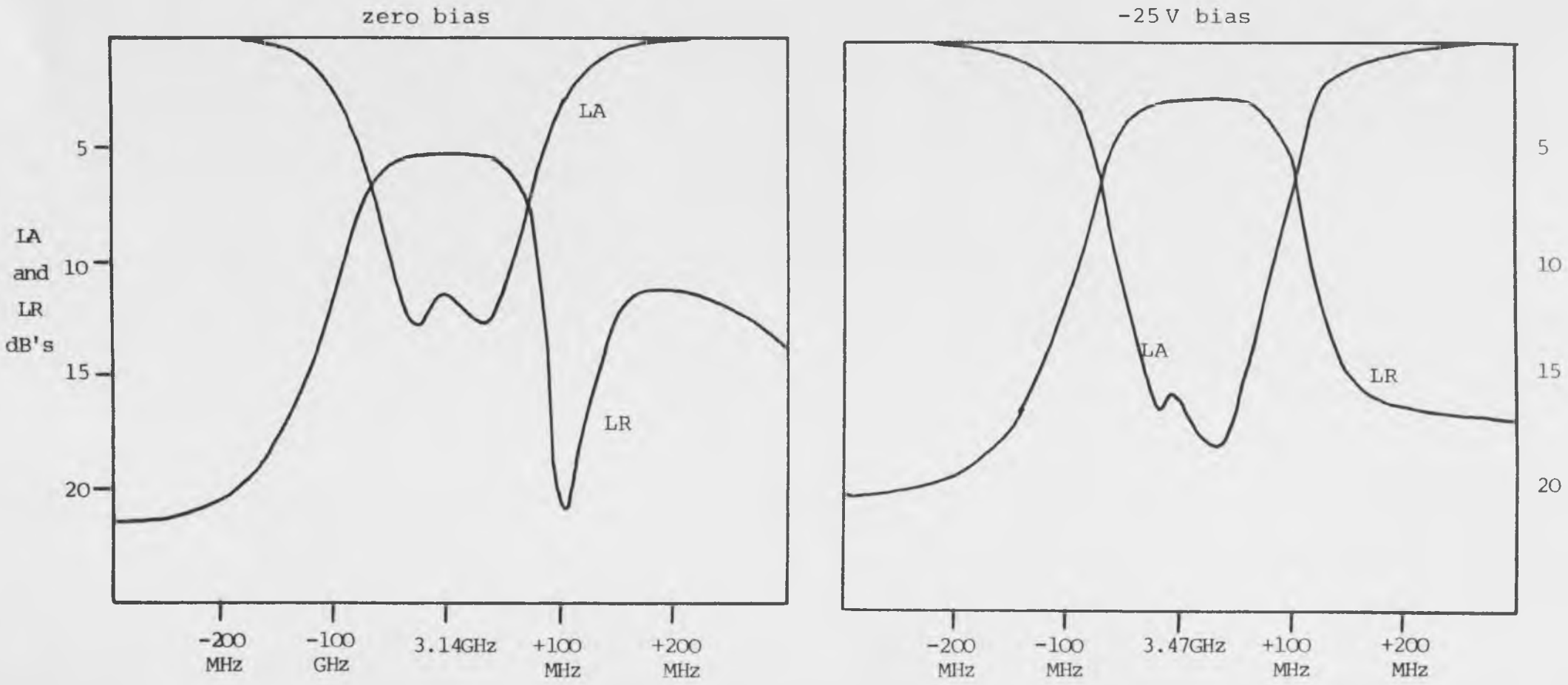

Fig. 2.2.10 2 Stage varactor tuned filter response with a coupling gap of 0.005"

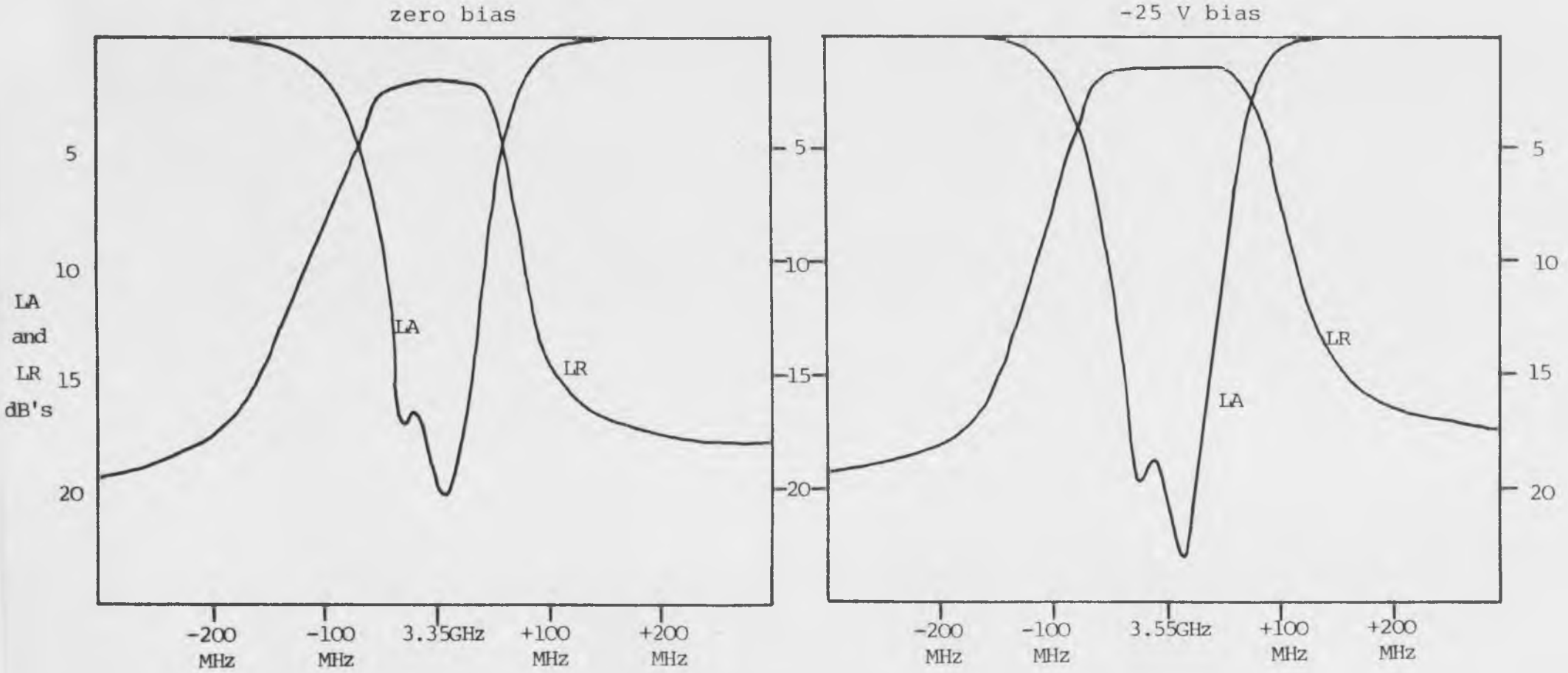

Fig. 2.2.11 2 Stage varactor tuned filter response with a coupling gap of 0.005" and weakly coupled varactors

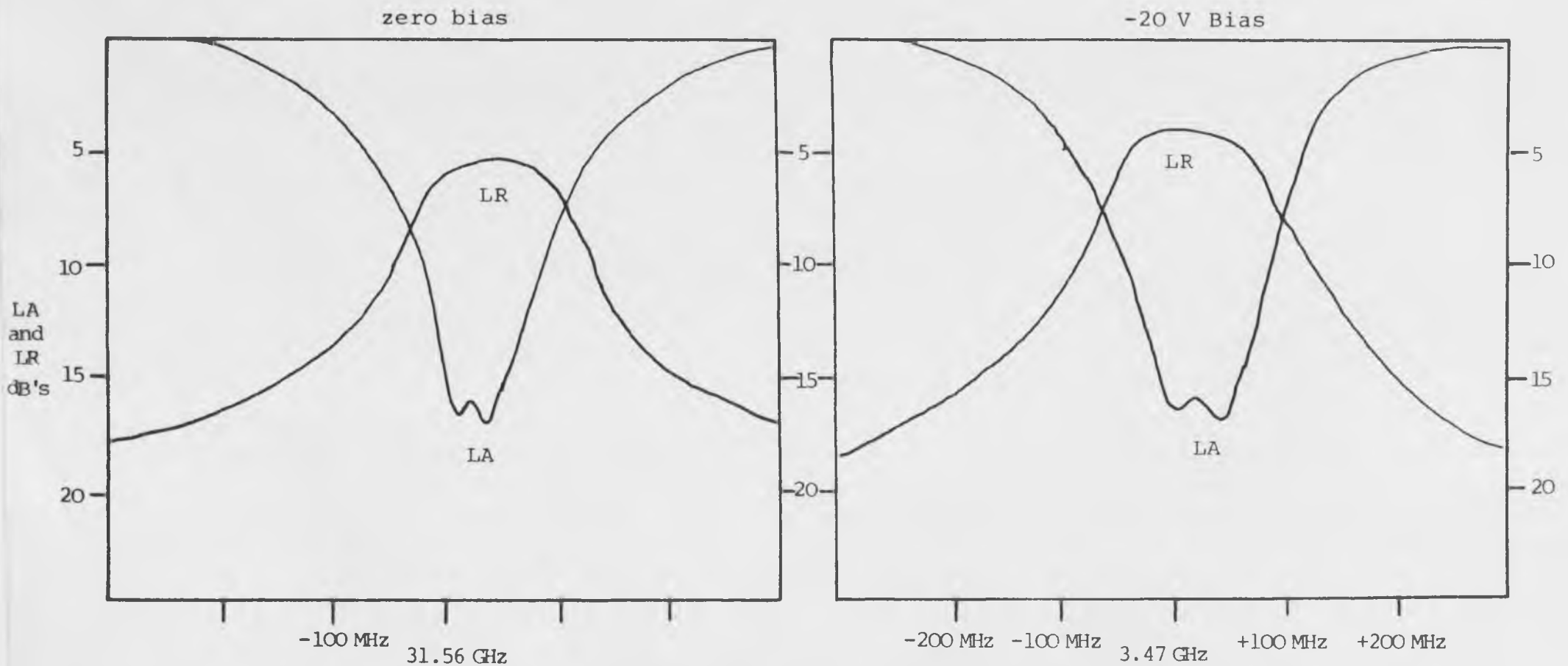

Fig. 2.2.12 2 stage varactor tuned filter response with 0.01" coupling gaps

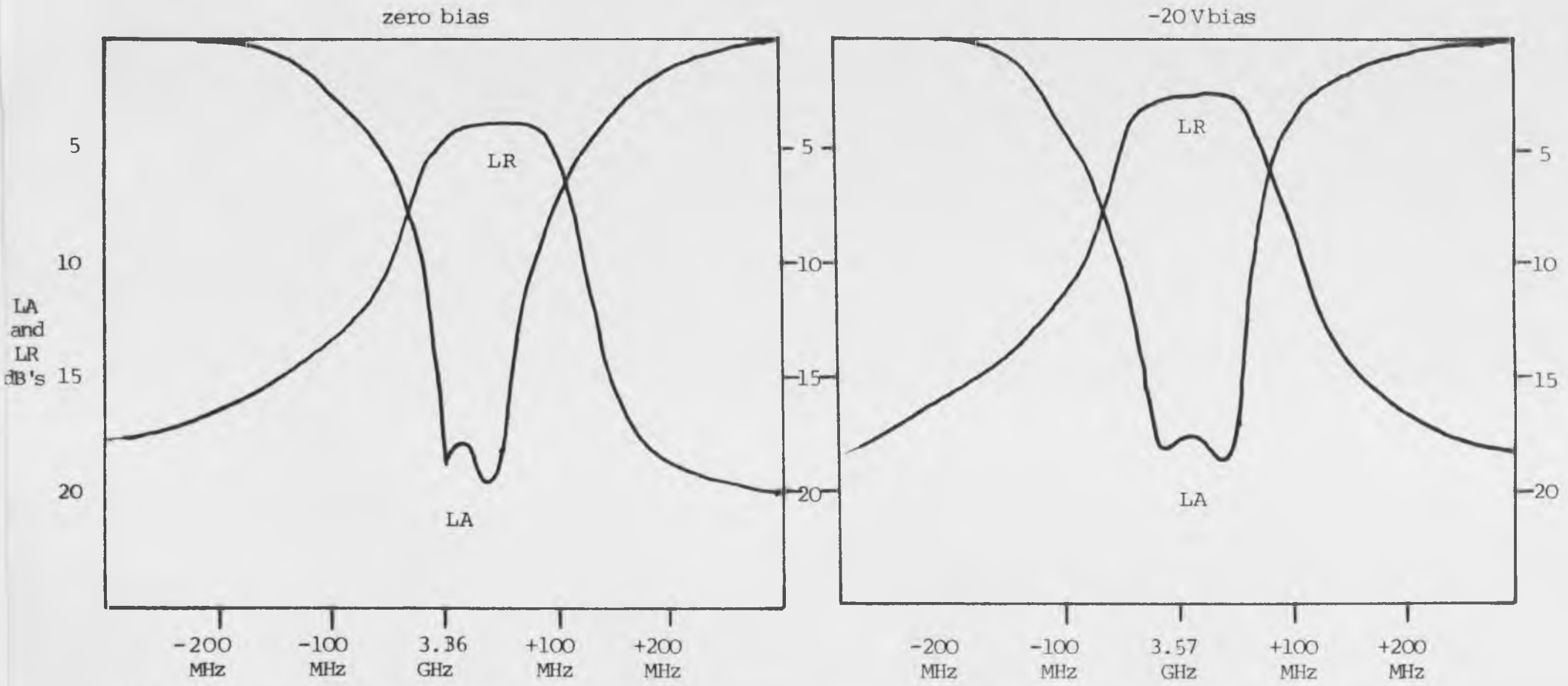

Fig. 2.2.13 2 stage varactor tuned filter response with 0.01" coupling gaps and loosely coupled varactors

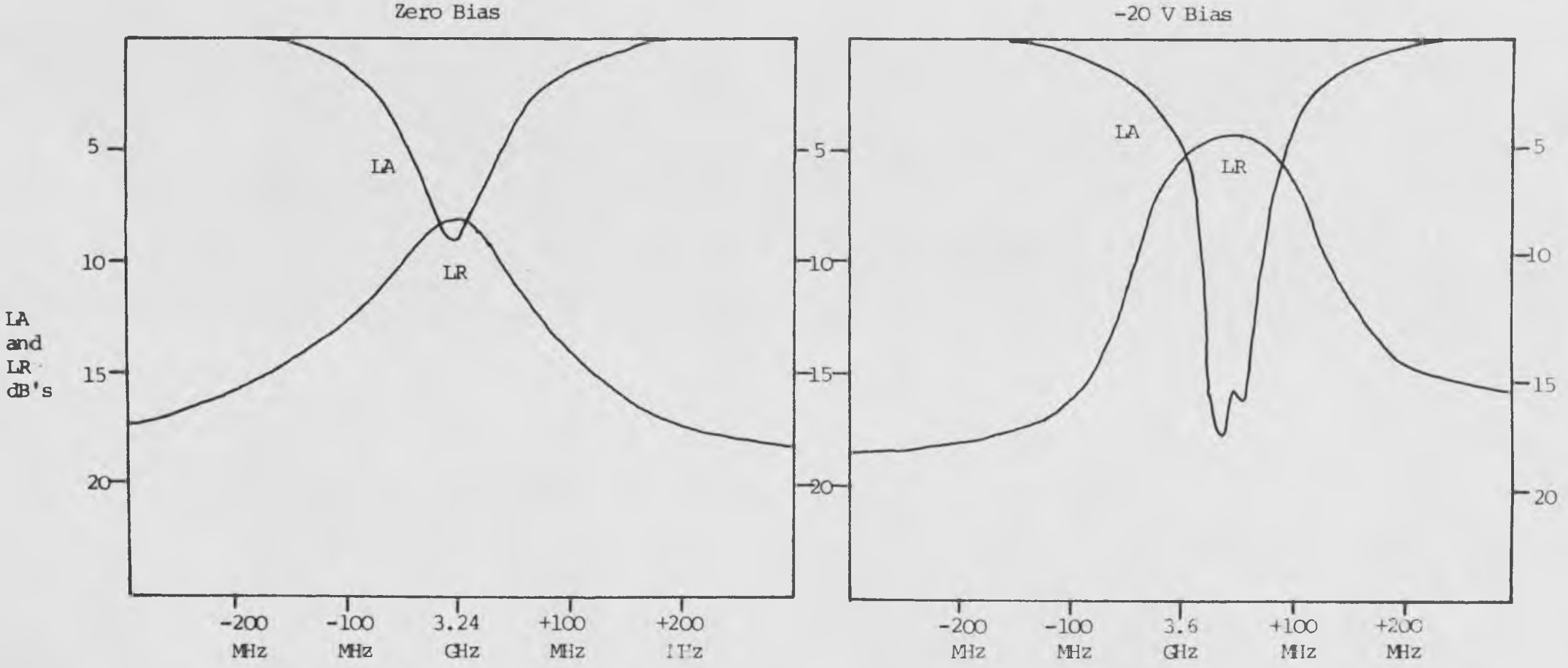

Fig. 2.2.14 2 stage varactor tuned filter response with 0.018" coupling gaps

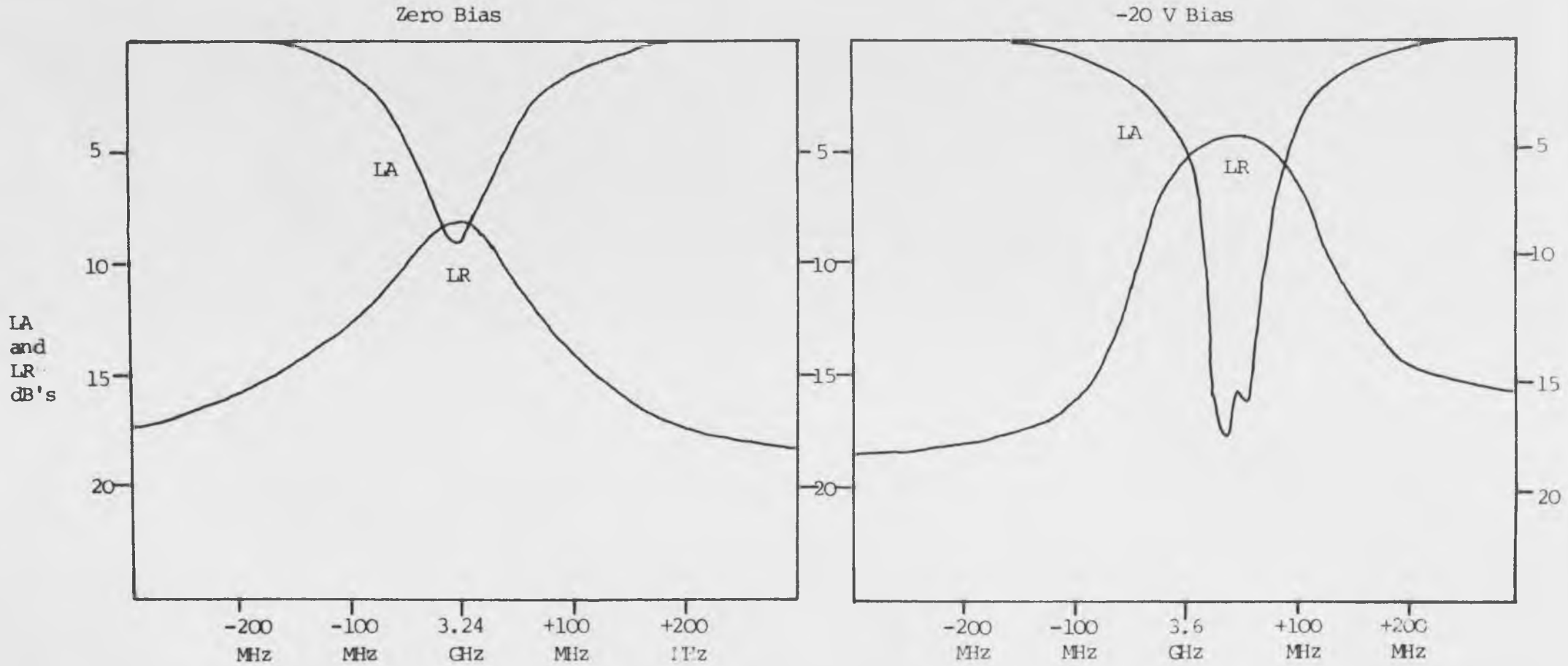

Fig. 2.2.14 2 stage varactor tuned filter response with 0.018" coupling gaps

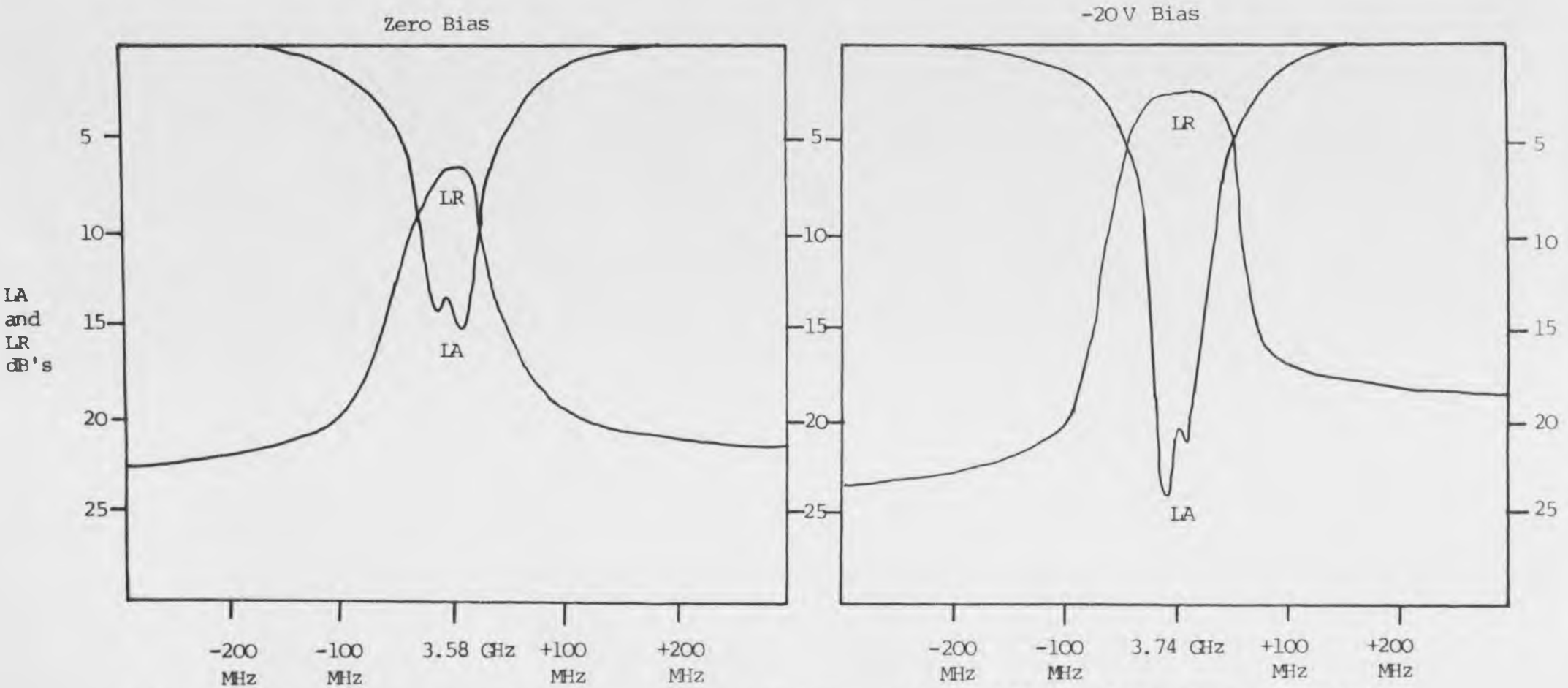

Fig. 2.2.15 2 stage varactor tuned filter response with 0.018" coupling gaps and weakly cupled varactors

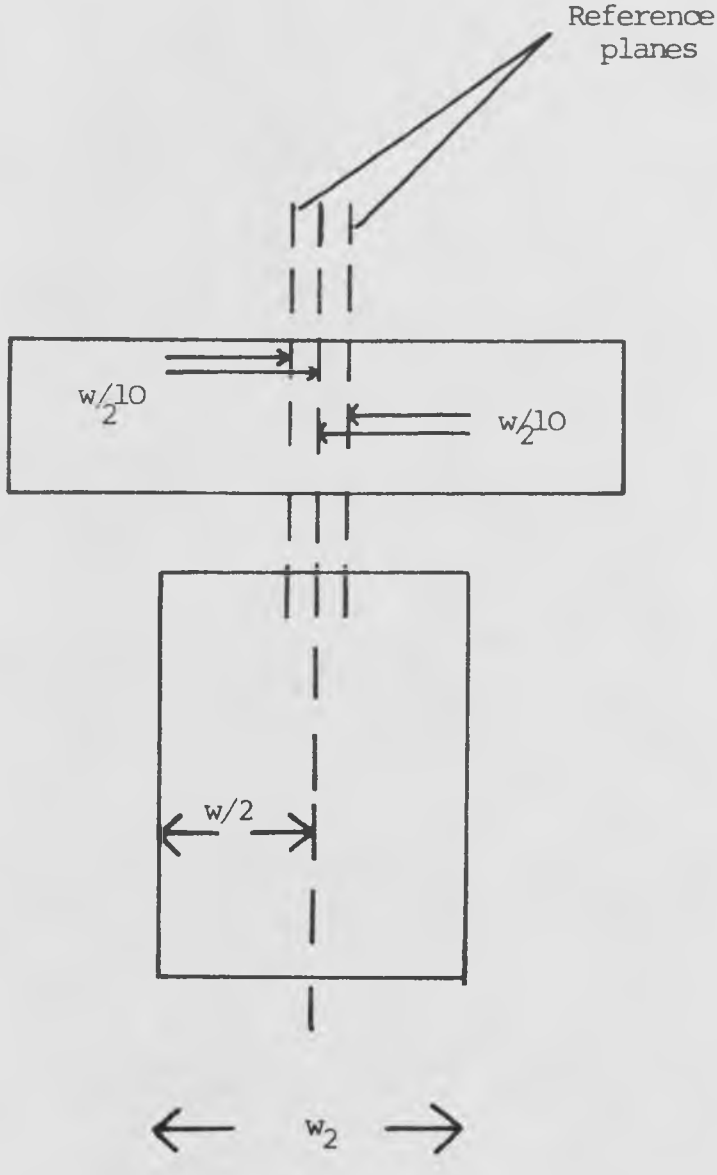

Fig. 2.2.16 Measured reference plane locations of the bandstop resonators

The S.S.S circuit board layout of this filter is shown in Fig. 2.2.17. The filter was mechanically tuned to a centre frequency of 10GHz and the measured performance is shown in Fig. 2.2.18.

The frequency response of the filter exhibited a greater selectivity and a lower level of passband return loss on the higher side of the stopband than on the lower side. A possible explanation of this would be that the phase shift between the resonators were incorrect. The resonators were coupled by a transmission line (assumed lossless) with the transfer matrix (normalised to a 1 Ω system) below.

$$[T] = \begin{bmatrix} \cos(\theta) & j\sin(\theta) \\ j\sin(\theta) & \cos(\theta) \end{bmatrix} \qquad (2.2.7)$$

Where $\theta = aw$

This matrix can be decomposed into the product below,

$$\begin{bmatrix} \sqrt{\sin(\theta)} & 0 \\ 0 & \frac{1}{\sqrt{\sin(\theta)}} \end{bmatrix} \begin{bmatrix} 1 & 0 \\ -j\cos(\theta) & 1 \end{bmatrix} \begin{bmatrix} 0 & j \\ j & 0 \end{bmatrix} \cdot$$

$$\cdot \begin{bmatrix} 1 & 0 \\ -j\cos(\theta) & 1 \end{bmatrix} \begin{bmatrix} 1/\sqrt{\sin(\theta)} & 0 \\ 0 & \sqrt{\sin(\theta)} \end{bmatrix} \qquad (2.2.8)$$

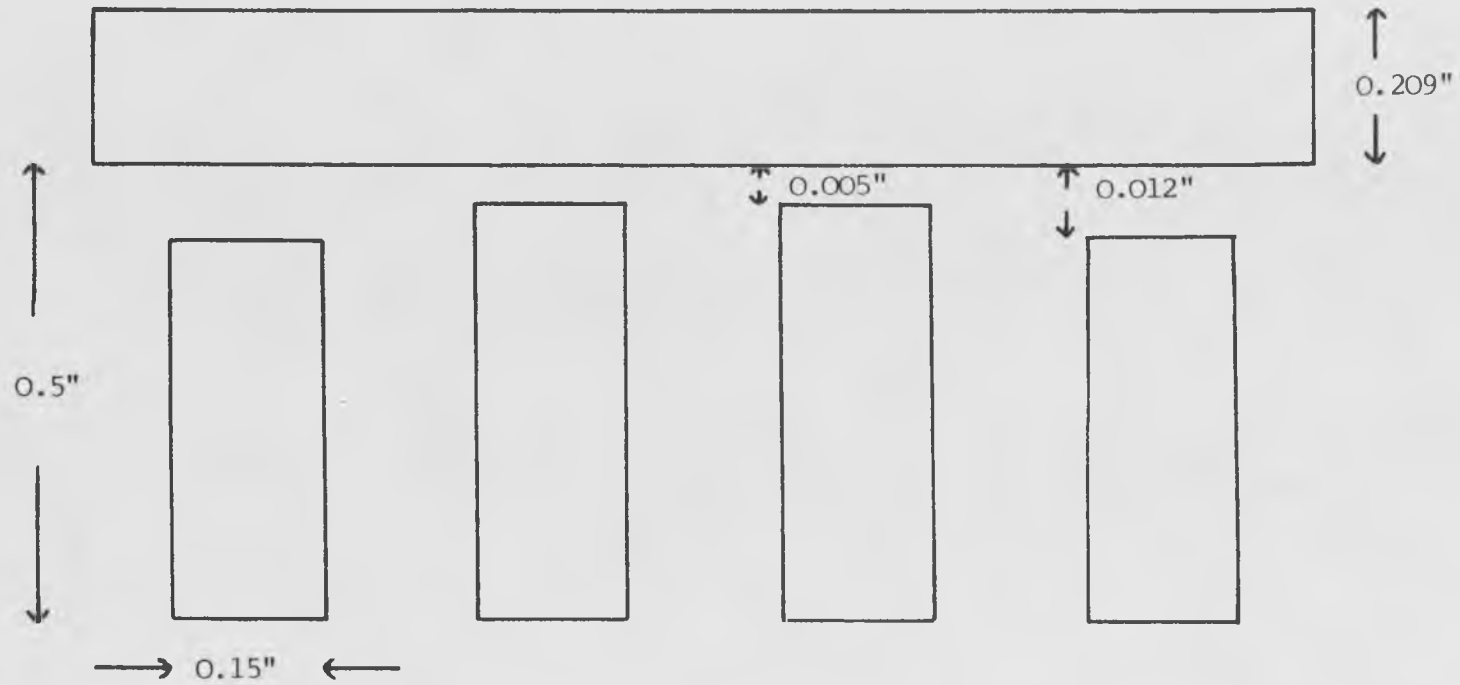

Fig. 2.2.17 Dimensions of 4 stage bandstop filter

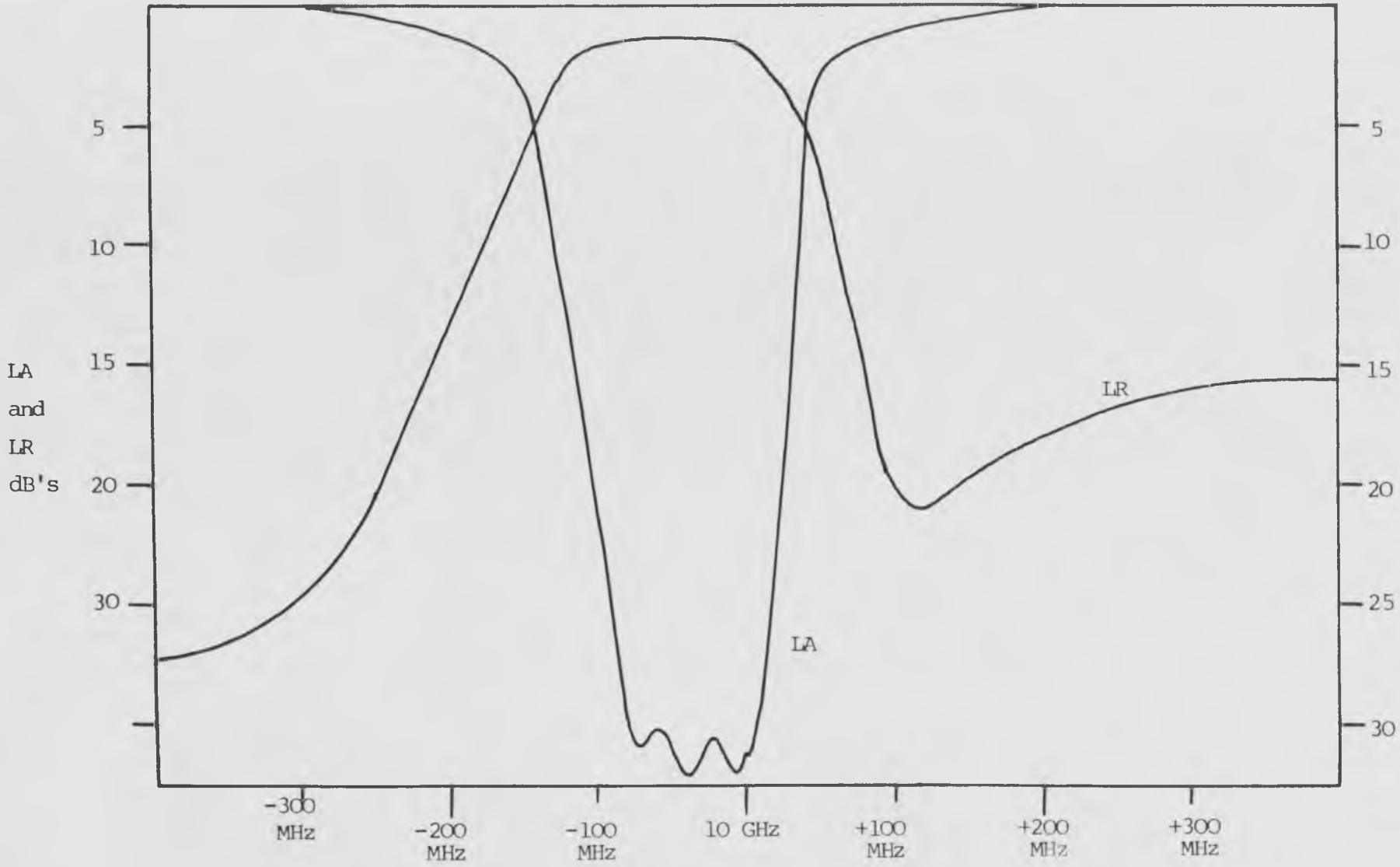

Fig. 2.2.18 Measured performance of four stage bandstop filter

The matrix product of 2.2.8 represents an ideal unity impedance inverter shunted on each side by frequency dependent reactances and terminated in frequency dependent transformers [Fig. 2.2.19]. If the transmission line were exactly 90^{o} long then 2.2.8 would degenerate into the required unity impedance inverter. For lengths of line other than 90^{o} the shunt reactances become finite and load the resonators, thus causing the asymmetric frequency response, also the transformers will no longer have unity turns ratio and the filter passband return loss will be degraded. This effect is shown in Fig. 2.2.20 for a prototype bandstop filter with the computed frequency response given for phase shifts between resonators of 60^{o}, 90^{o} and 120^{o}.

However, the filter response shown in Fig. 2.2.19 was evident when the phase shift between the resonators was exactly 90^{o}. The correct explanation of this phenomenon can be attributed to the basic properties of the resonators. The equivalent circuit of the bandstop resonator including a lumped tuning capacitor is shown in Fig. 2.2.21. The input impedance of this resonator is

$$Zin(jw) = \frac{j[Z_o^2 C_1 C2w^2 \tan(aw) - w(C1+C2)Z_o - \tan(aw)]}{wC1[\tan(aw) + wC2Zo]} \qquad (2.2.9)$$

The resonator possesses a transmission zero and a transmission pole, these being defined by the zeros of the numerator and denominator of 2.2.9. The frequency of perfect transmission is slightly greater than the transmission zero

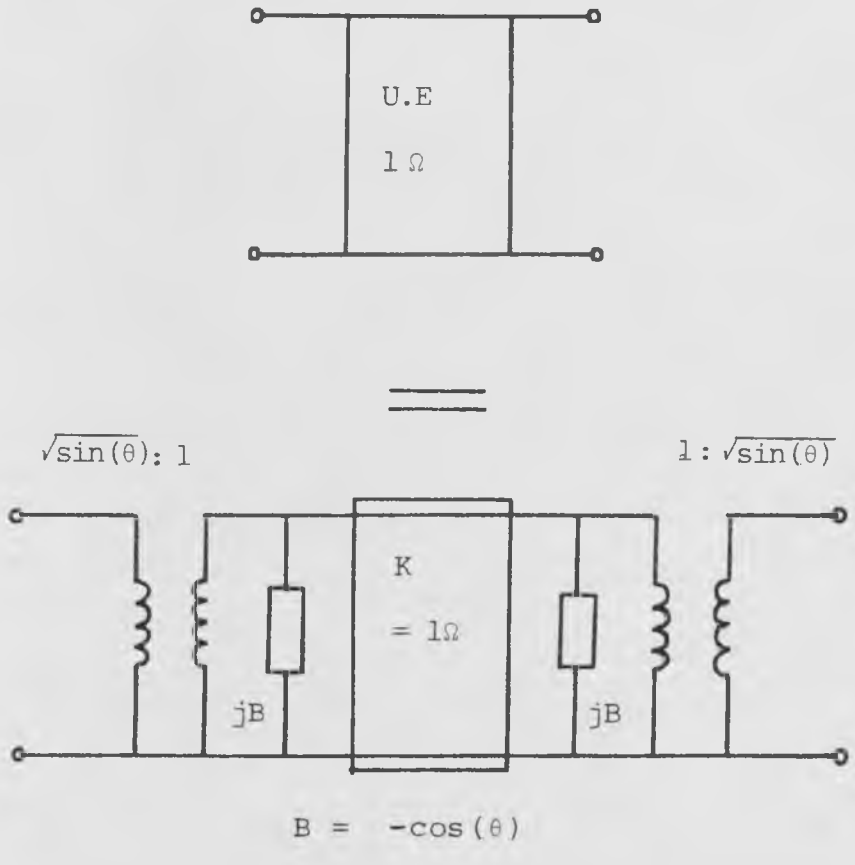

Fig. 2.2.19 Equivalent circuit of a unit element of transmission line

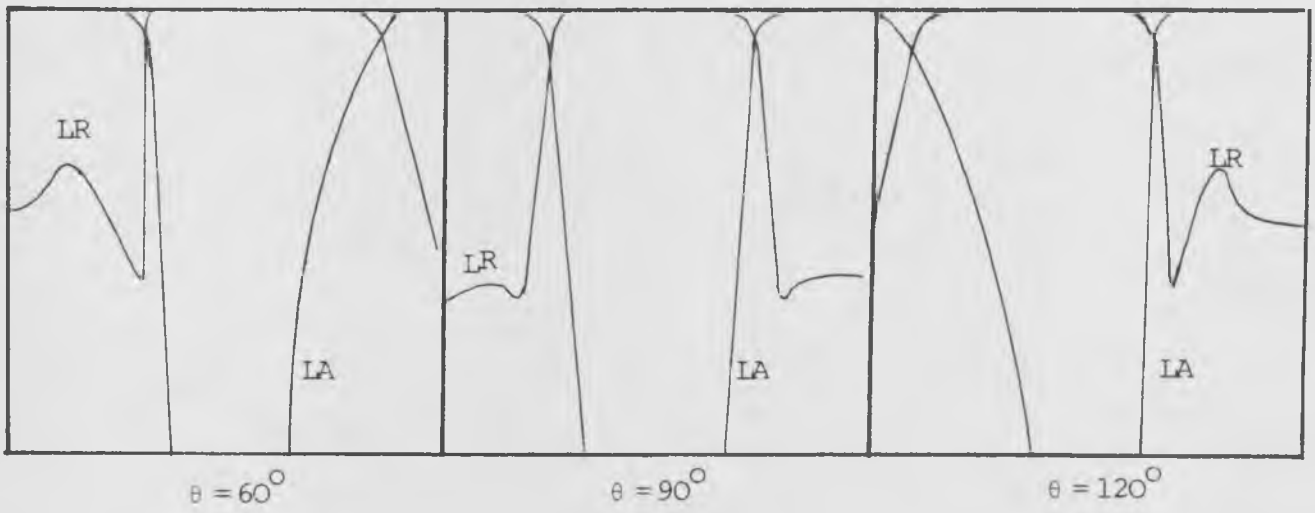

Fig. 2.2.20 The effect on bandstop filter performance of varying the phase shift between the resonators

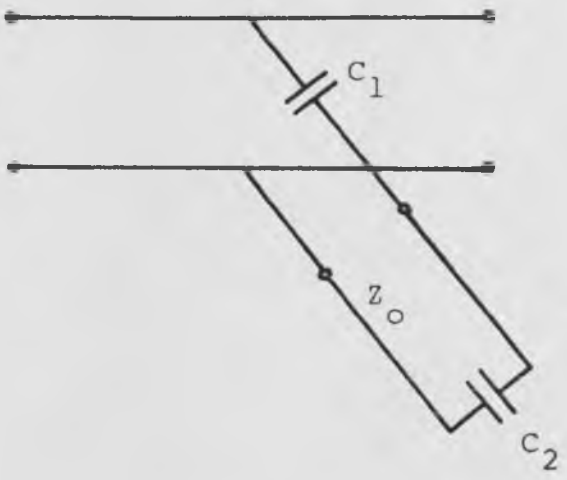

Fig. 2.2.21 Equivalent circuit of a tunable bandstop resonator

frequency, thus the impedance of the resonator will change more rapidly for frequencies above the transmission zero frequency than below it. This has the effect of making the frequency response of a basic resonator coupled to a main line more selective on the high side of the resonant frequency than below it. Thus since the resonators are inherantly assymmetric, the frequency response of a multistage bandstop filter with resonators coupled by 90^{o} phase shifters will also be assymetric.

In chapter three, a technique is constructed for evaluating the correct phase shift between the bandstop resonators to compensate for their inherent assymetry.

2.3 Tunable Microwave Bandpass Filters

There are many bandpass filters suitable for realisation in S.S.S. These include, for example, the combline filter [2.6], the interdigital filter [2.7] and the capacitive gap coupled transmission line filter [2.8]. An initial decision was made to avoid short circuited transmission lines in the S.S.S medium as these would contribute to the filter loss. The other major consideration was that varactor diodes and their bias filters must be easily incorporated into the circuit.

With the above considerations in mind the initial choice of filter was the S.S.S structure shown in Fig. 2.3.1. Basically, this filter is composed of open circuited transmission line resonators of between one quarter and one half wavelength long capacitively coupled to unit elements of transmission line. The

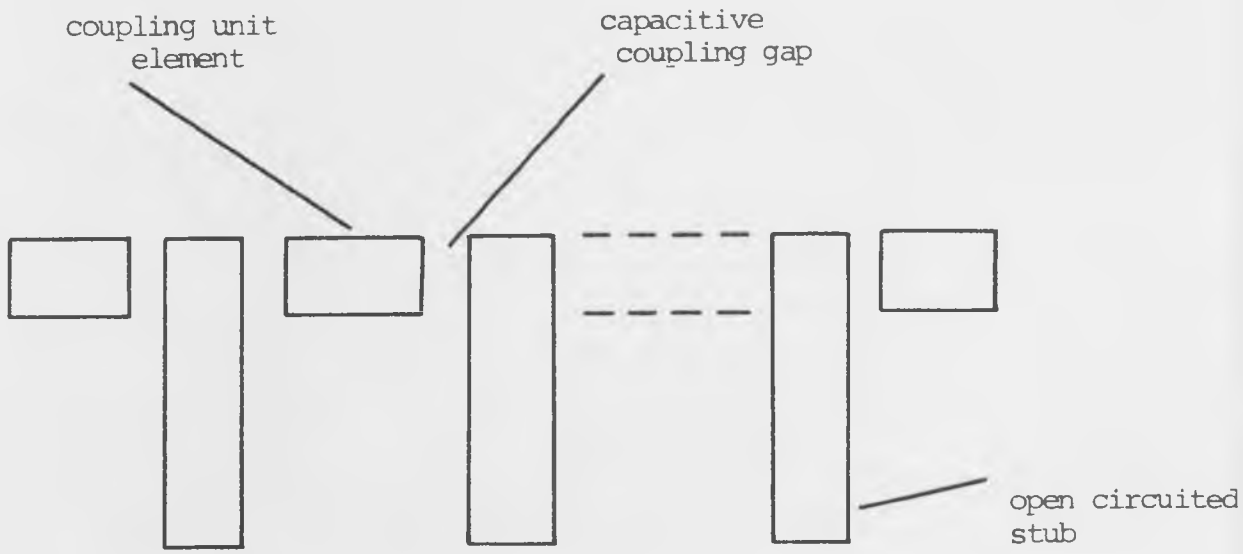

Fig. 2.3.1 Structure of S.S.S bandpass filter

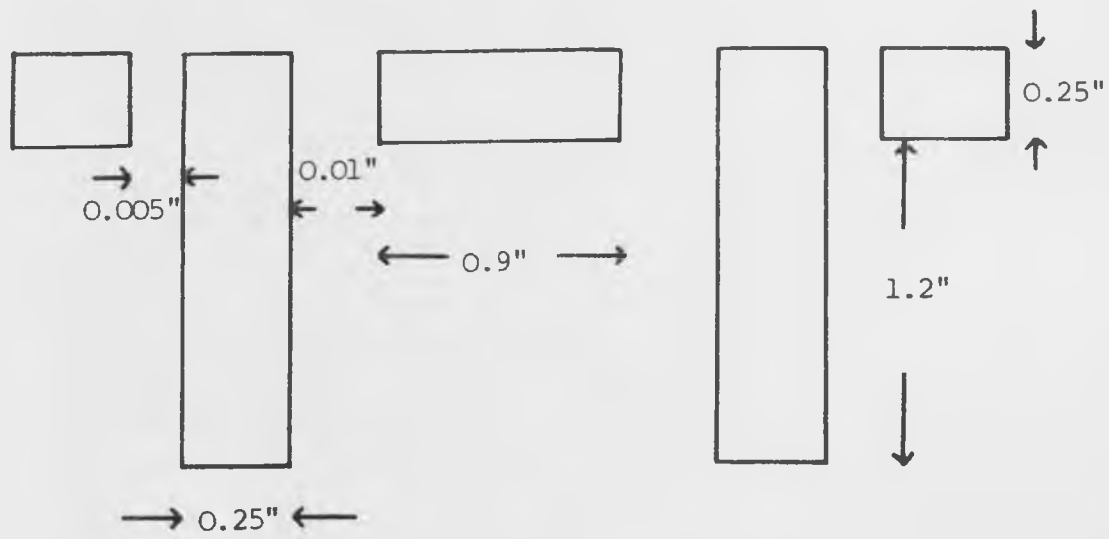

Fig. 2.3.2 Dimensions of two stage bandpass filter

equivalent circuit of this filter is not presented since exact design techniques are not discussed in this chapter.

A two resonator bandpass filter was constructed for the purpose of investigating the effects of tuning. The S.S.S circuit board layout of this filter is shown in Fig. 2.3.2. The resonators were designed to be 135^{o} long at passband centre and the unit element coupling the resonators was 75^{o} long. The capacitive gaps coupling the unit element to the resonators were made 0.01" wide as this was roughly the same value as that used for decoupling bandstop resonators in section 2.2. The measured performance of this filter is shown for two values of tuned frequency in Fig. 2.3.3. Tuning was achieved by capacitive tuning screws located over the ends of the resonators.

When tuned to 3.22 GHz the filter exhibited an acceptable frequency response with a passband return loss of 12.5 dB and a bandwidth of 43 MHz . The passband insertion loss was 1.8 dB which is comparable to coaxial filters of the same physical size. [The ground plane spacing was 0.3"]. However when the filter was tuned to 2.8 GHz the response deteriorated drastically with the dissipation loss becoming very high. This phenomenon is known as undercoupling [2.9] and is a result of the coupling between the resonators being highly dependent on frequency. A technique for overcoming this problem is developed in chapter four.

An attempt was made to varactor tune the two resonator bandpass filter. DC4373B varactors were used and they were decoupled by 0.5pF capacitors to increase their Q factor.

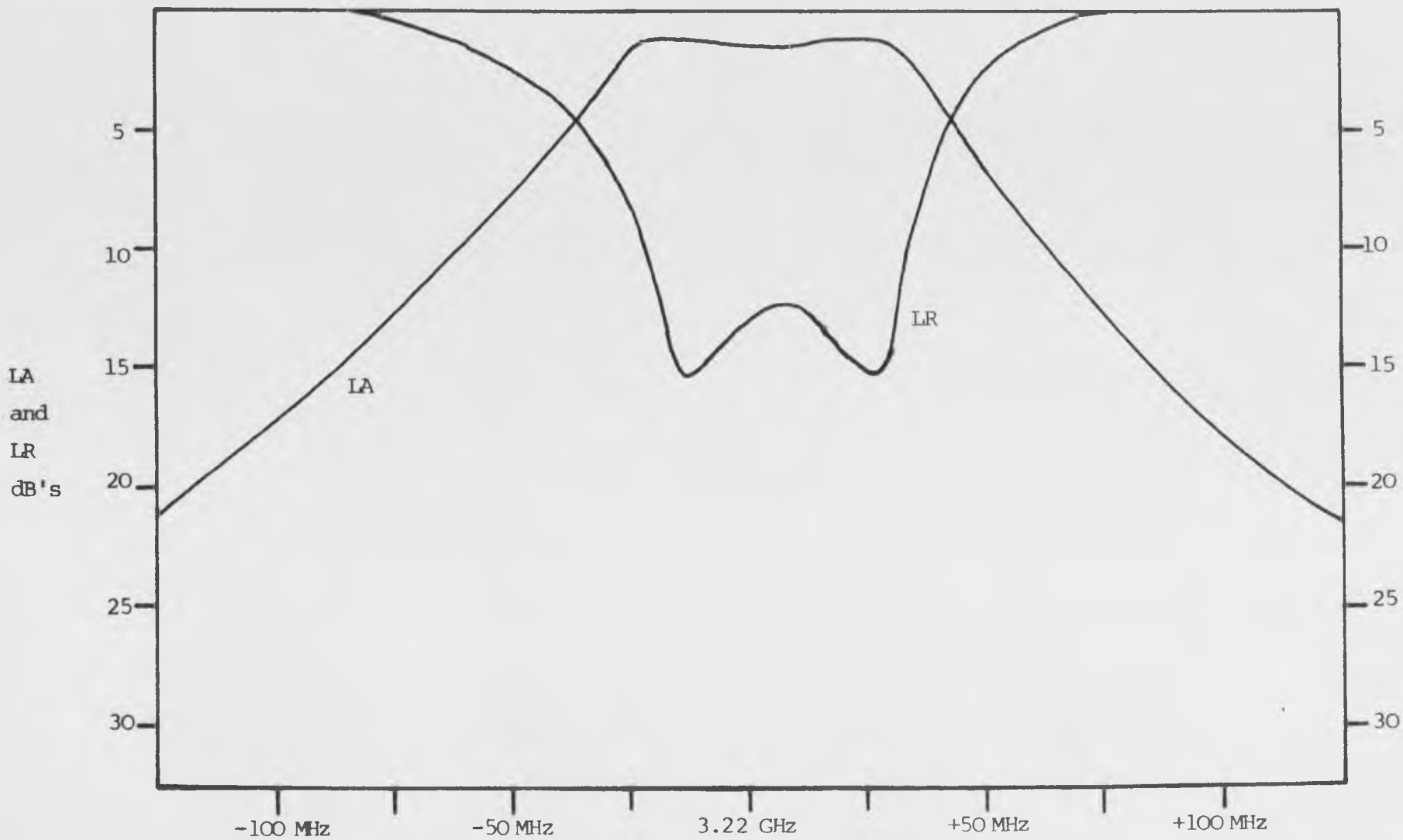

Fig. 2.3.3 a) Measured performance of 2 stage bandpass filter

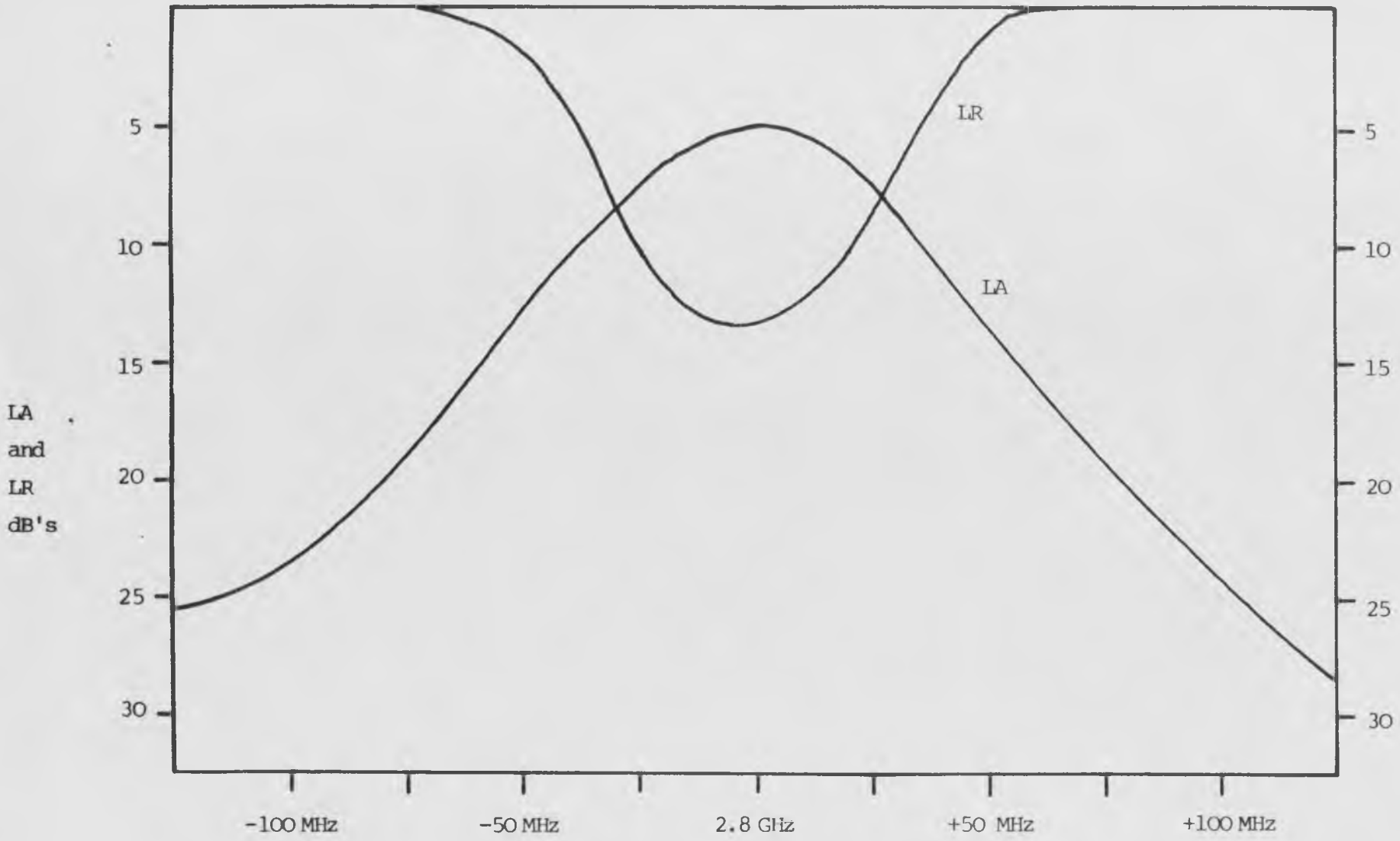

Fig. 2.3.3 b) Measured performance of 2 stage bandpass filter after tuning down in frequency

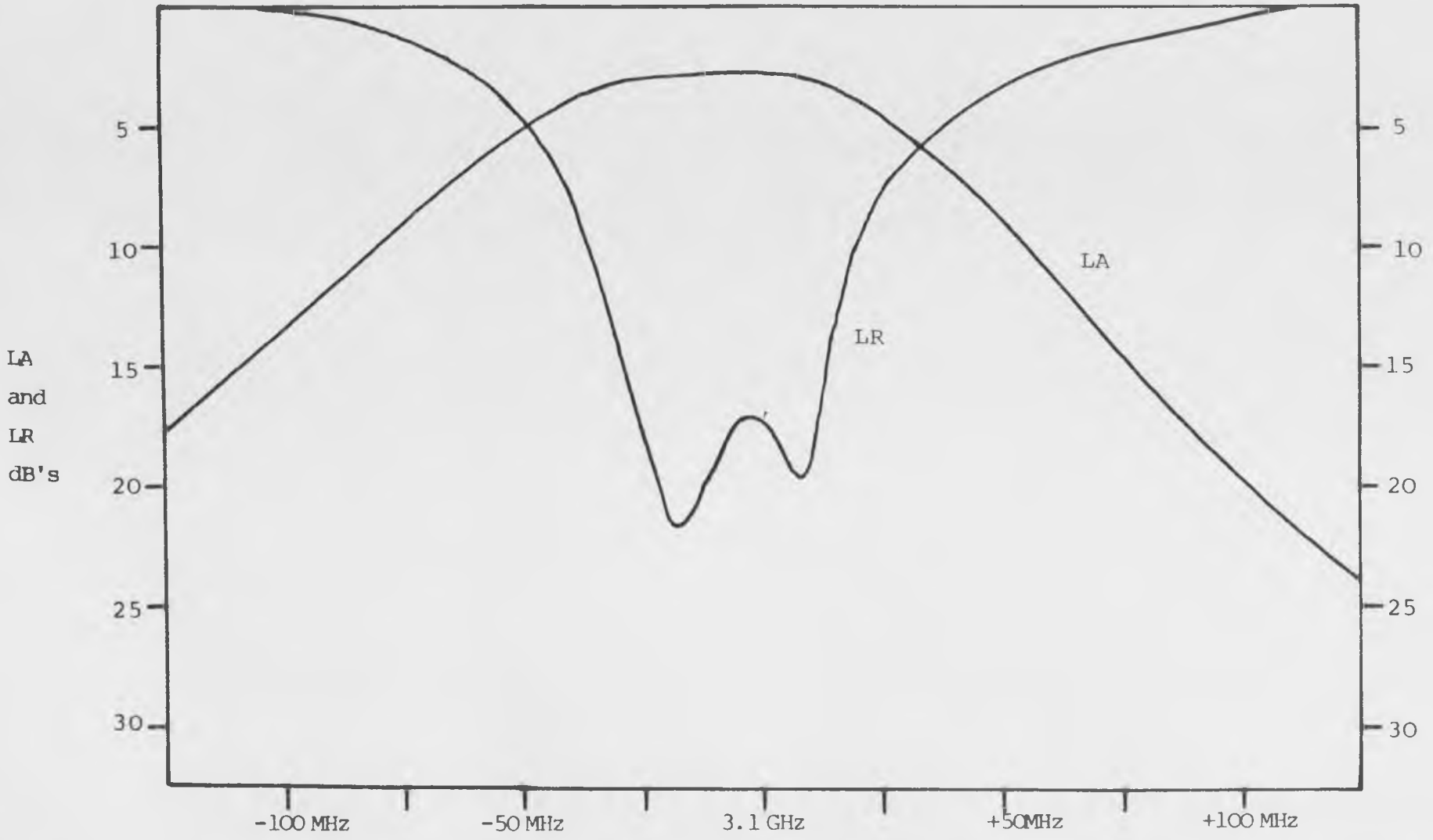

Fig. 2.3.4 Measured performance of varactor tuned bandpass filter at zero bias

The measured performance of this filter at zero bias is shown in Fig. 2.3.4. A passband insertion loss of 2.5dB and a tuning bandwidth of 8% were achieved. The frequency response of this filter deteriorated rapidly with tuning as expected but the loss performance at zero bias was encouraging and suggested that with a suitable filter design, useful low loss varactor tuned bandpass filters were feasible.

2.4 Conclusions

2.4.1 Varactor Loss

Experimental results show that low loss varactor tuned two section bandstop and bandpass filters can be constructed, and they will exhibit tuning bandwidths of approximately 10%. To improve upon these results it is necessary to use higher quality varactor diodes. All preceding work in this thesis involves the use of the Microwave Associates MA46620G varactor. This diode has a similar capacitance and capacitance variation to the AEI 4373B varactor but has an epitaxial layer resistance of only 1.25 Ω at zero bias. This corresponds to a 2.4 times increase in Q factor as compared with the AEI varactor.

In addition all the filters described in the remainder of this thesis were designed for 3dB bandwidths of at least 5%. Combined with the higher quality varactors this enables much broader tuning bandwidths to be achieved.

2.4.2 Circuit Design Techniques

All the filters described in this chapter were designed on a largely intuitive basis with the objective merely being to observe the effects of varactor loss and tuning on filter performance. Experimental results show that a technique for evaluating the correct phase shift between the resonators of bandstop filters is required and that a bandpass filter circuit suitable for broadband tuning must be developed. In addition since loss is a major cause of the deterioration of varactor tuned filter performance, techniques of predicting its effect must be developed.

References

2.1 'Coupled rectangular bars between parallel plates'
W.J. Getsinger
IRE. TRANS M.I.T. JAN 1962

2.2 'Microwave filters, impedance matching networks and coupling structures', pp168-172
Matthaei, Young and Jones, McGraw Hill

2.3 Ref 2.2 pp243-244

2.4 J.E. Dean, Ph.D. Thesis
Dept. of Electrical and Electronic Engineering
The University of Leeds

2.5 G.R. Dyer, Ph.D. Thesis
Department of Electrical and Electronic Engineering
The University of Leeds

2.6 Ref 2.2 pp497-505

2.7 Ref 2.2 pp614-625

2.8 Ref 2.2 pp440-450

2.9 Ref 2.2 pp663-668

Appendix 2.1

The graphs on the following pages show the even and odd mode fringing capacitances of coupled rectangular bars between parallel ground planes as a function of bar separation. They also show the coupling capacitance between the bars and the fringing capacitance from an isolated bar.

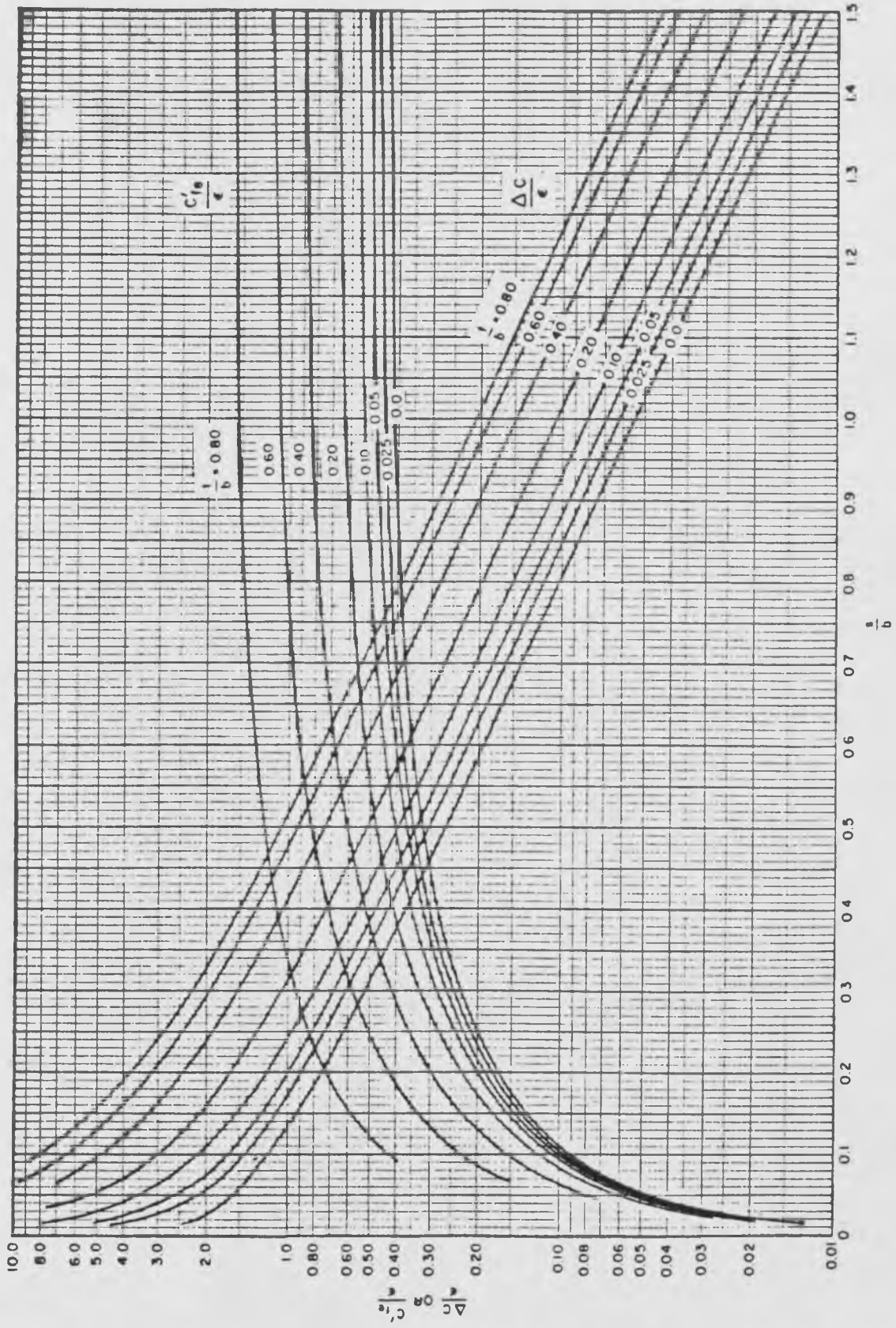

Even mode fringing capacitance and coupling capacitance between coupled rectangular bars

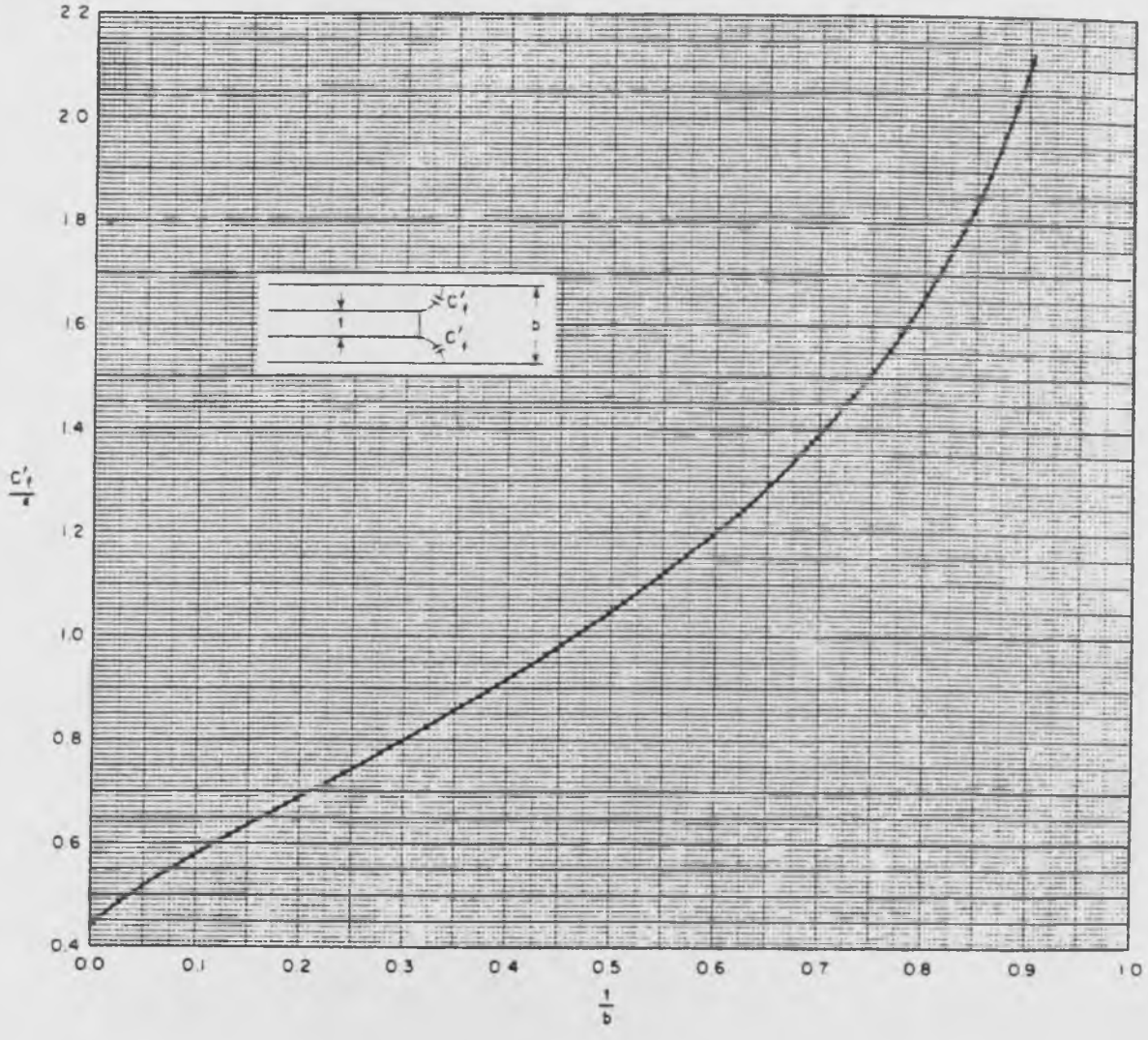

Fringing capacitance from an isolated rectangular bar

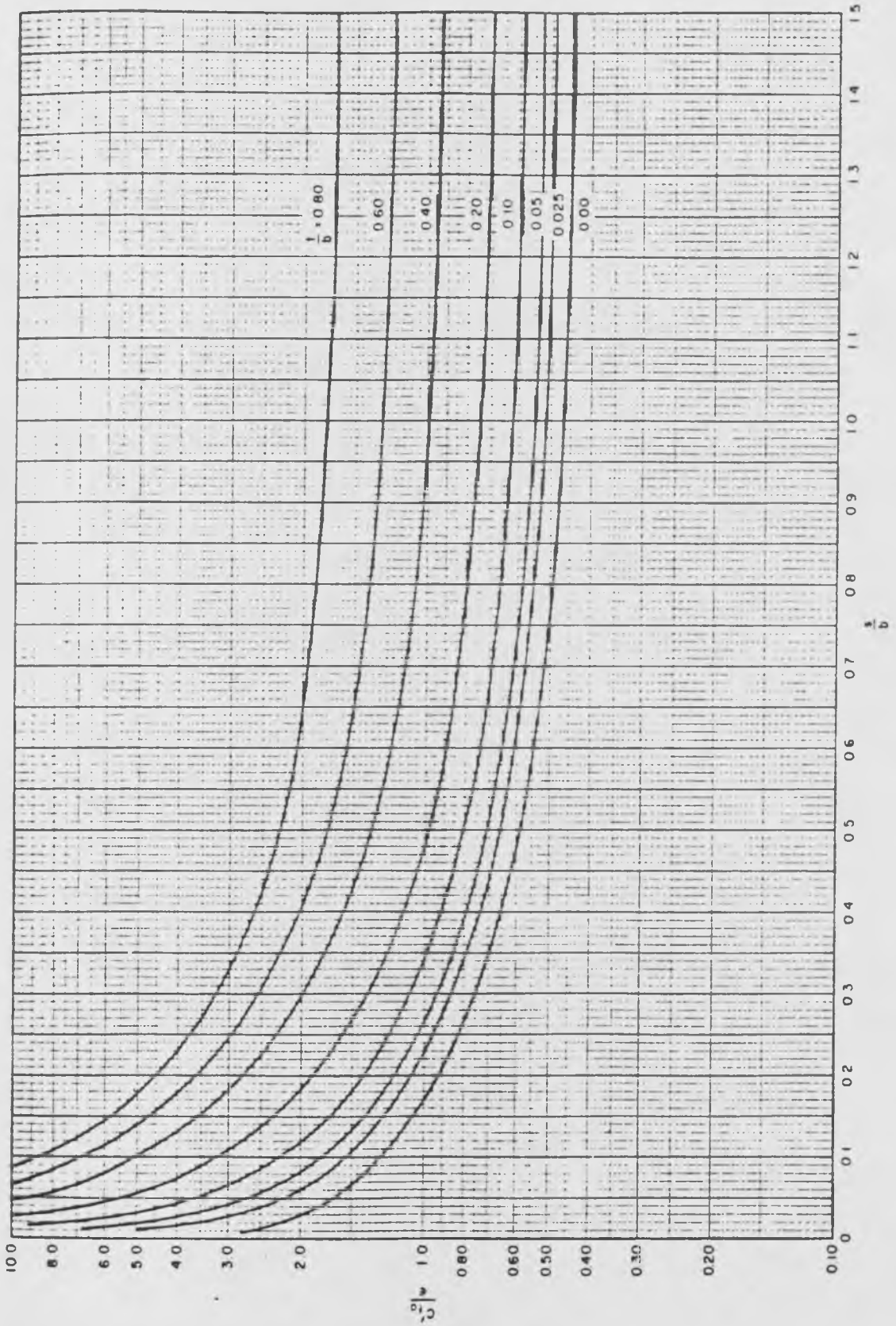

Odd mode fringing capacitance of coupled rectangular bars

3 TUNABLE MICROWAVE BANDSTOP FILTERS

3.1 Introduction

In chapter two it was shown that in order to achieve the optimum symmetrical bandstop filter response, it is necessary to couple the resonators with transmission lines of phase shift not equal to 90^{o}. In this chapter a design procedure has been developed which enables the correct phase shifts between resonators to be evaluated. Two fixed frequency S.S.S bandstop filters have been designed and constructed using this technique. Both filters were designed from an inverse Chebyshev prototype and had a centre frequency of 4 GHz and respective 40 dB stopband bandwidths of 1% and 10%. Both devices performed extremely well, exhibiting the required symmetrical frequency response, broad low V.S.W.R passbands and high levels of stopband insertion loss. A computer analysis program was developed to examine the effects of dissipation loss and the computed results showed excellent agreement with the measured performances.

A varactor tuned bandstop filter has been designed using the new procedure for computing the phase shifts between the filter resonators. In this case the optimum phase shift was chosen to be at the exact centre of the tuning bandwidth. The tunable filter was a three resonator device designed to tune from 3.5 GHz to 4.5 GHz with a 1% 20 dB stopband bandwidth. A computer analysis program has been developed in order that the effects of varactor loss can be predicted and the computed results agree closely with the measured performance of the varactor tuned filter.

3.2 Theory of Symmetrical Bandstop Filters

The equivalent circuit of the S.S.S bandstop filter is shown in Fig. 3.2.1. The input admittance of the rth resonator of this filter can easily be shown to be

$$Y_r(j\omega) = \frac{j[\omega Cl_r[Z_r \omega C2_r + \tan(a\omega)]]}{[\omega Z_r(Cl_r + C2_r) - \tan(a\omega)[Z_r^2 \omega^2 Cl_r C2_r - 1]]}$$

$Y_r(j\omega)$ possess a pole at ωp_r which corresponds to the rth transmission zero of the filter. $Y_r(j\omega)$ also posesses a zero at a frequency ωz_r, slightly higher than ωp_r. It is this zero which causes $Y_r(j\omega)$ to vary more rapidly at frequencies above ωp_r than below ωp_r and thus the resonator frequency response is asymmetric.

For frequencies close to ωp_r, $y_r(j\omega)$ can be approximated by the bilinear function below:

$$Y_r(j\omega) \simeq \frac{j(\omega - \omega z_r)}{K_r(\omega - \omega p_r)(\omega z_r - \omega p_r)} \qquad (3.2.2)$$

Differentiating 3.2.1 with respect to ω and evaluating at ωp_r we obtain

$$K_r = \frac{\partial}{\partial \omega}[1/Y_r(j\omega)]\Big|_{\omega=\omega p_r} \qquad (3.2.3)$$

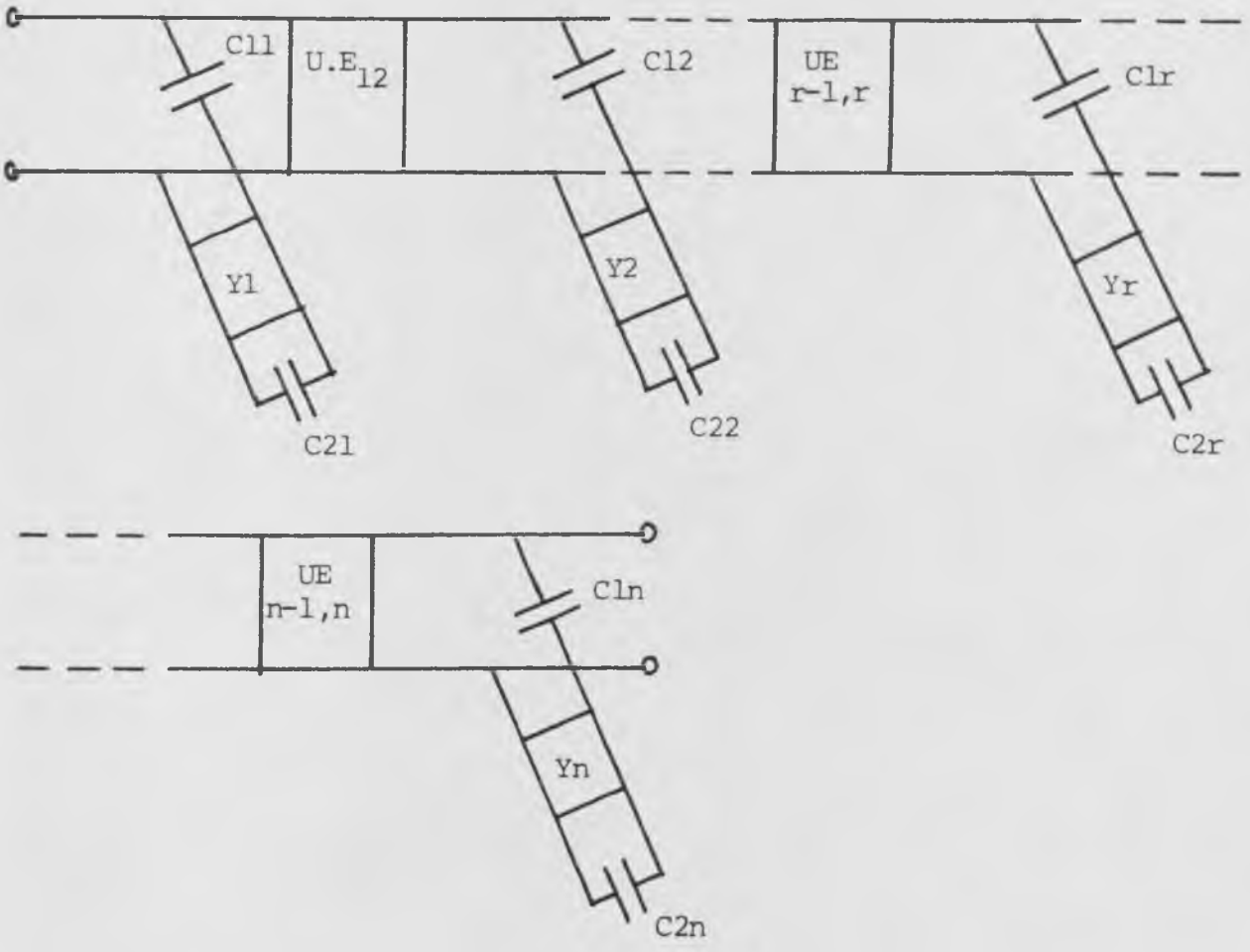

Fig. 3.2.1 The equivalent circuit of the S.S.S bandstop filter

$$K_r = \frac{a(1+\tan^2(a\omega p_r))(Z_r^2 C1_r C2_r \omega p_r^2 - 1) + 2\tan(a\omega p_r) Z_r^2 C1_r C2_r - Z_r(C1_r + C2_r)}{\omega p_r [Z_r \omega p_r C2_r + \tan(a\omega p_r)]} \qquad (3.2.4)$$

The values of ωz_r and ωp_r are obtained from the zeros of the numerator and denominator of 3.2.1 as below.

$$\tan(a\omega z_r)/\omega z_r = -Z_r C2_r \qquad (3.2.5)$$

$$\tan(a\omega p_r)[Z_r^2 \omega p_r^2 C1_r C2_r - 1] = \omega p_r Z_r [C1_r + C2_r] \qquad (3.2.6)$$

The expression 3.2.2 for $Y_r(j\omega)$ can be decomposed by extracting the residue at ωp_r to obtain

$$Y_r(j\omega) = jB_r - j/(\omega L_r - X_r) \qquad (3.2.7)$$

where

$$B_r = 1/K_r(\omega z_r - \omega p_r) \qquad (3.2.8)$$

$$L_r = K_r \qquad (3.2.9)$$

$$X_r = K_r \omega p_r \qquad (3.2.10)$$

$Y_r(j\omega)$ has thus been approximated by a resonator composed of an inductor and a frequency invarient reactance, which is shunted by another frequency invariant reactance. If the shunt reactance were removed from the resonator, the remaining resonator would possess a linear reactance as a function of

frequency and this would produce the required symmetrical filter response. Thus it is necessary to construct a technique to remove B_r from each resonator.

The resonator is now decomposed into the network shown in Fig. 3.2.2. The notation in Fig. 3.2.2 is as follows:

$$Y'_r(j\omega) = -jn_r^2(\omega L_r - X_r) \tag{3.2.11}$$

$$B_r = B'_r + B''_r \tag{3.2.12}$$

Applying this procedure to every resonator and coupling the rth and r+ith resonators via unity impedance phase shifters with phase shift $\theta_{r,r+1}$ we obtain the typical coupling network shown in Fig. 3.2.3 with the transfer matrix below

$$\begin{bmatrix} 1/n_r & 0 \\ 0 & n_r \end{bmatrix} \begin{bmatrix} 1 & 0 \\ jB''_r & 1 \end{bmatrix} \begin{bmatrix} \cos(\theta_{r,r+1}) & j\sin(\theta_{r,r+1}) \\ j\sin(\theta_{r,r+1}) & \cos(\theta_{r,r+1}) \end{bmatrix}$$

$$\begin{bmatrix} 1 & 0 \\ jB'_{r+1} & 1 \end{bmatrix} \begin{bmatrix} n_{r+1} & 0 \\ 0 & 1/n_{r+1} \end{bmatrix} \tag{3.2.13}$$

After multiplying out 3.2.13 to form a single matrix we obtain

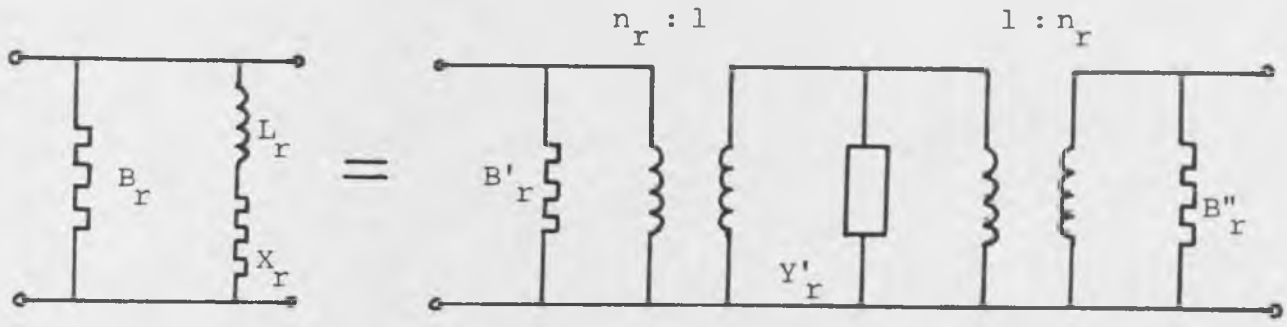

Fig. 3.2.2 Decomposition of the basic bandstop resonator

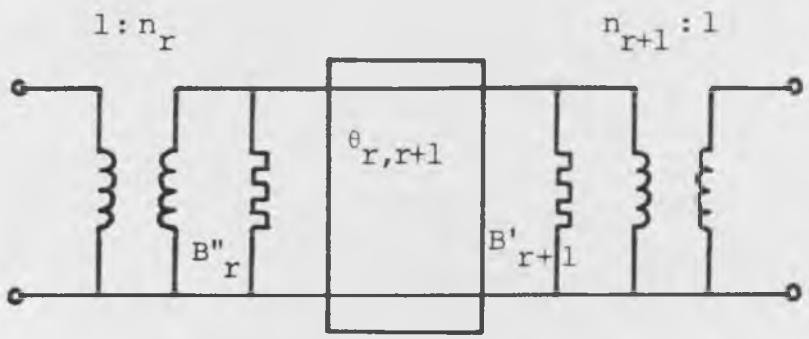

Fig. 3.2.3 The typical coupling network between the resonators of the bandstop filter

$$\begin{bmatrix} \frac{n_{r+1}}{n_r}\left[\cos(\theta_{r,r+1}) - \beta'_{r+1}\sin(\theta_{r,r+1})\right] & \frac{j\sin(\theta_{r,r+1})}{n_r n_{r+1}} \\ jn_r n_{r+1}\left[B''_r[\cos(\theta_{r,r+1}) - B'_{r+1}\sin(\theta_{r,r+1})\right] & \frac{n_r}{n_{r+1}}\begin{bmatrix}\cos(\theta_{r,r+1}) \\ -B''_r\sin(\theta_{r,r+1})\end{bmatrix} \end{bmatrix} \qquad (3.2.14$$

This matrix can be equated to that of an ideal admittance inverter under the condition that

$$\cos(\theta_{r,r+1}) = B''_r\sin(\theta_{r,r+1}) = B_{r+1}'\sin(\theta_{r,r+1}) \qquad (3.2.15)$$

The admittance of the inverter is

$$K_{r,r+1} = n_r n_{r+1}/\sin(\theta_{r,r+1}) \qquad (3.2.16)$$

The initial conditions are

$$n_1 = 1 \quad \text{and} \quad B'_1 = 0 \qquad (3.2.17)$$

Provided that the above conditions are satisfied the elements B_r in each resonator have now been absorbed into the phase shifters thus forming ideal impedance inverters between the resonators.

The design equations for the symmetrical bandstop

filter can now be developed. The design is based on the inverse Chebyshev bandstop prototype filter shown in Fig. 3.2.4. This prototype is derived from the inverse Chebyshev natural highpass prototype filter using the slope reactance parameter technique [3.1]. The bandstop prototype element values are given by the following equations:-

$$L_r = \frac{2\alpha + \cos(\theta_r)}{4\omega_o \eta \sin(\theta_r)} \qquad (3.2.18)$$

$$C_r = \frac{4\eta \sin(\theta_r)}{\omega o(2\alpha - \cos(\theta_r))} \qquad (3.2.19)$$

with

$$\omega_o = \sqrt{\omega_1 \omega_2} \qquad (3.2.20)$$

$$\alpha = \omega_o/(\omega_2 - \omega_1) \qquad (3.2.21)$$

$$\theta_r = (2r-1)\pi/2n \qquad (3.2.22)$$

$$n \geq \frac{L_A + L_R + 6}{20 \operatorname{Log}(S + \sqrt{S^2-1})} \qquad (3.2.23)$$

$$\eta = \sinh[\tfrac{1}{h} \sinh^{-1}(1/\varepsilon)] \qquad (3.2.24)$$

$$\varepsilon = [10^{(LA/10)} - 1]^{-\frac{1}{2}} \qquad (3.2.25)$$

where

ω_1 and ω_2 are the prescribed stopband edge frequencies

LA is the stopband insertion loss at ω_1 and ω_2

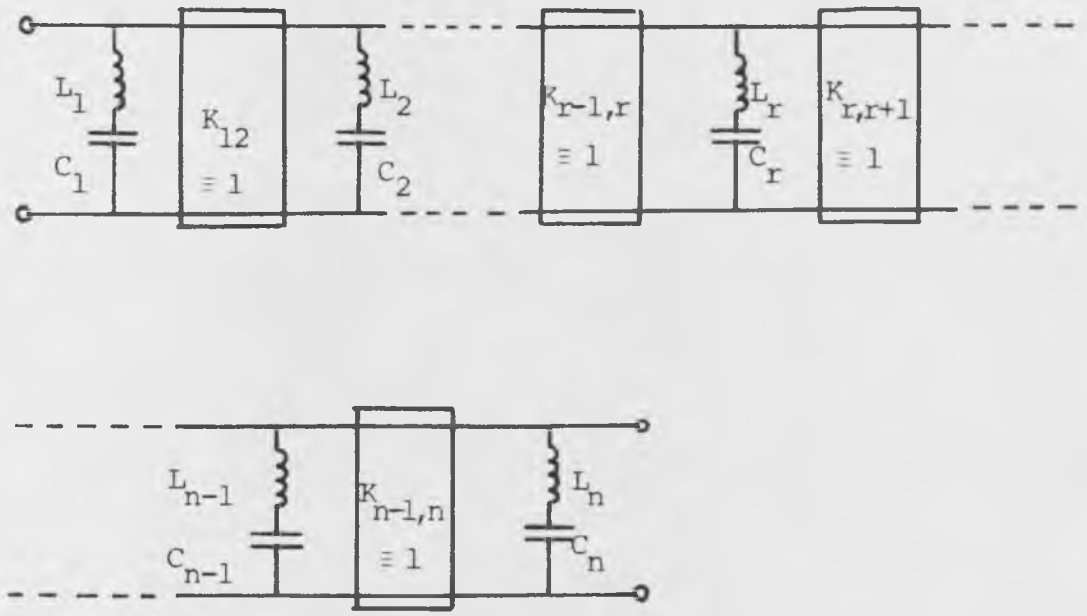

Fig. 3.2.4 The Inverse Chebyshev prototype bandstop filter

LR is the return loss at the passband edge frequencies.

S is the ratio of the passband to stopband bandwidths.

The resonant frequencies and bandwidths of the prototype resonators are given by

$$\omega o_r = \frac{1}{\sqrt{L_r C_r}} \tag{3.2.26}$$

$$\Delta\omega_r = \frac{1}{2L_r} \tag{3.2.27}$$

In order to obtain the element values for the microwave resonators, the expressions for their central frequencies and bandwidths must be equated with the values obtained from 3.2.26 and 3.2.27. Thus from 3.2.6 with ωp_r equal to ωo_r we obtain

$$\tan(a\omega o_r)[Z^2_r \omega o_r^2 C1_r C2_r - 1] = \omega o_r Z_r [C1_r + C2_r] \tag{3.2.28}$$

The bandwidth of the rth resonator can easily be shown to be to a good approximation

$$\Delta\omega_r = [\frac{\partial}{\partial\omega}[1/Y_r(j\omega)]]^{-1} \Big|_{\omega = \omega o_r} \tag{3.2.29}$$

Thus from 3.2.3 and 3.2.29 we have

$$\Delta\omega_r = K_r \tag{3.2.30}$$

From 3.2.4 and 3.2.30 we obtain

$$\Delta\omega_r = \frac{\omega o_r Cl_r [Z_r \omega o_r C2_r + \tan(a\omega O_r)]}{a(1+\tan^2(a\omega o_r))[Z_r^2 \omega o_r^2 Cl_r C2_r - 1] + 2\tan(a\omega o_r) Z_r^2 \omega o_r Cl_r C2_r - Z_r(Cl_r + C2_r)} \qquad (3.2.31)$$

To obtain the resonator element values, firstly any one of the variables Z_r, Cl_r and $C2_r$ can be prescribed to have a known value equal for all r, equations 3.2.28 and 3.2.31 can then be solved simultaneously for the remaining variables. This procedure can easily be achieved numerically, using for example, the Newton-Raphson procedure [3.2].

The phase shifts between the resonators at the stop-band centre frequency can now be evaluated. Firstly, remembering that the rth resonator has been scaled by a factor n_r^2, we obtain

$$K_r = n_r^2 / \Delta\omega_r \qquad (3.2.32)$$

Then compute ωz_r from

$$\omega z_r / \tan(a\omega z_r) = -1/(Z_r C2_r) \qquad (3.2.33)$$

which can easily be solved numerically.

Next we obtain B_r from

$$B_r = 1/K_r(\omega z_r - \omega p_r) \qquad (3.2.34)$$

with

$$B_r = B'_r + B''_r \qquad (3.2.35)$$

And

$$B_{r+1}' = B_r' \tag{3.2.36}$$

Rearranging 3.2.15 we obtain the phase shift between the resonators.

$$\theta_{r,r+1} = \cot^{-1}(B_r'') \tag{3.2.37}$$

From 3.2.16 with $K_{r,r+1} = 1$ (for the inverse Chebyshev prototype) the recurrence formulae for the scaling factors n_r are obtained.

$$n_{r+1} = \sin(\theta_{r,r+1})/n_r \tag{3.2.38}$$

With initial conditions

$$n_1 = 1 \tag{3.2.39}$$

$$B_1' = 0 \tag{3.2.40}$$

In summary, we apply 3.2.18 to 3.2.31 to obtain the resonator element values and then calculate the phase shifts from 3.2.32 to 3.2.40.

It is of importance to note that the scaling procedure used in this design process will modify the bandwidths of the resonators. However, the change in bandwidth is negligible. This is because the correct phase shift between the resonators is always greater than 75^{o} in practice, and from 3.2.38 we have

$$n_r \cdot n_{r+1} = \sin(\theta_{r,r+1})$$

Thus for $\theta_{r,r+1} > 75^{o}$ then

$$n_r \cdot n_{r+1} > 0.966$$

The effect of the scaling factors on the resonator bandwidths is thus of little importance.

3.3 Design of Fixed Frequency Symmetrical Bandstop Filters

3.3.1 Specifications of the filters

Two S.S.S bandstop filters were designed to the following specifications.

Design 1

Centre frequency	4 GHz
Minimum stopband ripple level	40 dB
Stopband bandwidth	40 MHz
20 dB return loss bandwidth	66 MHz

Design 2

Centre frequency	4 GHz
Minimum stopband ripple level	40 dB
Stopband bandwidth	400 MHz
20 dB return loss bandwidth	660 MHz

The physical design and construction of each of these filters was very similar, thus only Design 1 which is the more important, narrowband specification is presented in detail.

3.3.2 Physical Design of the Bandstop Filters

Design 1

The theoretical design process described in section 3.2 enables one set of the resonator element values, $C1_r$, $C2_r$ and Z_r to be prescribed. In the case of fixed frequency filters it is not necessary for the tuning capacitors to be equal, thus equations 3.2.28 and 3.2.31 should be solved simultaneously for $C1_r$ and $C2_r$. In the particular case of this design which is for a 1% stopband bandwidth at 4 GHz there was no real need to solve for $C1_r$ since the 3 dB bandwidths of the resonators could be used directly to obtain the coupling gaps from the resonators to the main line from Fig. 2.1.9.

The phase lengths of the resonators used in this filter were designed to be 160° at 4 GHz and the resonator characteristic impedances were all chosen to be 50 Ω. The method described in section 3.2 was then applied to calculate the 3 dB bandwidths of the resonators and the phase shifts between them. This procedure also evaluated the values of the tuning capacitors $C2_r$, these were all found to be less than 0.25pF which are easily realisable using capacitive tuning screws. The values of the resonator bandwidths and the phase shifts between them are shown in Fig. 3.3.1.

The conversion from electrical to physical parameters is now easily performed. First, a ground plane spacing of 0.15" was chosen, previous results indicated that this would

Resonator number	1	2	3	4	5	6	7
Bandwidth of resonator MHz	9	25	35	40.5	35	25	9
ψ r,r+1	84.6	87.4	83.7	83.7	87.4	84.6	

Fig. 3.3.1 The computed values of the bandwidths of the phase shifts between the resonators of the narrow band bandstop filter

give a reasonable value of resonator Q factor.

Secondly from Fig. 3.3.1 and Fig. 2.1.9 the coupling gaps between the resontors and the main line are obtained.

The widths of the 50 Ω resonators in a 0.15" deep cavity were calculated to be 0.213" using the method described in section 2.1.2.

The physical lengths of the main line separating the resonators are calculated as follows.

At the stopband centre frequency ωo, we have

$$\psi_{r,r+1} = \frac{\omega o Lm}{c} \qquad (3.3.1)$$

where

Lm = length of main line between resonators

c = velocity of electromagnetic propogation in air.

The reference plane locations between the resonators must also be taken into account in this calculation. From 3.3.1 and Fig. 2.2.17 we have

$$Lm' = \frac{c\psi_{r,r+1}}{\omega o} + \frac{w_r}{10} + \frac{w_{r+1}}{10} \qquad (3.3.2)$$

where

w_r = width of rth resonator

Equation 3.3.2 enables the calculation of the exact required length of main line between the centre lines of the resonators.

The phase lengths of the resonators were all required to be 160^o at 4 GHz. This corresponds to a physical length

of 1.319". The reference plane locations of the resonators due to fringing at one end and the discontinuity at the coupling region must be taken into account. From 2.1.14 the required physical length of each resonator is

$$LRES_r = 1.319" - u_r - 0.23b - \frac{wm}{4} \qquad (3.3.3)$$

where

u_r = the width of the rth coupling gap
w_m = the width of the main line
b = the ground plane spacing

The main line was to be located at a distance 0.05" from the inner side wall of the S.S.S housing, the width of this line after allowing for the increase in fringing capacitance to the side wall, was calculated using the method described in section 2.1.2 and was

$$wm = 0.209"$$

The lengths of the resonators were thus

$$LRES_r = 1.232" - u_r \qquad (3.3.4)$$

The physical layout of the S.S.S circuit board for the bandstop filter is shown in Fig. 3.3.2.

Design of the housing for the bandstop filter

The design of the S.S.S housing was very similar to that described in chapter 2. The major difference was that

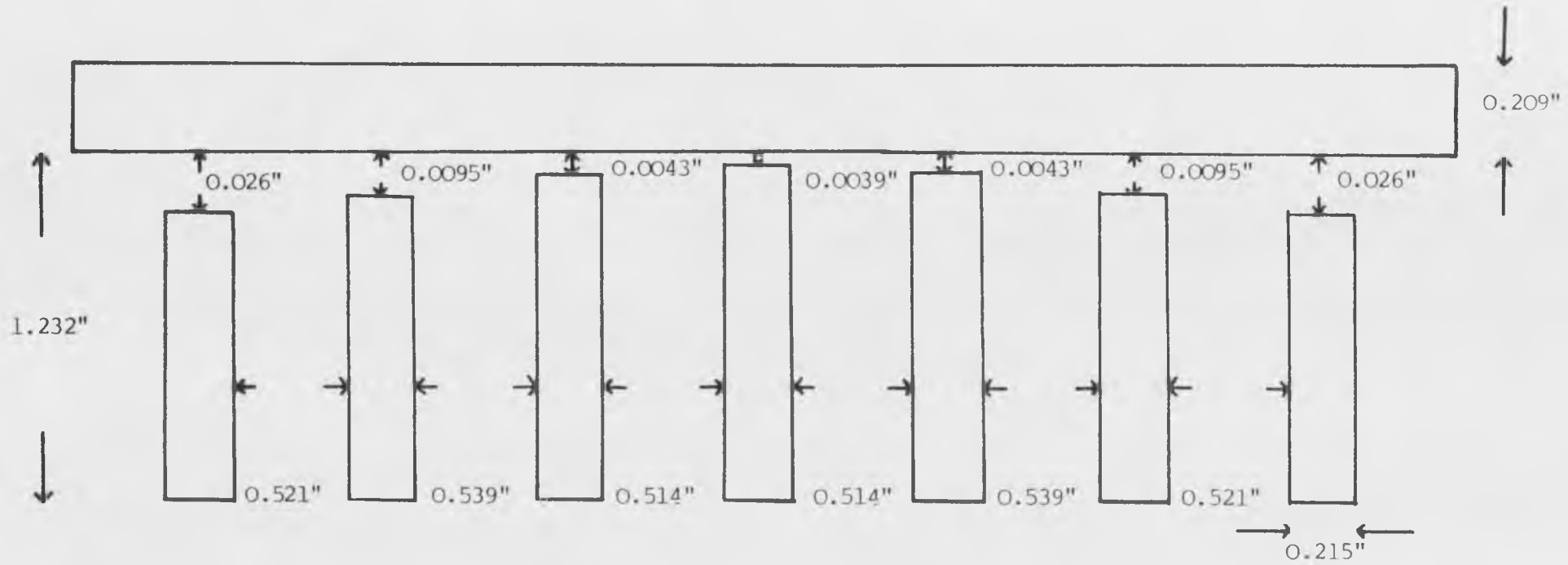

Fig. 3.3.2 The dimensions of the circuit board of the narrow band bandstop filter

due to the length of the housing, spurious mode propogation could be a severe problem. The actual length of the interior of the housing was 5.11". This would enable a TE_{101} mode to resonate at 3.65 GHz. To overcome this problem, inductive posts were inserted between the resonators, so that the top of the housing was electrically connected to the bottom [Fig. 3.3.3]. These posts were approximately one quarter wave length apart at 4 GHz and would raise the box resonant frequency to 8.71 GHz.

Tuning screws were located in the top of the housing so that they were over the ends of the resonators. An important practical point to note is that these screws were positioned adjacent to nylon plugs, this gave them more rigidity and made fine tuning relatively simple.

The S.S.S housing was copper plated to reduce its loss and the assembled filter is shown in photograph no 1.

Design 2

The only significant difference between this design and design 1 was that the larger bandwidth of the filter resulted in values of coupling capacitors Cl_r to the main line which were too large to be realised with practical values of coupling gaps. To overcome this problem it was necessary to print the resonators on opposite sides to and overlapping the main line [Fig. 3.3.4]. The coupling capacitors were then realised by parallel plates. No exact procedure is known for calculating the overlap required to produce a desired capacitance. In practice the capacitor was assumed to be a

Photograph no. 1

4 GHz Bandstop Filter

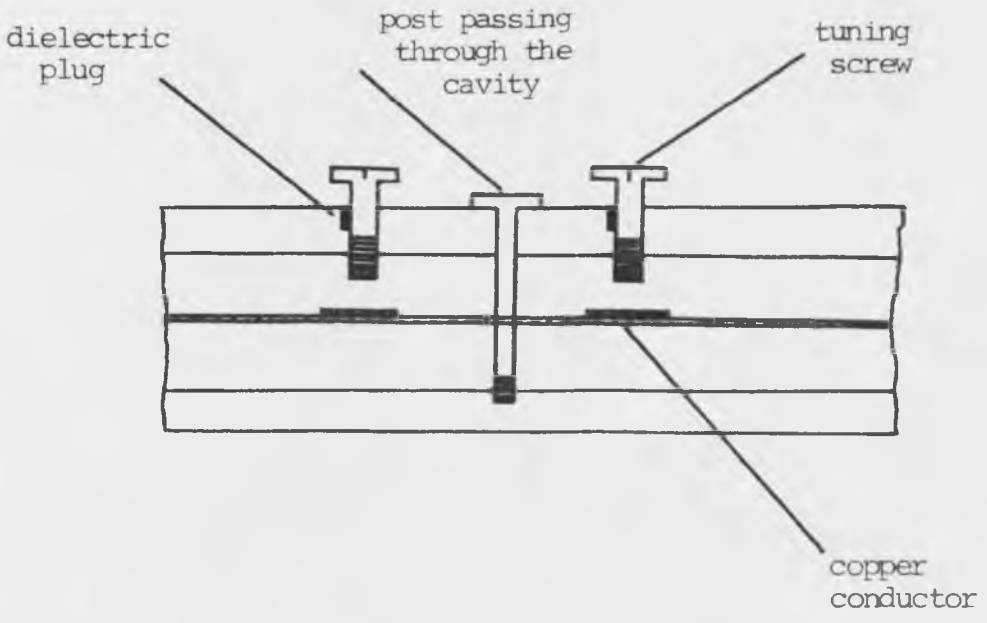

Fig. 3.3.3 Showing the method of suppressing higher ordered modes in the bandstop filter

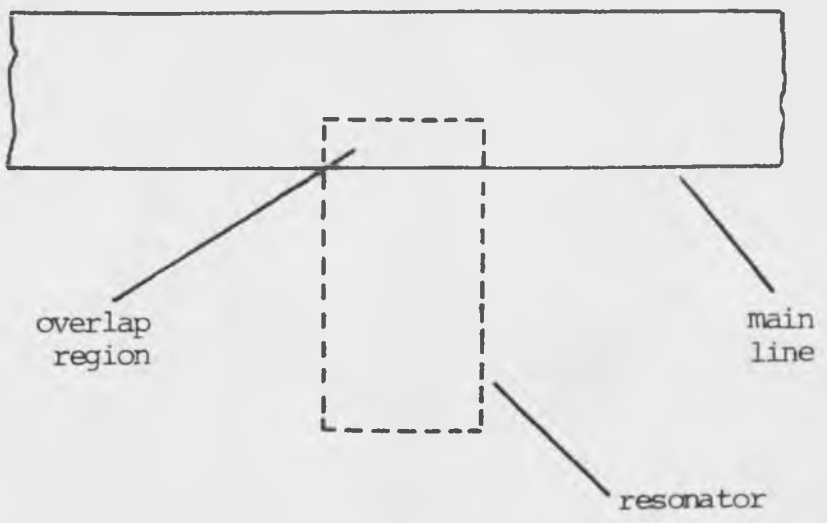

Fig. 3.3.4 Overlapping capacitor realisation of large capacitance

a simple parallel plate capacitor through the dielectric circuit board [εr = 2.22] and an increase in capacitance of 50% due to fringing was assumed. The details of the design of this filter are not presented because of the similarity to design 1.

3.3.3 Measured Performances of the Bandstop Filters

The measured frequency responses of the two bandstop filters are shown in Figs 3.3.5 and 3.3.6. The performances are summarised below.

Design 1

Stopband centre frequency	4 GHz
1 dB stopband bandwidth	90 MHz
3 dB stopband bandwidth	62.5 MHz
40dB stopband bandwidth	40 MHz
Mid-stopband return loss	1 dB
Minimum passband return loss	14 dB to 7 GHz

Design 2

Stopband centre frequency	4 GHz
1 dB stopband bandwidth	670 MHz
3 dB stopband bandwidth	600 MHz
40 dB stopband bandwidth	400 MHz
Mid-stopband return loss	0.4 dB
Minimum passband return loss	14 dB to 7 GHz

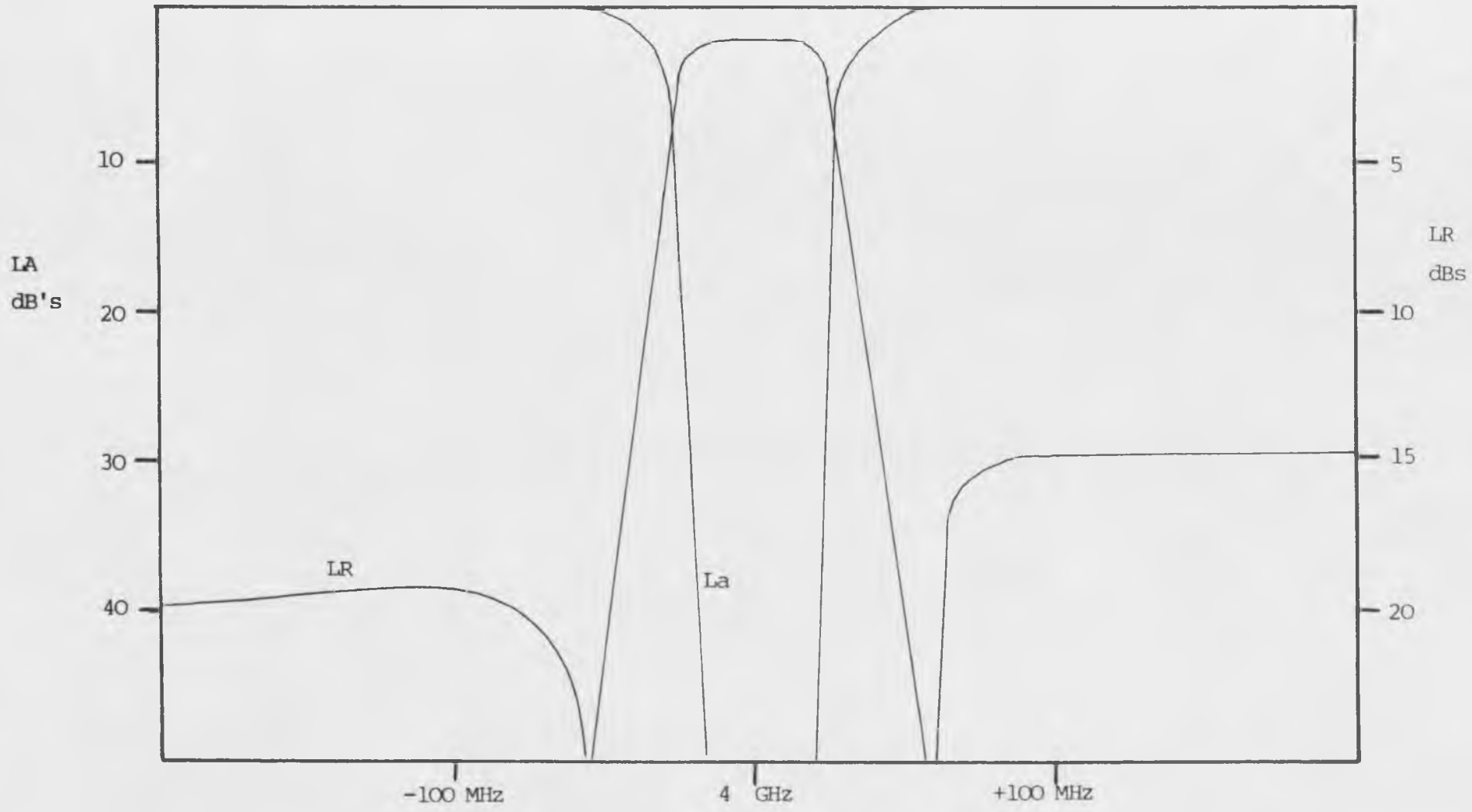

Fig. 3.3.5 Measured performance of narrowband bandstop filter

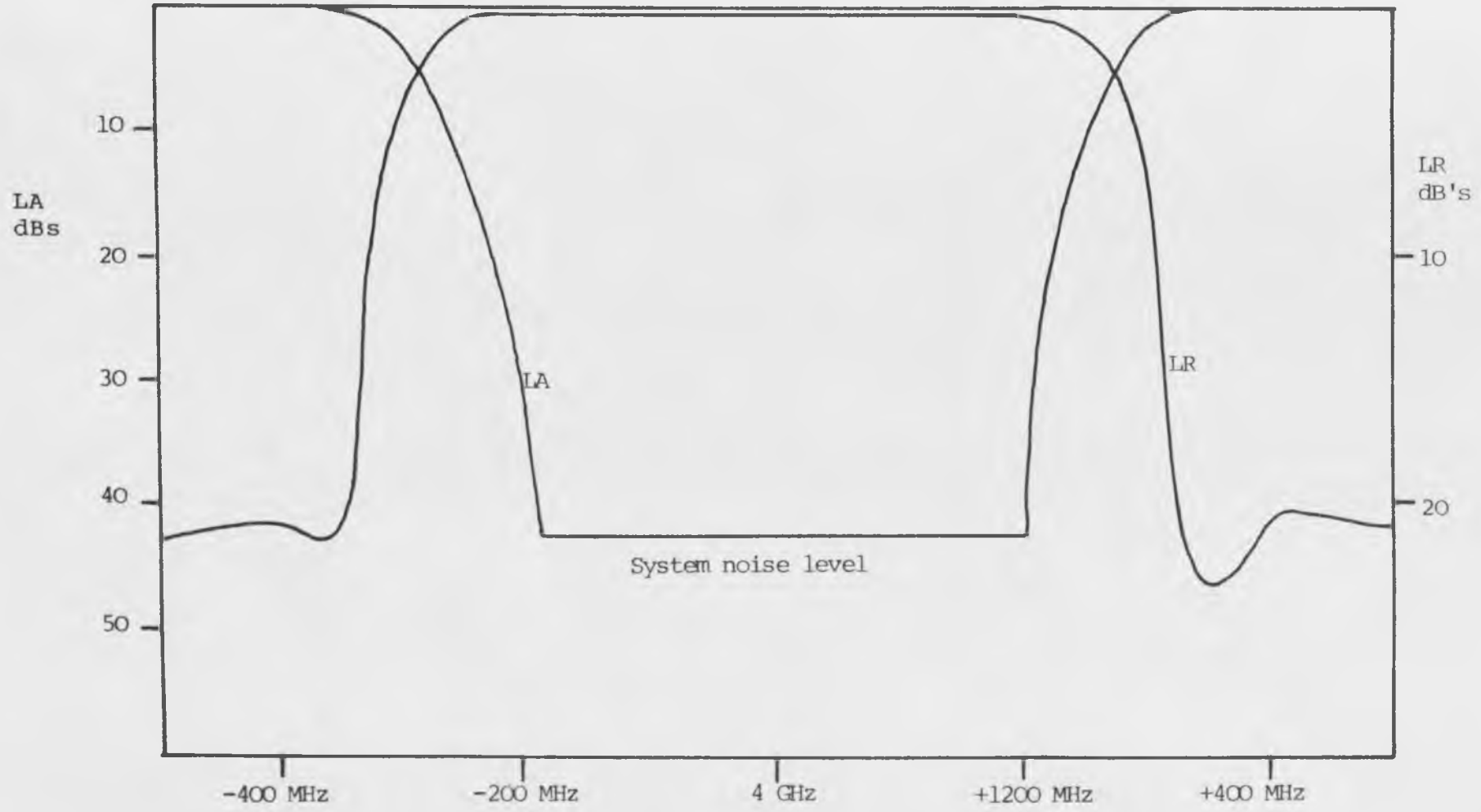

Fig. 3.3.6 Measured performance of 10% bandwidth bandstop filter

Both filters exhibited the required symmetrical frequency response and a high passband return loss. The good passband return loss was a consequence of using a straight through transmission line for coupling the resonators. The 10% bandwidth filter exhibited almost the exact designed specification. However the 1% bandwidth filter suffered from a reduction of selectivity due to the finite Q factor of the S.S.S medium. The designed passband to 40 dB stopband ratio of this filter was 1.66:1, in practice, the 1 dB to 40 dB ratio was 2.25:1 and the 3 dB to 40 dB ratio was 1.5:1. The selectivity of this filter could be increased by increasing the ground plane spacing, thus increasing the resonator Q factors. However, there is obviously a limit beyond which it is not practicable to increase the ground plane spacing. For example, consider the case of a filter with 50 Ω resonators. The width of the resonators is given by

$$w = \frac{b}{4}\left[\frac{c}{\varepsilon} - \frac{4cf'}{\varepsilon}\right] \qquad (3.3.5)$$

For 50 Ω resonators $c/\varepsilon = 7.54$ and for large ground plane spacings $\frac{cf'}{\varepsilon} = 0.45$, thus

$$w = 1.43\,b \qquad (3.3.6)$$

The phase shift between the resonators must be approximately 90^{o} and the physical distance between the edges of the resonators is

$$s = 39.3\,\frac{\pi}{2}\,\frac{c}{\omega_o} - 1.43\,b \qquad (3.3.7)$$

where c is the velocity of electromagnetic propogation in air and s and b are in inches.

The value of s must have a minimum value since if the resonators are too close to each other there will be significant coupling between them. Experimental results have shown that the value of s should satisfy the inequality

$$s > 0.3b \qquad (3.3.8)$$

Tesets on filters not satisfying this inequality show that the stopband response may deteriorate to the point of becoming an all pass response.

From 3.3.7 and 3.3.8 we obtain

$$b\omega o < 1.07 \times 10^{10} \qquad (3.3.9)$$

Thus for a stopband centre frequency of 4 GHz we obtain

$$b < 0.425"$$

It is important to note that the impedances of the resonators could be increased beyond 50 Ω, this would reduce their width and thus the ground plane spacing could be increased. However the Q factor of S.S.S transmission lines decreases linearly with impedance and thus no advantage would be gained from doing this.

3.3.4 Computer Analysis of S.S.S Fixed Frequency Filters

A computer program was written to analyse the effect of resistive loss on the performance of fixed frequency S.S.S

bandstop filters. In this program the main line and resonator transmission lines were represented by the general transfer matrix for a lossy transmission line, which is

$$\begin{bmatrix} \cosh(\gamma L) & Z_o \sinh(\gamma L) \\ Y_o \sinh(\gamma L) & \cosh(\gamma L) \end{bmatrix} \tag{3.3.10}$$

where to a good approximation for low loss lines [3.3]

$$\gamma = \alpha + j\beta \tag{3.3.11}$$

$$\alpha = \beta/2Q_c \tag{3.3.12}$$

$$\beta = \omega/c \tag{3.3.13}$$

Q_c is the quality factor of the S.S.S transmission lines contributed by conductor losses [Fig. 3.3.7]. [3.4] The dielectric losses of the S.S.S lines were assumed to be insignificant.

The computed response of the 1% bandwidth filter described in section 3.3.3 is shown in Fig. 3.3.8, this shows excellent agreement with the measured performance of the filter.

Because of the close agreement between the computed and measured performance of the bandstop filter, it was possible to use the program to predict the performance of any S.S.S bandstop filter. Fig. 3.3.9 shows the 1 dB to 40 dB and 3 dB to 40 dB bandwidth ratios of bandstop filters from degree 5 to degree 9, with bandwidths from 0.5% to 5%. This

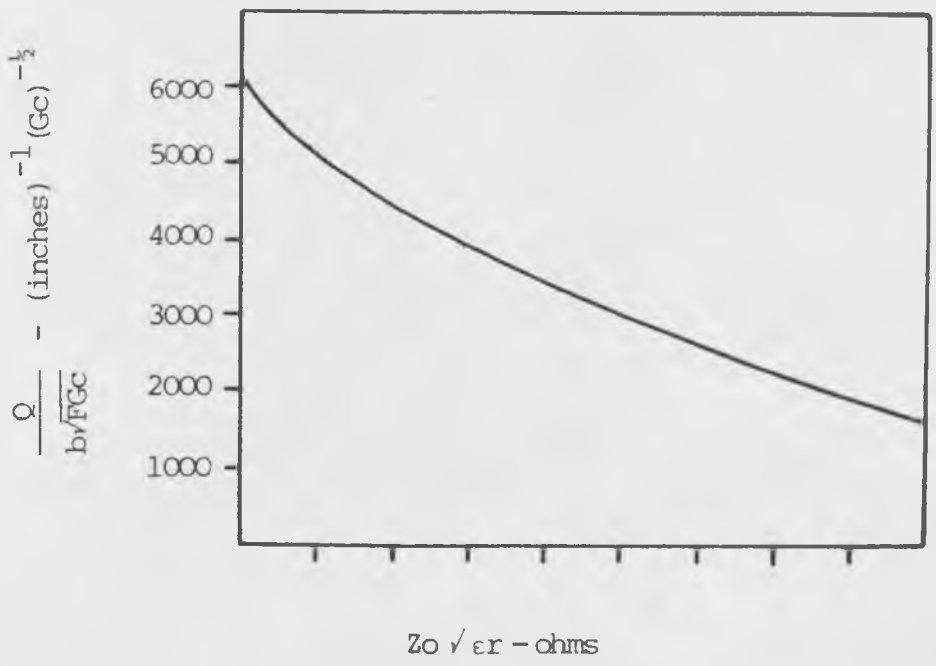

Fig. 3.3.7 The normalised Q factor of an S.S.S transmission line as a function of characteristic impedance. This refers to a zero thickness bar normalised to ground plane spacing and frequency

Fig. 3.3.8 Computed response of narrowband S.S.S bandstop filter

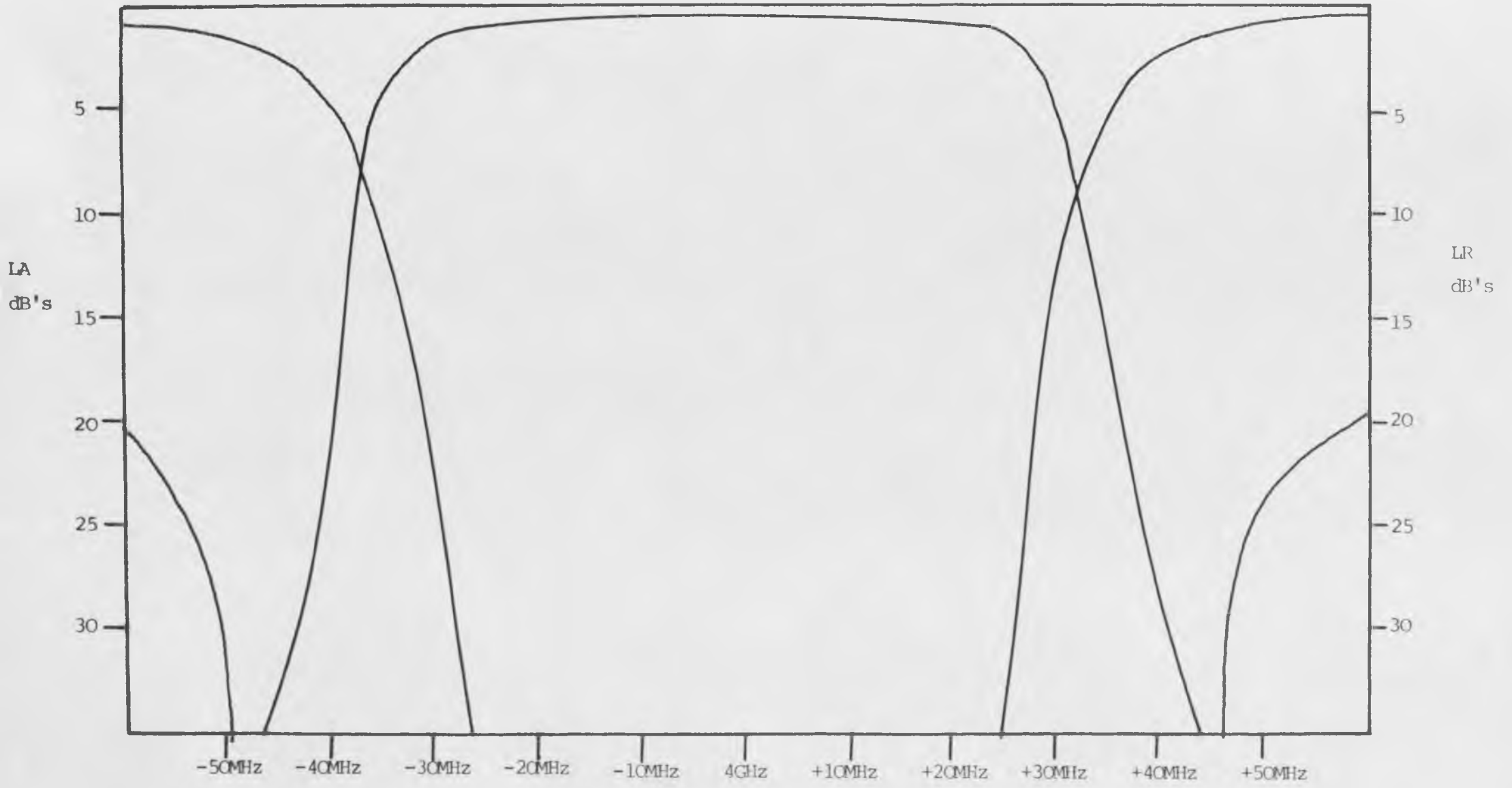

$\Delta\omega$ %	Degree 5		Degree 7		Degree 9	
	1 : 40	3 : 40	1 : 40	3 : 4	1 : 40	3 : 40
0.5	3.45	2.12	2.54	1.72	2.50	1.62
1	2.24	2.03	1.95	1.59	1.83	1.41
2	2.12	1.98	1.63	1.5	1.45	1.31
5	1.91	1.83	1.54	1.48	1.33	1.28
10	1.74	1.68	1.46	1.41	1.26	1.21

Fig. 3.3.9 Showing the computed 1 dB to 40 dB and 3 dB to 40 dB bandwidth ratios of S.S.S bandstop filters with 0.3" ground plane spacing and copper conductors

information was all derived from the analysis of 4 GHz filters with 0.3" ground plane spacings, however, since the filter Q factor is linearly proportional to ground plane spacing and proportional to the square root of frequency, it is possible to predict the performance of virtually any filter by simple extrapolation.

3.4 Varactor Tuned S.S.S Bandstop Filters

3.4.1 Computer Analysis of Varactor Tuned Filters

In chapter two it was seen that the performance of varactor tuned filters was critically dependent on the Q factor of the varactors (which is low at microwave frequencies) and the specification of the filter. It was thus necessary to be able to predict accurately the performance of any varactor tuned filter. This was achieved by computer analysis of the filters with the varactors modelled by their equivalent circuit. [Fig. 3.4.1]

The particular varactor to be used in the remainder of the work described in this thesis was the MA 46620 G device manufactured by Microwave Associates. This varactor had the highest Q factor of any presently available device, its equivalent circuit parameters were claimed to be as follows

Cj(0)	=	0.8pF $\pm$ 0.04pF
Cj(60V)	=	0.12pF $\pm$ 0.02pF
Rj(v)	=	$\leq$ 1.5Ω
Cp1	=	0.19pF $\pm$ 0.02pF
Cp2	=	0.04pF $\pm$ 0.01pF
Lp	=	400pH $\pm$ 50p H

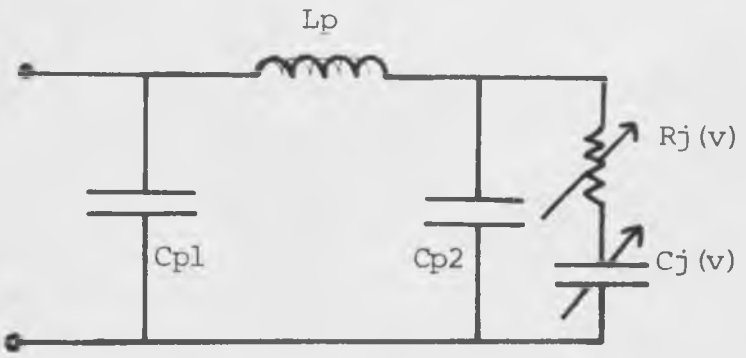

Fig. 3.4.1 MA 46620G varactor equivalent circuit

These parameters were checked using the measurement techniques discussed in section 2.2.2. The measured value of bondwire inductance of 1400pH contradicted the manufacturers claim of 400pH. It would thus seem wise to be wary of manufacturers claims and always measure varactor properties before proceeding with a design.

A computer analysis program was written in order to predict the performance of varactor tuned filters as a function of degree and bandwidth. The circuit model of the MA46620G varactor was used in the analysis. The varactor tuned filters were analysed for bandwidths from 0.5% to 5% and degrees of 2, 3 and 4 for values of Cj of 0.8pF, 0.4pF and 0.11pF. The computed 1dB to 20dB and 3dB to 20db bandwidth ratios of the filters are presented in Fig. 3.4.2. All the data presented was for filters with direct varactor coupling to the resonators, corresponding to a tuning bandwidth of 25%. The bandwidths of the filters presented in Fig. 3.4.2 are the 20dB bandwidths at the middle of the tuning band, these varied by a factor of 1.6:1 across the tuning band.

The centre frequency of all the filters shown in Fig. 3.4.2 was 4GHz. In order to predict the performance of filters with other centre frequencies the change in filter Q factor with frequency must be taken into account. The Q factor of the varactors is inversely proportional to frequency and the Q factor of the S.S.S medium is too large to be significant. Thus, since the Q factor of the filter is proportional to its bandwidth, the analysis of any filter can be achieved simply

	Cj = 0.8 pF		Cj = 0.4 pF		Cj = 0.2 pF	
20 dB bandwidth %	Select-ivity 1:20 dB	Select-ivity 3:20 dB	Select-ivity 1:20 dB	Select-ivity 3:20 dB	Select-ivity 1:20 dB	Select-ivity 3:20 dB
0.5	Not applicable since stopband rejection only 12dB		13	9	4.33	3.16
1	14.01	9.5	4.66	3.44	4.13	2.95
2	4.50	3.31	3.90	3.12	3.46	2.84
5	3.19	2.70	3.05	2.58	3.13	2.66

Fig. 3.4.2a Computed performance of second degree varactor tuned bandstop filters. This shows the 1 dB to 20 dB and 3 dB to 20 dB selectivities of the filters as a function of varactor capacitance and stopband bandwidth

	Cj = 0.8 pF		Cj = 0.4 pF		Cj = 0.2 pF	
20 dB bandwidth %	Select-ivity 1:20 dB	Select-ivity 3:20 dB	Select-ivity 1:20 dB	Select-ivity 3:20 dB	Select-ivity 1:20 dB	Select-ivity 3:20 dB
0.5	Not applicable since maximum rejection only 13.7dB		6.92	4.05	3.91	2.48
1	8.55	4.73	4.20	2.66	3.04	2.15
2	5.03	2.71	3.44	2.20	2.58	2.08
5	3.19	2.00	2.14	1.81	1.97	1.73

Fig. 3.4.2b Computed performance of third degree varactor tuned bandstop filters. This shows the 1 dB to 20 dB and 3 dB to 20 dB selectivities of the filter as a function of varactor capacitance and stopband bandwidth.

	Cj = 0.8 pF		Cj = 0.4 pF		Cj = 0.2 pF	
20 dB bandwidth %	Select-ivity 1:20 dB	Select-ivity 3:20 dB	Select-ivity 1:20 dB	Select-ivity 3:20 dB	Select-ivity 1:20 dB	Select-ivity 3:20 dB
0.5	Not applicable since maximum rejection only 15 dB		5.10	3.40	2.64	2.05
1	6.43	3.95	2.88	2.16	2.29	1.83
2	3.41	2.52	2.21	1.89	2.07	1.64
5	2.25	1.85	1.76	1.61	1.70	1.53

Fig. 3.4.2c) Computed performance of fourth degree varactor tuned bandstop filters. This shows the 1 dB to 20 dB and 3 dB to 20 dB selectivities of the filter as a function of varactor capacitance and stopband bandwidth

by dividing the bandwidth by a factor equal to the increase or decrease in frequency from 4 GHz.

3.4.2 Design of a Varactor Tuned Bandstop Filter

The specification of the varactor tuned filter to be constructed was

Centre frequency	4 GHz ± 500 MHz
20 dB stopband bandwidth	50 MHz at 4 GHz
Degree	3
Passband return loss	20 dB

The computed performance of this filter is shown in Figs. 3.4.3 - 3.4.5.

The design of this filter was based upon the procedures outlined in sections 3.2 to 3.3.3. The only significant differences in the design of this filter as compared to the fixed frequency filters were as follows.

Choice of Prototype

The design was based on the Chebyshev prototype filter. This was purely for the purposes of ease of computer analysis. Since the inverse Chebyshev prototype filter has transmission zeros at intervals across the stopband of the filter, as the computer analysis program tuned the filter, the transmission zeros became misaligned and the response became meaningless. The transmission zeros of the Chebyshev filter are all at the same frequency and the problem does not occur when using this prototype. The modification to the design process involved in

Fig. 3.4.3 Computed performance of practical varactor tuned bandstop filter at zero bias

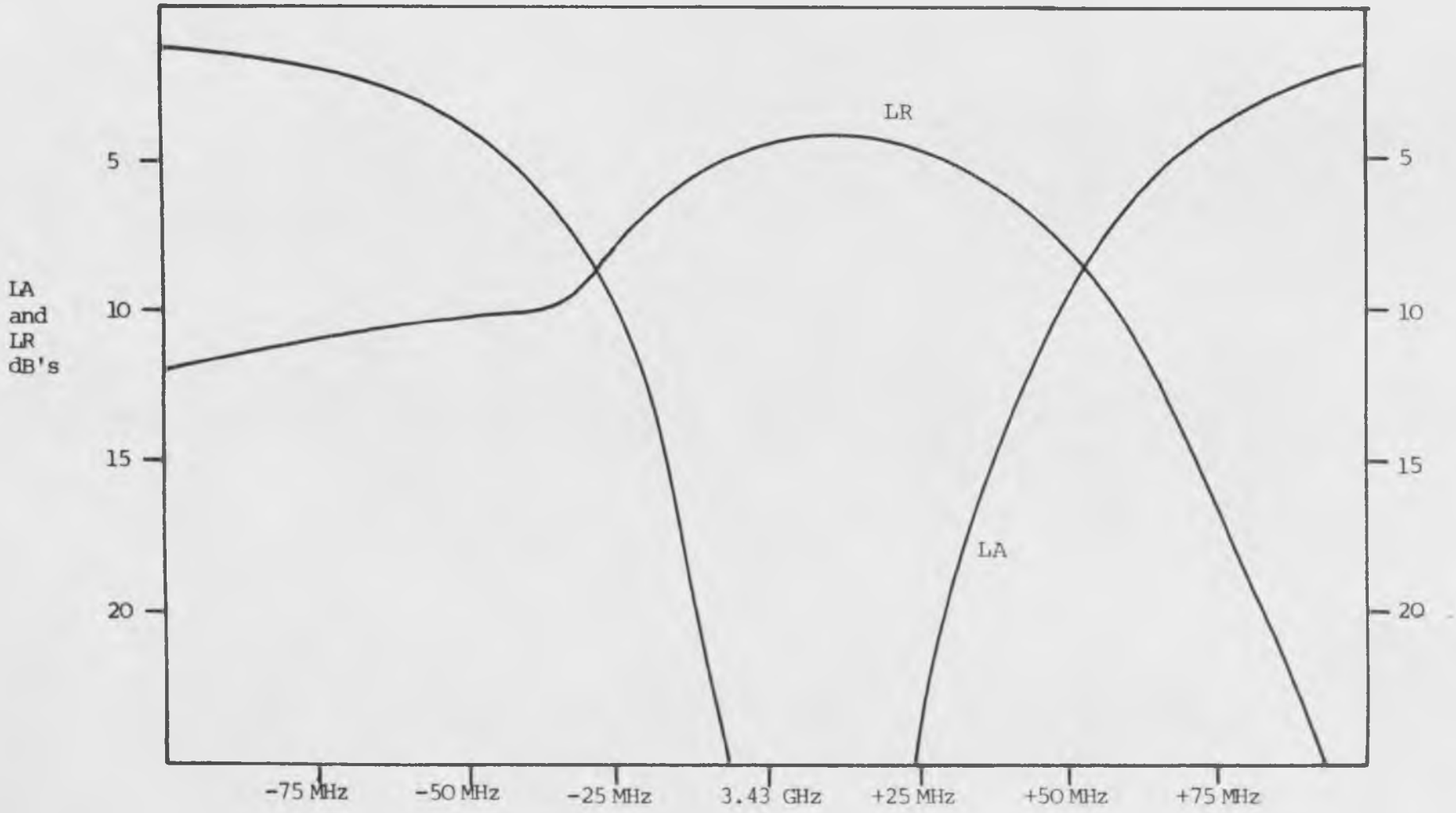

Fig. 3.4.4 Computed performance of practical varactor tuned bandstop filter at -4V bias

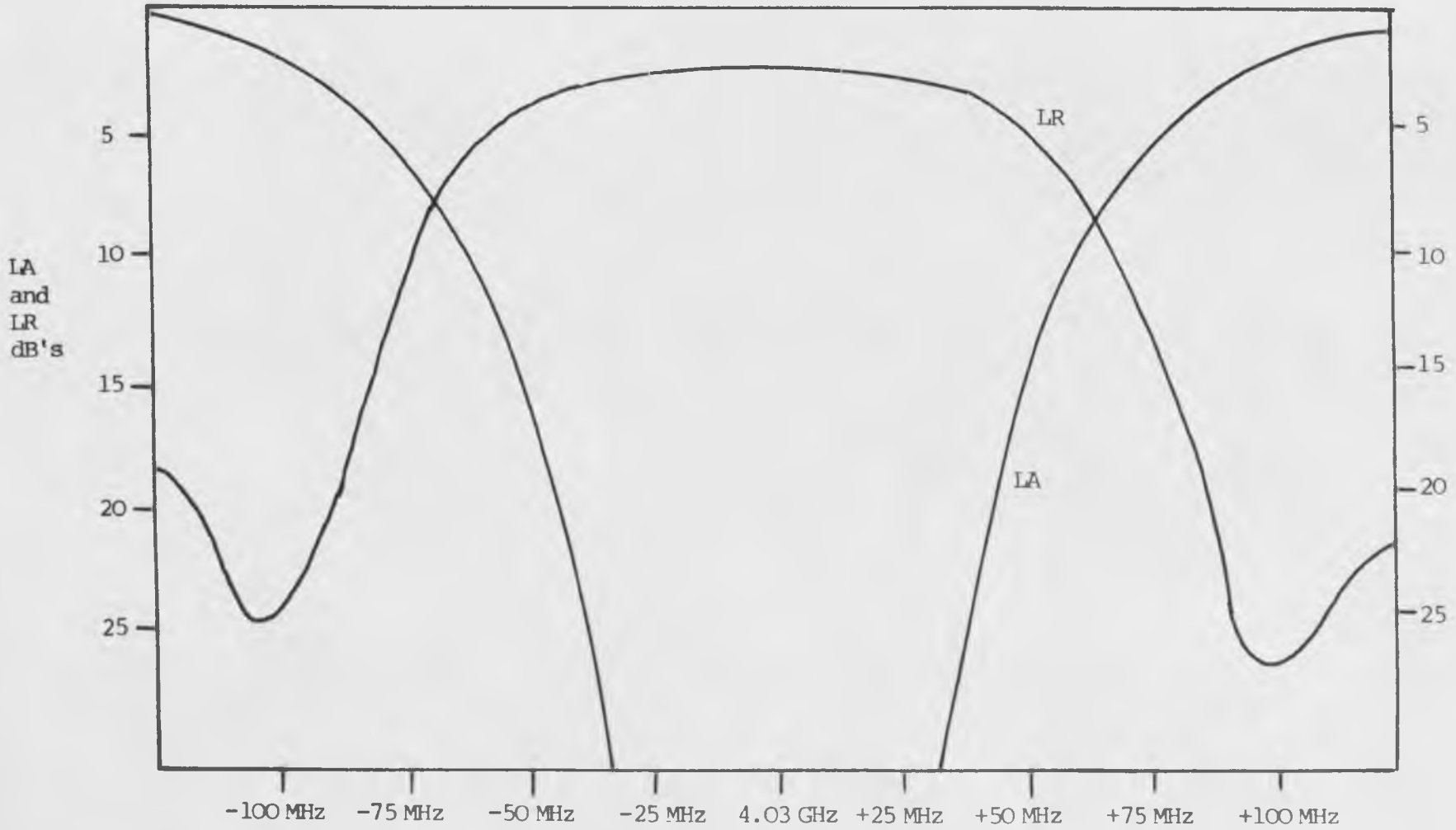

Fig. 3.4.5 Computed performance of practical varactor tuned bandstop filter at -30V bias

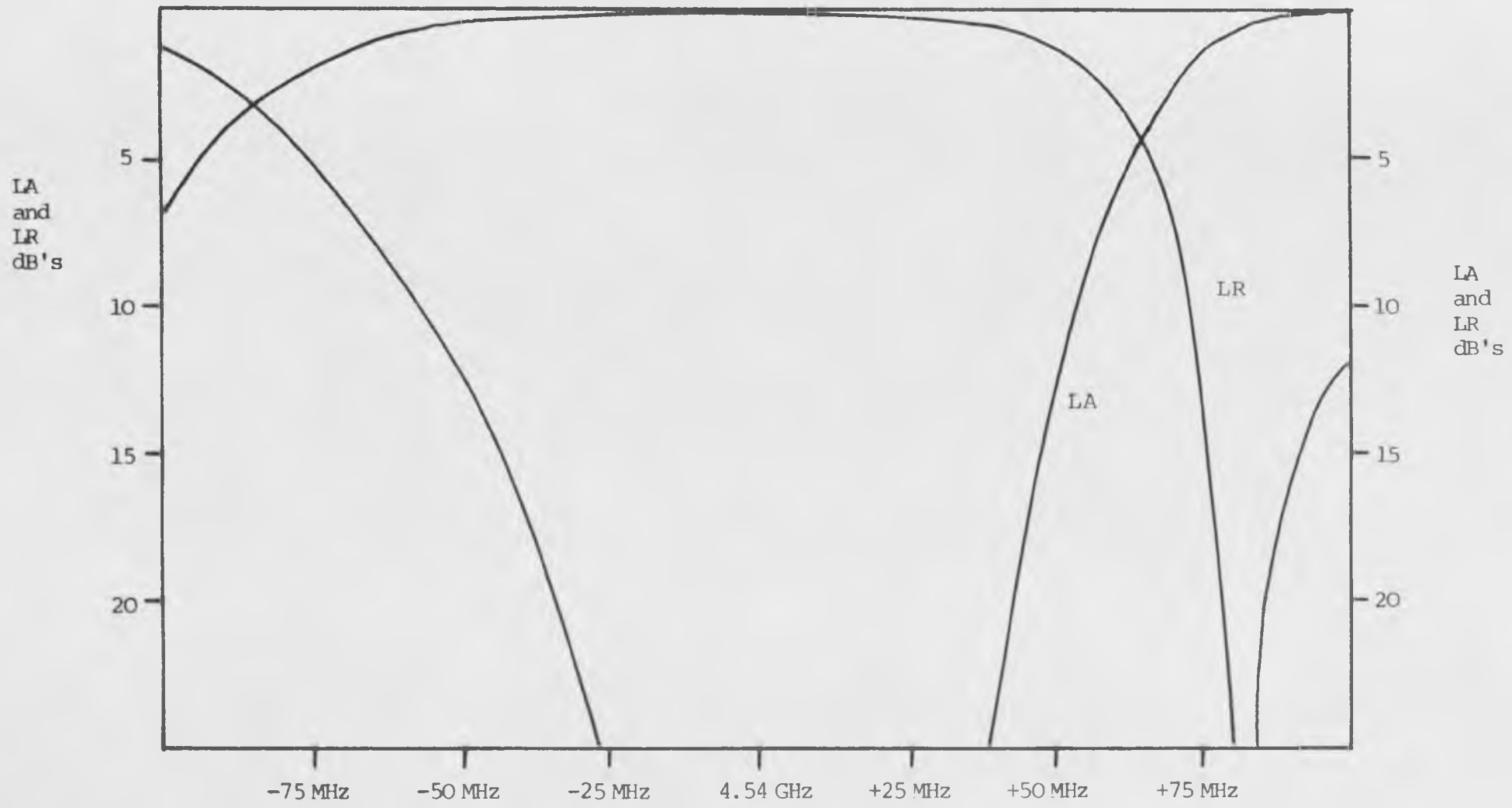

using this prototype is trivial, it merely involves using the element values given in ref. 3.5.

It is important to note that when designing the element values of the tunable bandstop filter, the tuning capacitors must be chosen and then equations 3.2.28 and 3.2.29 should be solved for the characteristic impedances of the resonators and the coupling capacitances to the main line.

Compensation for Varactor Inductance

The varactor capacitance, including package capacitance was 1pF at zero bias and 0.3pF at 60 volts bias. It would thus seem obvious that the filter should be designed for a midband tuning capacitance equal to the geometric mean of these two values. That is 0.55pF. However the bondwire inductance of the varactor has the effect of lowering the centre frequency of the filter. To compensate for this the filter was designed for a midband tuning capacitor value of 0.65pF.

The element values of the tunable bandstop filter were as follows

Resonator	Impedance of resonator	Coupling capacitance to main line
1	76.5 Ω	1.72×10^{-13} F
2	76 Ω	1.66×10^{-13} F
3	76.5 Ω	1.72×10^{-13} F

The phase lengths between the resonators were computed to be 84.6° at 4 GHz and the phase lengths of the resonators were 125° at 4 GHz.

The ground plane spacing of the cavity was chosen to be 0.3" and the physical dimensions of the resonators and coupling gaps were calculated using the methods described in section 3.2.2.

Design of the Main Through Line

A method of reducing the width of the main line was described in section 2.1.2. This involved locating the main line near to the side wall so that the fringing capacitance to ground was increased. In practice, this requires very accurate alignment of the circuit board which may not always be achieved. Any errors in circuit board alignment would result in a change in impedance of the main line and a consequent degradation in the passband return loss of the filter. An alternative to this technique is to print a grounded strip very close to the main line as shown in Fig. 3.4.6. The advantage of this technique is that since the main line will always be the same distance to ground, independence of errors in circuit board location, then good, reproducible passband return loss levels can be achieved. Also, because printed circuits can be printed to within an accuracy of 0.0005", then considerable reduction in width of the main line can be achieved. In this particular case the width of the main line was reduced from 0.4" to 0.273" by

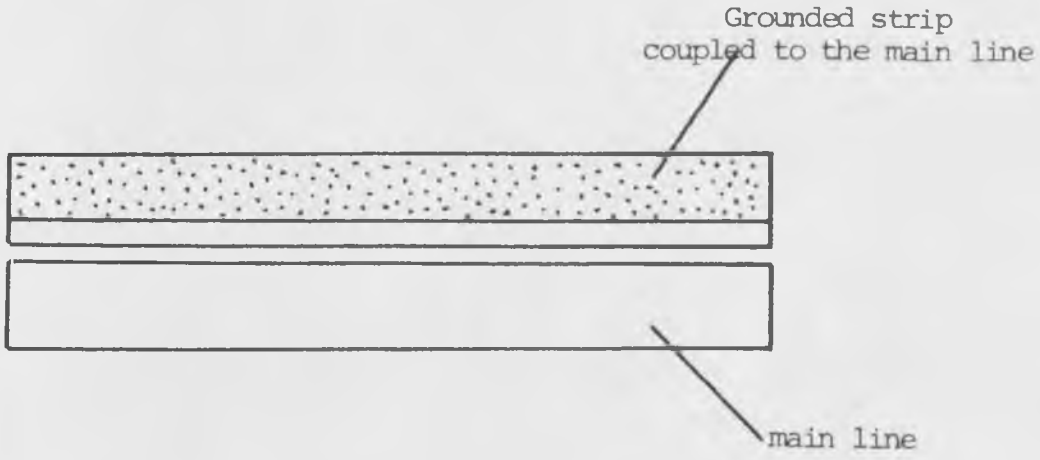

Fig. 3.4.6 Grounded strip realisation of thin lines

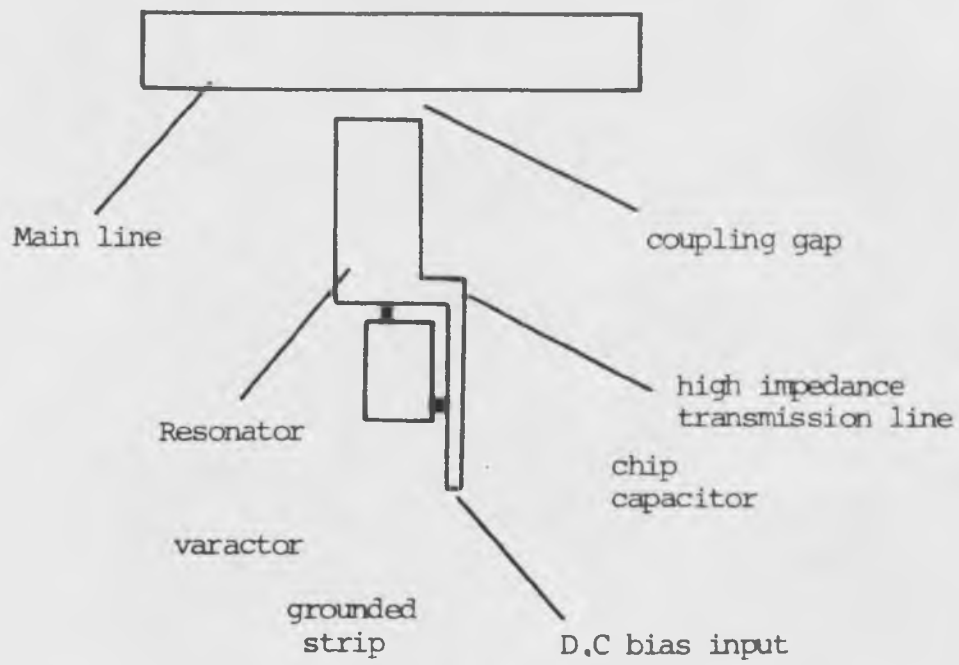

Fig. 3.4.7 Realisation of bias choke

printing the grounded strip at a distance of 0.01" from the main line.

Design of Bias Chokes

In section 2.2.3 the design of stepped impedance transmission line bias chokes was discussed. Unfortunately, a two section quarter wave stepped impedance filter operating at 4 GHz will be approximately 1.4" long. It is desirable to minimise the physical size of devices for use in military systems. Thus an alternative technique is to use a single section of high impedance quarter wave transmission terminated in a shunt capacitor to ground. [Fig. 3.4.7] This technique halves the length of the bias filter and removes the need to realise very low impedance transmission lines. The particular bias filter used in this design had a quarter wave frequency of 4 GHz and an impedance of 200 Ω, the shunt capacitor was a 10pF chip capacitor manufactured by A.T.C. capacitors and this was guaranteed non-resonant for frequencies below 10 GHz.

The transfer matrix of the bias choke is

$$\begin{bmatrix} \cos(\theta) & jZ\sin(\theta) \\ jY\sin(\theta) & \cos(\theta) \end{bmatrix} \begin{bmatrix} 1 & 0 \\ j\omega C & 1 \end{bmatrix} \qquad (3.4.1)$$

$$\begin{bmatrix} \cos(\theta) & -\omega CZ\sin(\theta) \\ j[Y\sin(\theta) + & \omega C\cos(\theta) \end{bmatrix} \begin{bmatrix} jZ\sin(\theta) \\ \cos(\theta) \end{bmatrix} \qquad (3.4.2)$$

The insertion loss of this filter operating in a 1Ω system is expressed by

$$LA = 10Log[1 + 0.25[(\omega(Z\sin(\theta))^2 + ((Z-Y)\sin(\theta) - \omega(\cos(\theta))^2]] \quad (3.4.3)$$

where C and Z are normalised to a 1Ω system.

Evaluating 3.4.3 at 4 GHz we obtain

$$LA(4GHz) = 28.6dB$$

This filter thus produces a superior insertion loss to the stepped impedance filter and is only half the physical length.

The layout and dimensions of the circuir board of the tunable bandstop filter are shown in Fig. 3.4.8.

The design of the housing for the tunable filter was slightly more complex than that for the fixed frequency filters in that d.c connectors had to be incorporated. Also both the housing and the circuit board were gold plated so that good ohmic contacts could be achieved where d.c short circuits were required. Photograph no 2 shows the assembled filter with the top half of the housing removed.

The measured performance of the varactor tuned bandstop filter is shown in Figs. 3.4.9 to 3.4.11. This performance is summarised below

Bias Voltages	0V, 0.02V, 0.01V
Centre Frequency	3.04 GHz
1 dB Stopband Bandwidth	430 MHz
3 dB Stopband Bandwidth	380 MHz
20dB Stopband Bandwidth	0 MHz
Mid-Stopband Return Loss	8 dB
Passband Return Loss	> 20dB to 6 GHz
	> 13dB to 7.2 GHz

Bias Voltages	4V, 4.41V, 4.2V
Centre Frequency	3.602 GHz
1 dB Stopband Bandwidth	421 MHz
3 dB Stopband Bandwidth	310 MHz
20dB Stopband Bandwidth	48 MHz
Mid Stopband Return Loss	3.2 dB
Passband Return loss	> 20 dB to 6.5 GHz
	> 15 dB to 7.2 GHz

Bias Voltages	25.4V, 30V, 27.1V
Centre Frequency	4.21 GHz
1 dB Stopband Bandwidth	417 MHz
3 dB Stopband Bandwidth	207 MHz
20dB Stopband Bandwidth	62 MHz
Mid-Stopband Return Loss	1.7 dB
Passband Return Loss	> 20 dB to 7 GHz

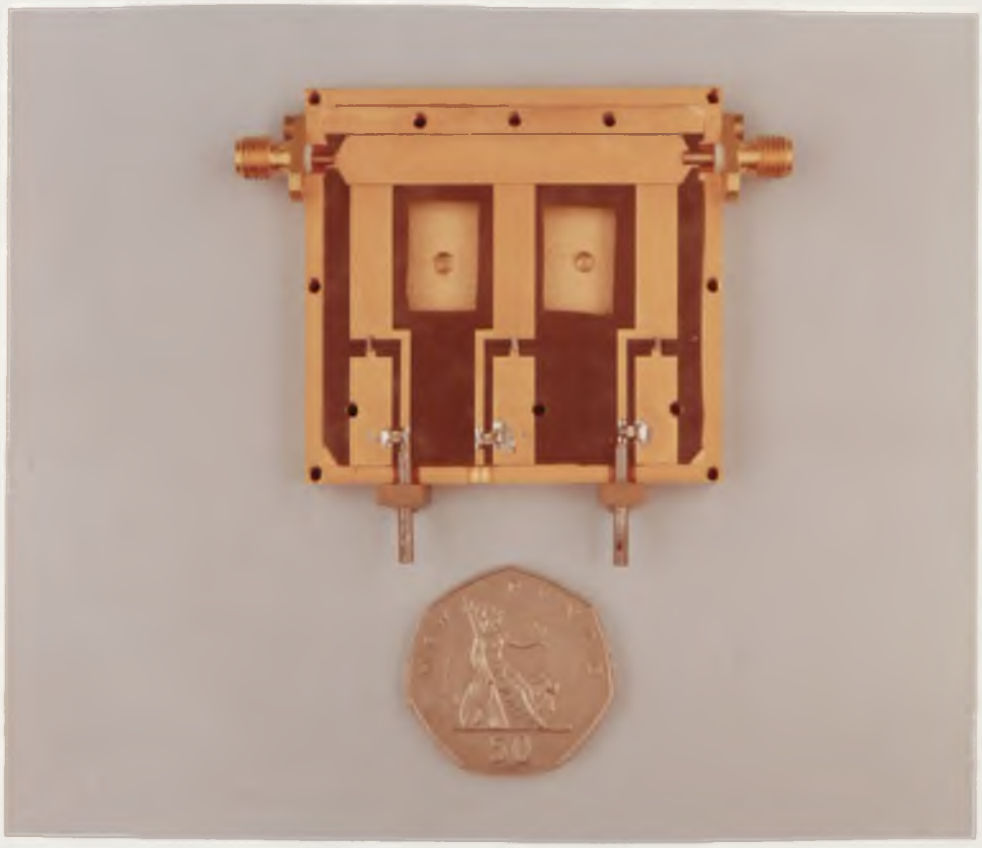

Photograph no. 2

Varactor Tuned Bandstop Filter

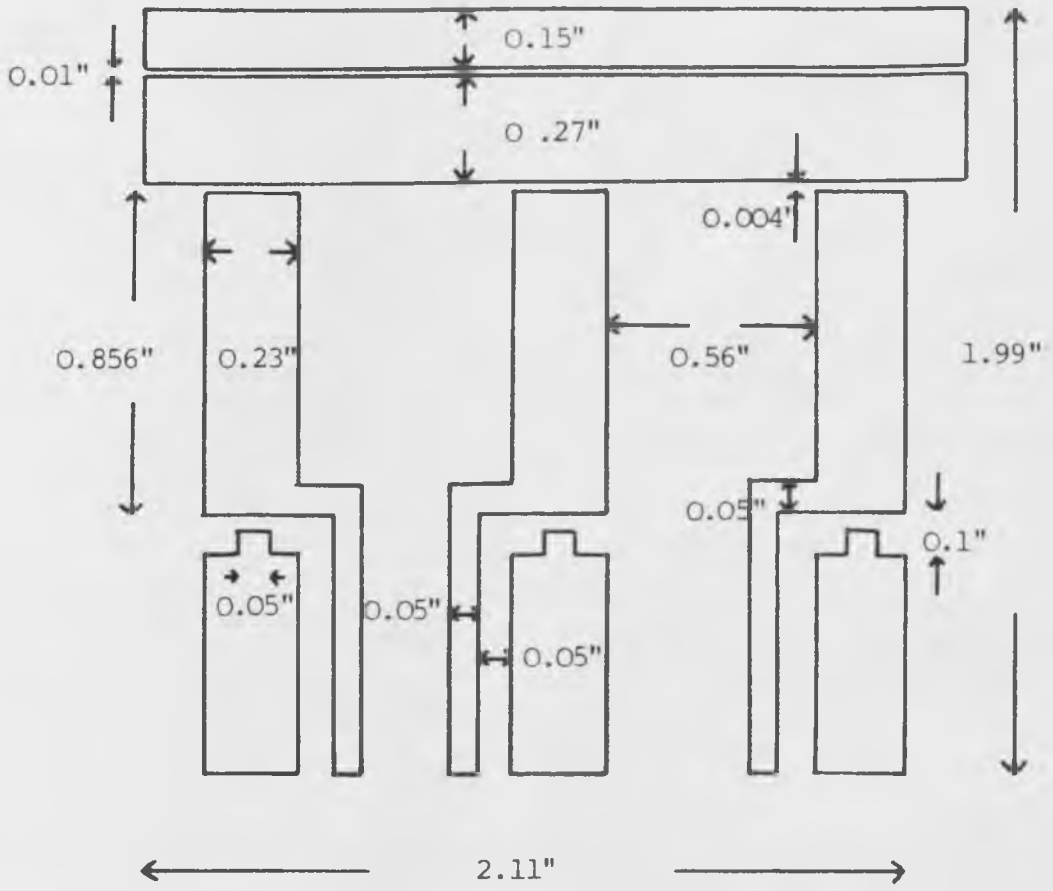

Fig. 3.4.8 Layout and dimensions of the S.S.S circuit board of the varactor tuned bandstop filter

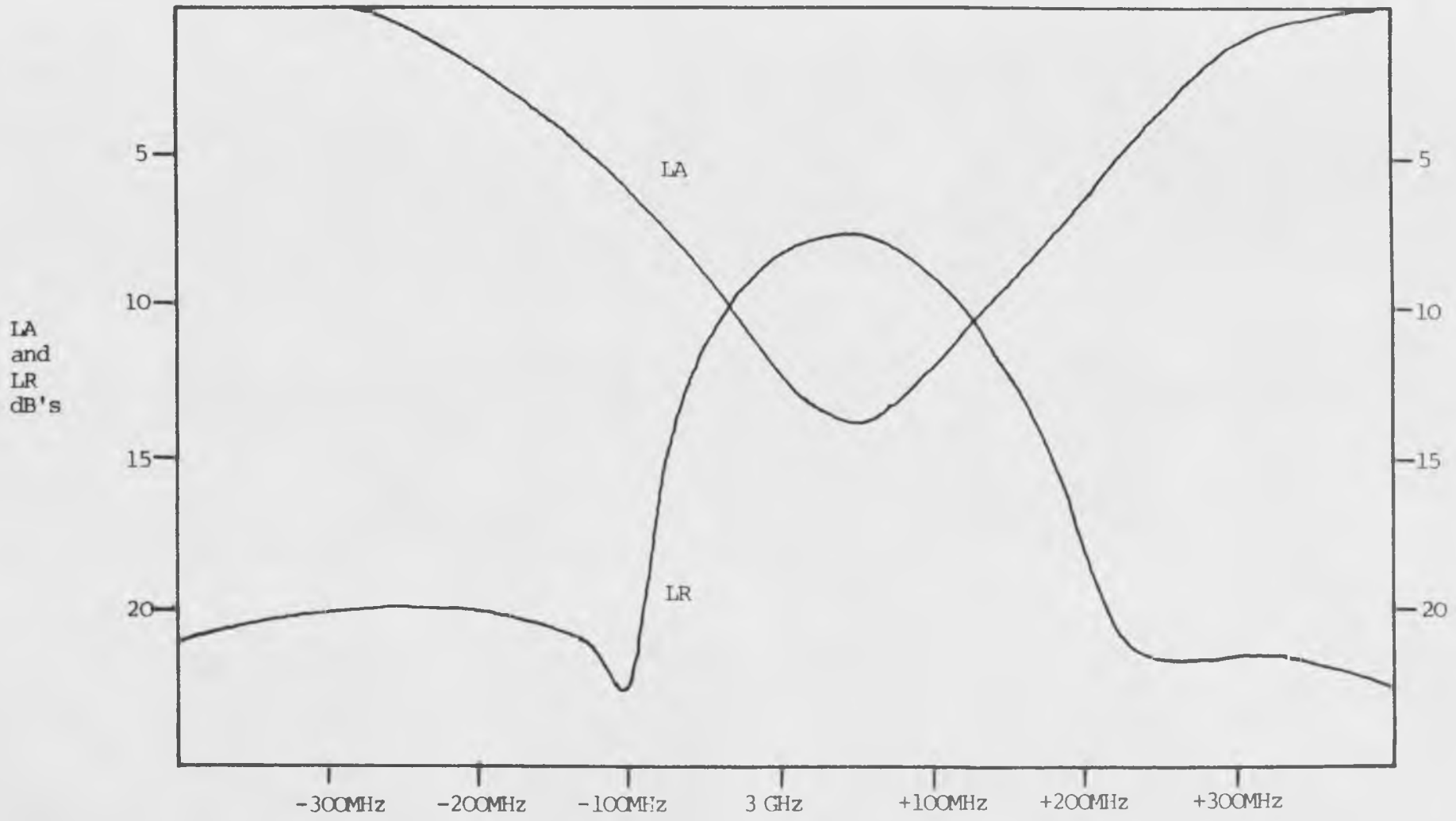

Fig. 3.4.9 Varactor tuned Bandstop Filter performance at zero bias

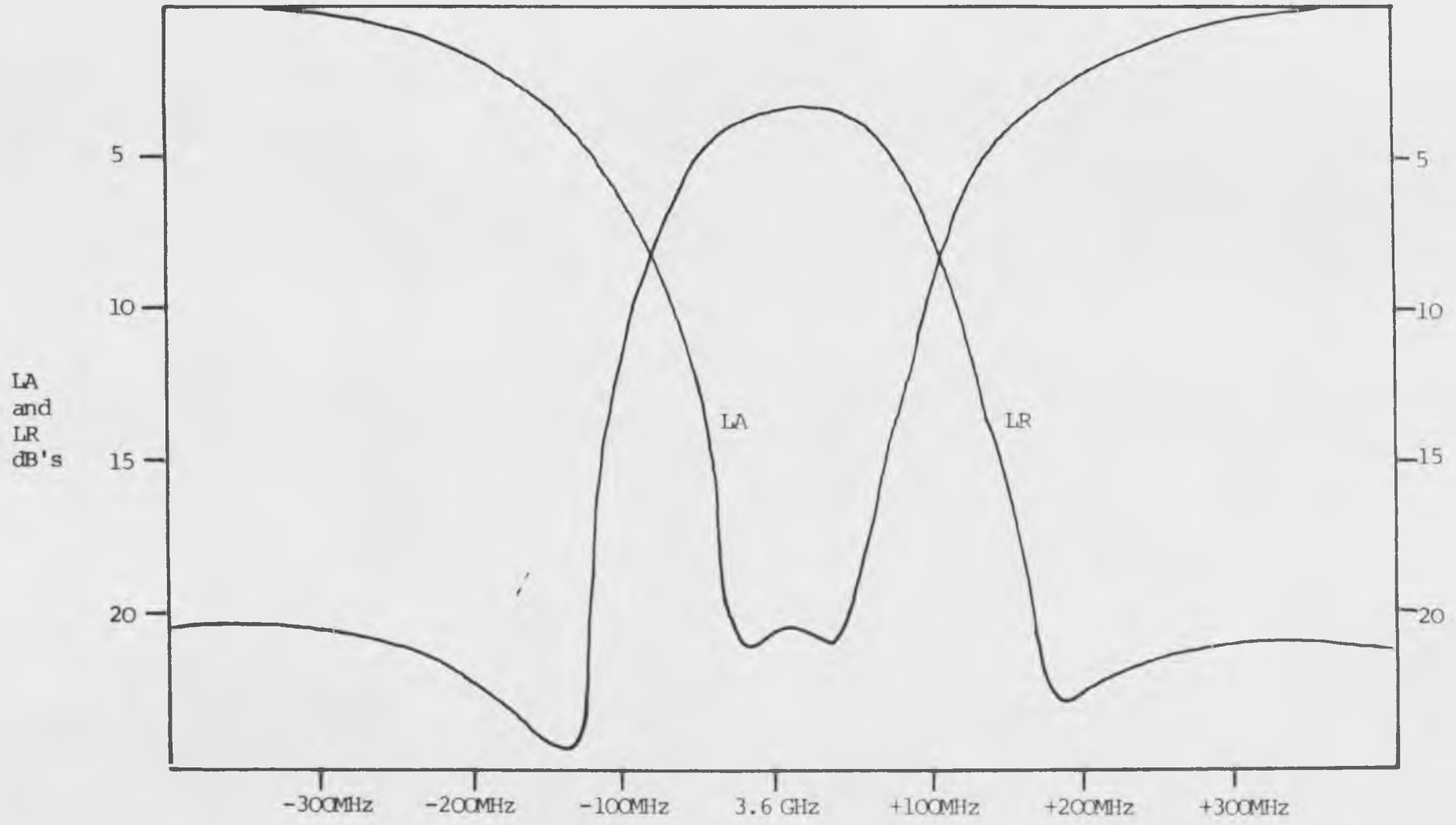

Fig. 3.4.10 Varactor tuned Bandstop Filters performance with bias voltages of approximately 4V

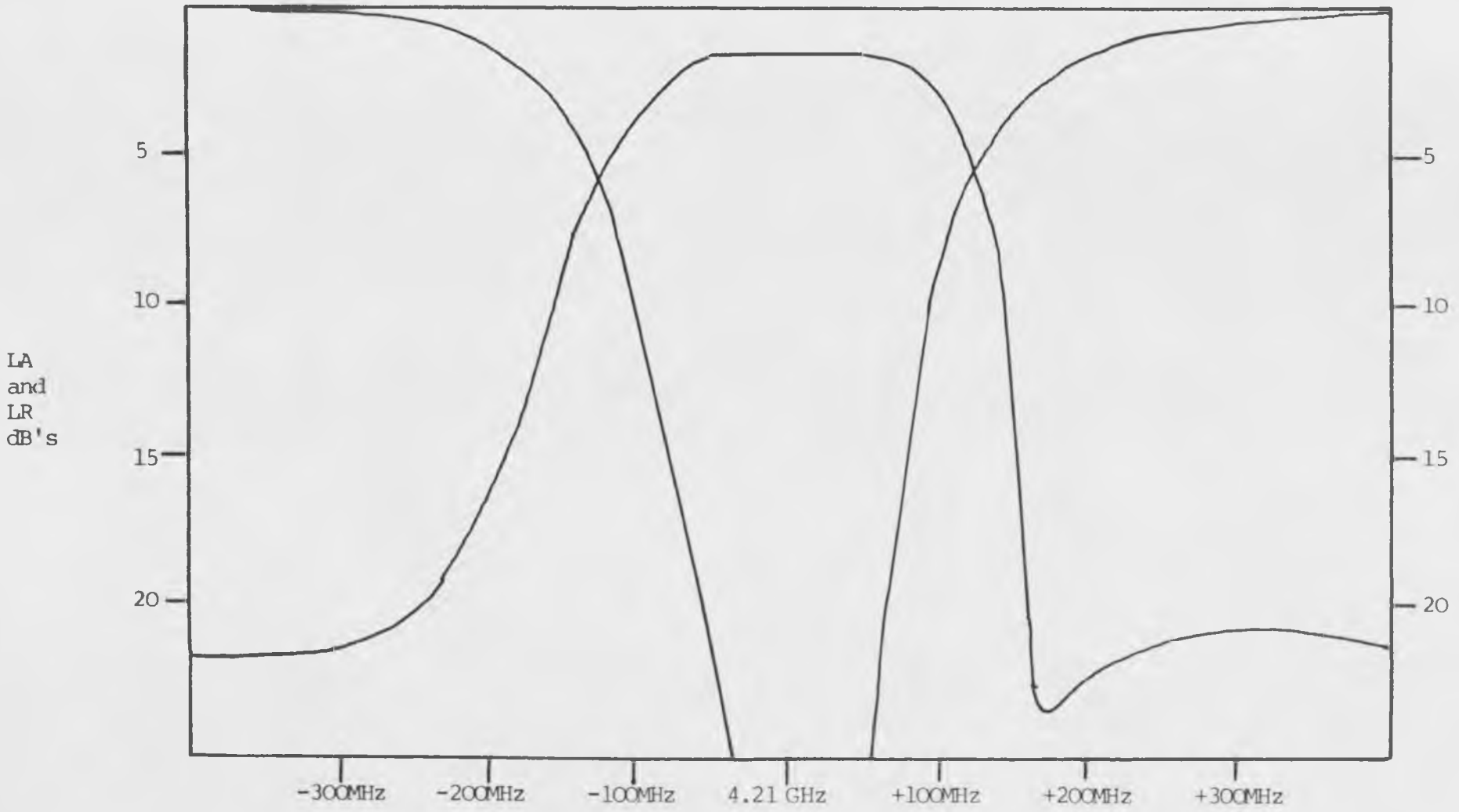

Fig. 3.4.11 Varactor tuned Bandstop Filter performance with bias voltages near 30V

The measured performance of the filter was in close agreement with theory except that the tuning range was shifted down in frequency by approximately 400MHz. This was caused by the high varactor bondwire inductance which was not fully allowed for in the design. This could however easily be compensated for by increasing the value of varactor capacitance used in the design process. It is important to note that the varactor bondwire inductance limits the maximum frequency of operation. This inductance will resonate the varactor at 4.5 GHz at zero bias and 8.2GHz at 60 Volts. Thus if a zero bias frequency of greater than 4.5 GHz is required the varactor must be decoupled to reduce its capacitance as described in Chapter 2.

In chapter 2 it was observed that multiple varactor filters could be tuned from a single power supply over tuning bandwidths of 10%. In the above example, due to the broader tuning bandwidth required, the varactors had to be independently tuned. This problem could be overcome by careful selection of matched varactors or by use of a digital control system with the required voltage frequency curve for each varactor stored in solid state memory.

3.5 The effects of large R.F signal levels on varactors tuned filter performance

In the design of varactor tuned filters the varactor is assumed to be a linear circuit element. That is, the current through the device is related to the voltage across the terminals of the device by a linear differential equation.

In reality, the varactor capacitance is a function of the instantaneous voltage across its terminals which is the sum of the d.c bias voltage and the instantaneous R.F signal voltage. Thus the varactor capacitance is a non-linear circuit element with the current and voltage related by non-linear differential equations. Parry (3.6) has shown that the relationship between the instantaneous charge stored and the voltage across the terminals of an ideal abrupt junction varactor is given by the following equation.

$$\Delta V = \frac{\Delta q^2}{4C^2_{(VB)}(VB+\psi)} + \frac{\Delta q}{C_{(VB)}} \qquad (3.5.1)$$

where

ΔV = Instantaneous voltage across the terminals

Δq = Instantaneous charge stored

VB = Bias Voltage

$C_{(VB)}$ = Varactor capacitance

From 3.5.1 it can be seen that even if the charge flowing through the varactor were sinusoidal the terminal voltage would possess second harmonic distortion. In reality the charge is not necessarily sinusoidal and an infinite number of harmonics may be generated. The large signal behaviour of varactor tuned filters is not easily predicted by analysis, it is better to predict the behaviour by actual measurements of particular filters.

The second harmonic and fundamental output powers of the varactor tuned bandstop filter were measured as a

function of input power and varactor bias voltage. These were measured by using a spectrum analyser as the load for the filter. The measurements were taken with the input signal at the same frequency as the stopband centre frequency of the filter.

Fig. 3.5.1 shows the ratio of the second and first harmonic powers as a function of input power at a bias voltage of approximately -1V on each varactor.

Examining Fig. 3.5.1 we see that at +5 dBm input power the second harmonic was 17 dB down on the fundamental output. No equipment was available for supplying more than 5 dBm of power, however the curve has approximately linear slope and by linear extrapolation we see that at +13 dBm input power the second harmonic power is equal to that of the fundamental. This is known as the second ordered intercept point.

Measurements taken as a function of bias voltage showed a general 6 dBm increase of intercept point each time the bias voltage was doubled. Unfortunately when the harmonic distortion was below -45 dBm it was difficult to measure above the system noise, but by extrapolation the intercept point at 10V bias would be 38dBm.

The physical basis for the reduction of distortion with increased bias voltage is that the varactor capacitance becomes less sensitive to bias as the bias is increased.

No third or higher ordered harmonics were detected. The physical basis for this is that the resonators are open circuited at frequencies away from the stopband centre

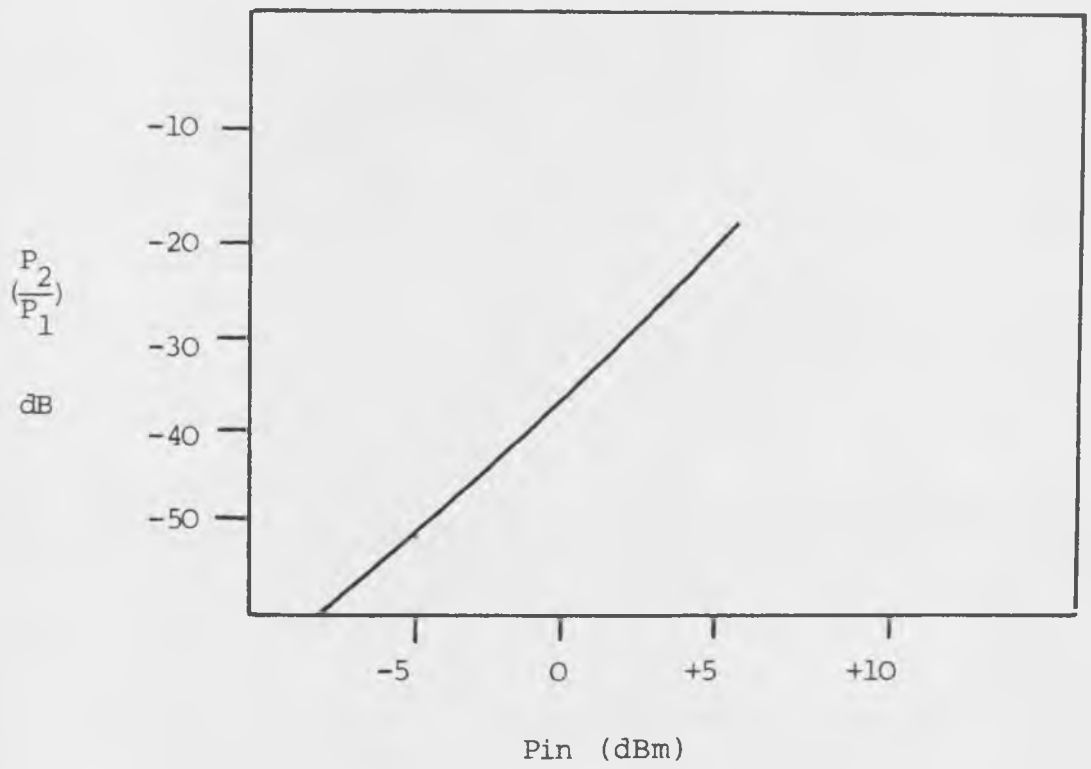

Fig. 3.5.1 Ratio of Second harmonic to Fundamental output powers as a function of input power for the varactor tuned bandstop filter

frequency and thus no harmonic currents can flow in the resonators, therefore in 3.5.1 only second harmonic voltages will be generated.

3.6 Conclusions

A novel design technique for symmetrical bandstop filters has been developed and explicit design formulae are presented. This theory has been used in the design of S.S.S fixed frequency filters and varactor tuned filters. Computer loss analysis of the filters is presented and this agrees closely with the measured performances of experimental devices.

References

3.1 'Theory of Electrical Filters'
pp70-71 J.D. Rhodes
Wiley

3.2 'Advanced Engineering Mathematics'
Erwin Kreysig
Wiley

3.3 'Microwave Filters, Impedance Matching Networks and Coupling Structures' Chapter 2
Matthaei, Young and Jones
McGraw Hill

3.4 Ref 3.3

3.5 Ref 3.1 pp48-49

3.6 'Microwave Frequency Dividers'
R. Parry
Internal Report for the Degree of Ph.D
Department of Electrical Engineering,
The University of Leeds

4. TUNABLE MICROWAVE BANDPASS FILTERS

4.1 Introduction

Initial attempts to construct a tunable bandpass filter were described in chapter two. This filter suffered from a frequency response shape which was highly dependent on tuned frequency. This problem was a consequence of the frequency dependent coupling between the resonators of the filter, the filter was thus mismatched when it was tuned away from the designed centre frequency.

To overcome this problem, a novel tunable combline filter has been developed. By suitable design of the redundant transformer elements at the input and output of the combline filter, it is possible to approximately cancel out the frequency dependence of the coupling between the resonators so that a good response can be maintained over large tuning bandwidths. The filter also possesses the additional important property of maintaining approximately constant absolute bandwidth over very large tuning ranges.

Design procedures are also presented for a tunable combline filter suitable for very narrow passband applications. This device uses open-circuited resonators thus avoiding lossy short circuits which can become a problem when passband bandwidths of less than 5% are required.

The design of a purely distributed circuit suitable for the realisation of narrowband S.S.S bandpass filters is also presented.

The practical design and measured performances of four filters are presented. The first is a two resonator varactor tuned combline filter designed to tune from 3GHz to 5GHz with a passband bandwidth of 5%. The second is a 3% bandwidth three resonator varactor tuned open circuited combline filter designed to tune from 3.5GHz to 4.5GHz. The other devices were fixed frequency 4GHz three resonator filters with 1% and 5% passband bandwidths. All four filters exhibited measured performances in excellent agreement with theoretical expectations.

4.2 Theoretical Design of Tunable Microwave Bandpass Filters

4.2.1 Theory of Tunable Combline Fitlers

The combline filter is shown in Fig. 4.2.1. It consists of a commensurate multi-wire line [4.1].with coupling constrained to be between adjacent lines. The lines are each short circuited to ground at the same end whilst opposite ends are terminated in lumped capacitors. At the resonant frequency of the filter, the lines are significantly less than one quarter of a wavelength long, indeed if the lumped capacitors were not present and the lines were one quarter wavelength long at resonance the network would be an all stop structure. Two advantages of this filter are its compact size and very broad stopband bandwidth, both of which have contributed to its use in multiplexer design [4.2].

The equivalent circuit of the combline filter is shown in Fig. 4.2.2. In Fig. 4.2.2 the resonators are composed of distributed inductors in parallel with lumped capacitors, which the coupling between resonators is achieved by series distributed inductors.

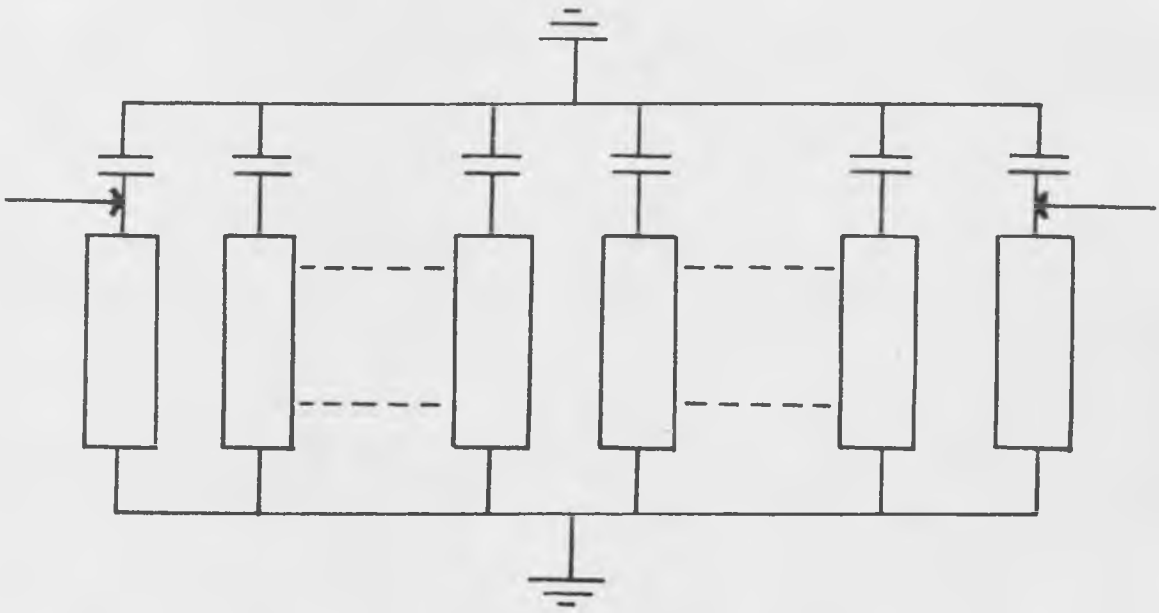

Fig. 4.2.1 The Combline Filter

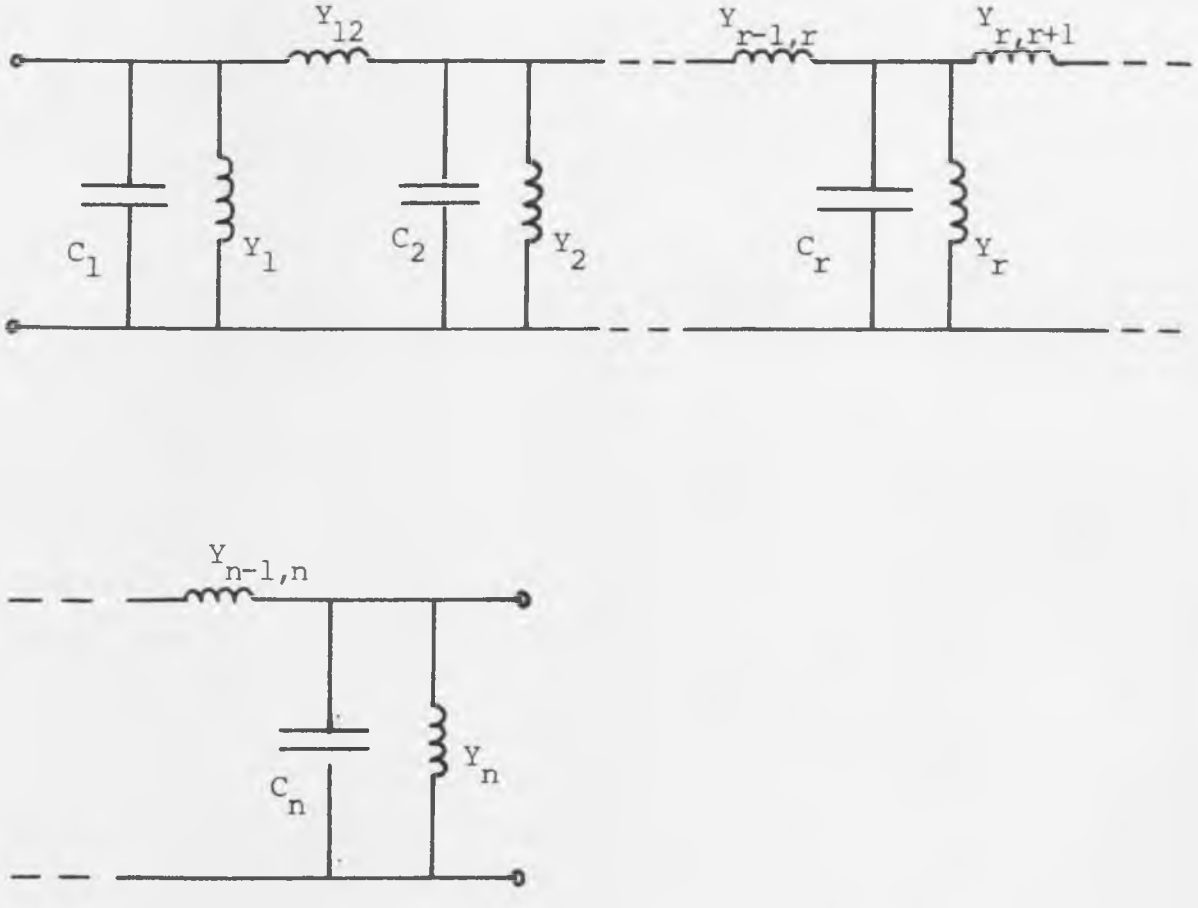

Fig. 4.2.2 Equivalent circuit of the Combline Filter

The method of designing the combline filter consists of transforming the equivalent circuit into a network composed of shunt resonators coupled by admittance inverters. The inverters are formed by shunting the series coupling inductors by identical elements of opposite sign [Fig. 4.2.3]. The transfer matrix between the rth and r+ith nodes in the network is then as follows

$$[T] = \begin{bmatrix} 1 & 0 \\ jY_{r,r+1}\tan(a\omega) & 1 \end{bmatrix} \begin{bmatrix} 1 & \frac{j\tan(a\omega)}{Y_{r,r+1}} \\ 0 & 1 \end{bmatrix} \begin{bmatrix} 1 & 0 \\ jY_{r,r+1}\tan(a\omega) & 1 \end{bmatrix} \tag{4.2.1}$$

$$= \begin{bmatrix} 0 & \frac{j\tan(a\omega)}{Y_{r,r+1}} \\ yY_{r,r+1}\tan(a\omega) & 0 \end{bmatrix} \tag{4.2.2}$$

which is the transfer matrix of an admittance inverter of characteristic admittance $K_{r,r+1}$ where

$$K_{r,r+1} = Y_{r,r+1}/\tan(a\omega) \tag{4.2.3}$$

From Fig. 4.2.3 the rth resonator can be seen to have an admittance Y(r) where

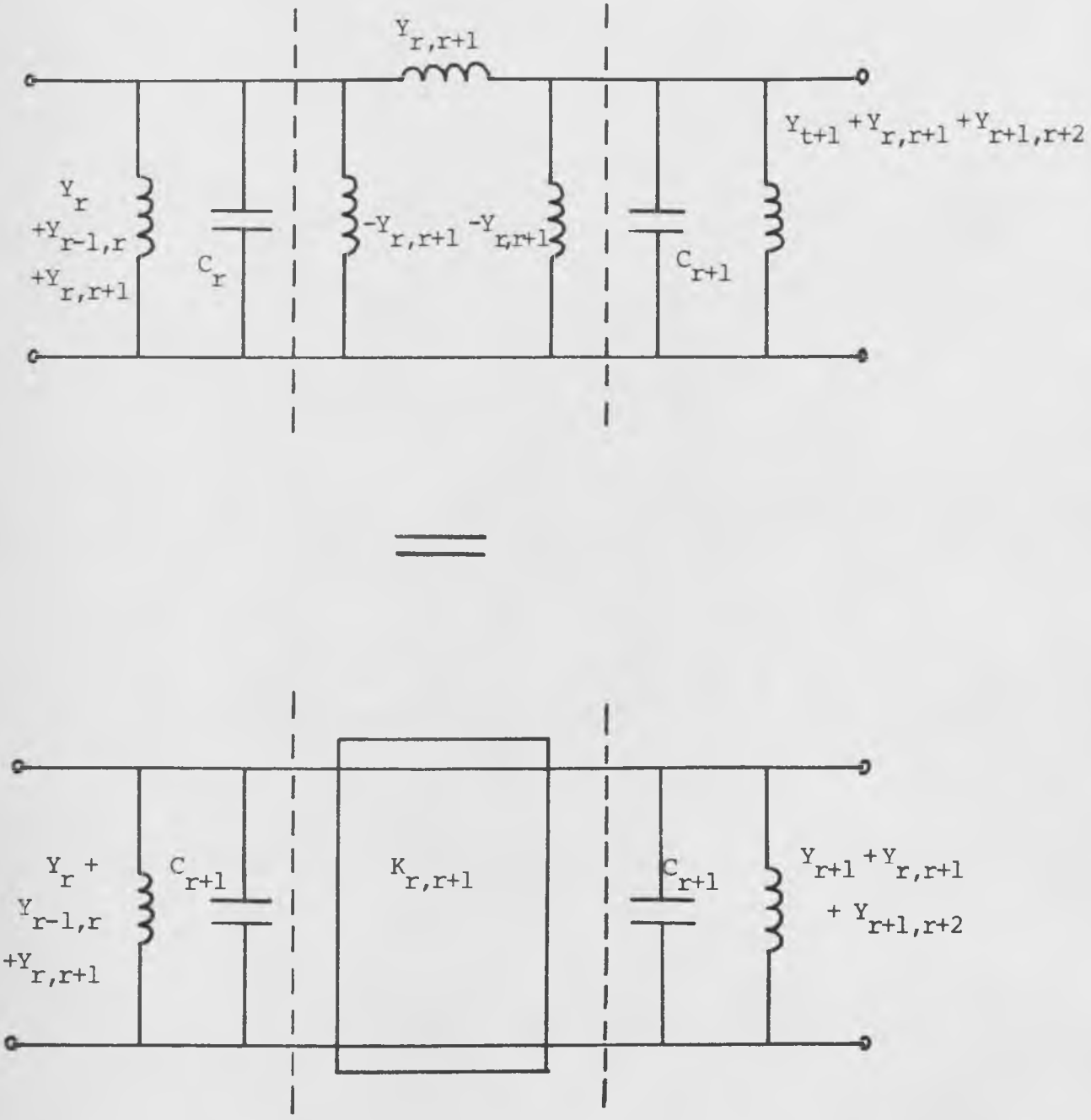

Fig. 4.2.3 Formation of admittance inverters in the combline filter

$$Y(r) = j[\omega C_r - (Y_r + Y_{r-1,r} + Y_{r,r+1})/\tan(a\omega)] \qquad (4.2.4)$$

The frequency dependence of the admittance inverters is now removed by scaling the entire network admittance, including the terminating resistors by a factor $\tan(a\omega)/\tan(a\omega o)$. After scaling we obtain

$$K_{r,r+1} = Y_{r,r+1} / \tan(a\omega_o) \qquad (4.2.5)$$

and

$$Y(r) = \frac{j}{\tan(a\omega_o)} [\omega C_r \tan(a\omega) - (Y_r + Y_{r-1,r} + Y_{r,r+1})] \qquad (4.2.6)$$

where ω_o is the passband centre frequency of the filter.

From the lowpass prototype filter shown in Fig. 4.2.4 we obtain the lowpass to bandpass frequency transformation below

$$\omega \rightarrow \alpha[\beta\omega\tan(a\omega) - 1] \qquad (4.2.7)$$

where

$$\alpha = [Y_r + Y_{r-1,r} + Y_{r,r+1}]/[CL_r \tan(a\omega_o)] \qquad (4.2.8)$$

and

$$\beta = C_r/[Y_r + Y_{r-1,r} + Y_{r,r+1}] \qquad (4.2.9)$$

Equating $\omega = \pm 1$ in the lowpass prototype to the band-edges $\omega 1$ and $\omega 2$ in the combline filter we obtain

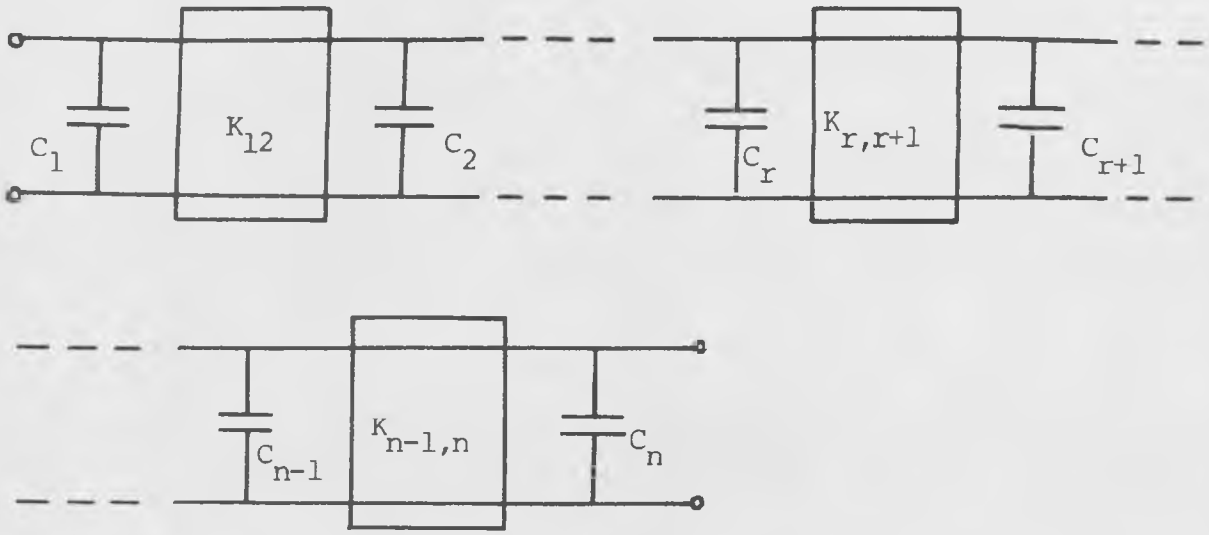

Fig. 4.2.4 The Lowpass Prototype Filter

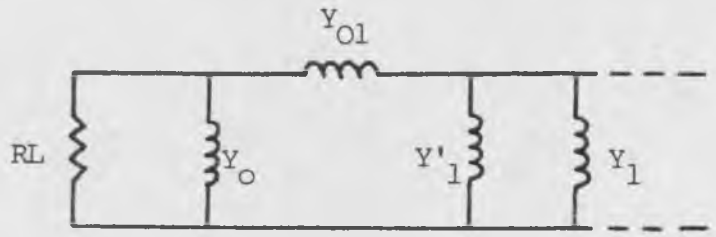

Fig. 4.2.5 The transformer elements at the input and output of the combline filter

$$-1 = \alpha(\beta\omega_1 \tan(a\omega_1) - 1) \qquad (4.2.10)$$

$$+1 = \alpha(\beta\omega_2 \tan(a\omega_2) - 1) \qquad (4.2.11)$$

The bandcentre frequency ω_o is defined as the resonant frequency of the filter, thus

$$\beta\omega_o \tan(a\omega_o) - 1 = 0 \qquad (4.2.12)$$

or

$$\beta = 1/(\omega_o \tan(a\omega_o)) \qquad (4.2.13)$$

For narrow passband bandwidths $\Delta\omega$ we can approximate the bandedge frequencies as follows

$$\omega_1 = \omega_o - \Delta\omega/2 \qquad (4.2.14)$$

$$\omega_2 = \omega_o + \Delta\omega/2 \qquad (4.2.15)$$

with

$$\Delta\omega << \omega_o$$

Using 4.2.14 and the trigonometric expansion of tan(A+B) we obtain

$$\tan(a\omega_1) \approx \frac{\tan(a\omega_o) - a\Delta\omega/2}{1 + a\Delta\omega/2 \tan(a\omega_o)} \qquad (4.2.16)$$

Now $\frac{a\Delta\omega}{2} \tan(a\omega_o) << 1$

Thus expanding [4.2.16] using the binomial theorum we obtain

$$\tan(a\omega_1) \approx [\tan(a\omega_o) - \frac{a\Delta\omega}{2}][1 - \frac{a\Delta\omega}{2}\tan(a\omega_o)] \qquad (4.2.17)$$

Similarly

$$\tan(a\omega_2) \approx [\tan(a\omega_o) + \frac{a\Delta\omega}{2}][1 + \frac{a\Delta\omega}{2}\tan(a\omega_o)] \qquad (4.2.18)$$

Now denoting $a\omega_o$ as θ_o, and substituting 4.2.17 into 4.2.10 and 4.2.18 into 4.2.11, and ignoring second order terms in $\Delta\omega$, then

$$-1 = \alpha[\beta[\omega_o\tan(\theta_o) - \frac{\Delta\omega}{2}[\tan(\theta_o) + \theta_o[1+\tan^2(\theta_o)]]]-1] \qquad (4.2.19)$$

And

$$+1 = \alpha[\beta[\omega_o\tan(\theta_o) + \frac{\Delta\omega}{2}[\tan(\theta_o) + \theta_o[1+\tan^2(\theta_o)]]]-1] \qquad (4.2.20)$$

Solving 4.2.19 and 4.2.20 simultaneously for $\Delta\omega$ yields

$$\Delta\omega = \frac{2}{\alpha\beta[\tan(\theta_o) + \theta_o(1+\tan^2(\theta_o))]} \qquad (4.2.21)$$

From 4.2.13 and 4.2.21 we obtain the expression for $\Delta\omega$ as a function of tuned frequency

$$\Delta\omega \approx \frac{2\omega_o\tan(\theta_o)}{\alpha[\tan(\theta_o) + \theta_o(1+\tan^2(\theta_o))]} \qquad (4.2.22)$$

The frequency dependent part of 4.2.22 is $F(\theta_o)$ where

$$F(\theta_o) = \frac{\theta_o \tan(\theta_o)}{\tan(\theta_o) + \theta_o[1 + \tan^2(\theta_o)]} \qquad (4.2.23)$$

For θ_o small we have

$$\tan(\theta_o) \simeq \theta_o \qquad (4.2.24)$$

and

$$F(\theta_o) \simeq \frac{\theta_o^2}{2\theta_o} \qquad (4.2.25)$$

which is an increasing function

As θ_o tends to 90^o we have

$$\tan(\theta_o) \to \infty \qquad (4.2.26)$$

and

$$F(\theta_o) \to 0 \qquad (4.2.27)$$

Thus the bandwidth of the combline filter has a turning point somewhere between $\theta_o = 0^o$ and $\theta_o = 90^o$.

Inverting 4.2.23 we obtain

$$[F(\theta_o)]^{-1} = \frac{1}{\theta_o} + \frac{1 + \tan^2(\theta_o)}{\tan(\theta_o)} \qquad (4.2.28)$$

$$= \frac{1}{\theta_o} + \frac{2}{\sin(2\theta_o)} \qquad (4.2.29)$$

Differentiating (4.2.29) and equating to zero to evaluate the turning point we obtain

$$\frac{1}{\theta_o^2} + \frac{4\cos(2\theta_o)}{\sin^2(2\theta_o)} = 0 \qquad (4.2.30)$$

4.2.30 can be solved numerically using the Newton Raphson technique to obtain

$$\theta_o = 52.885^o \qquad (4.2.31)$$

This value of θ_o is the point at which the bandwidth of the combline filter is maximised. The function $F(\theta_o)$ is shown below and it can be seen that the filter bandwidth is approximately constant, independent of tuned frequency, even over octave tuning bandwidths. The filter should be designed so that the electrical phase lengths of the resonators are 52.885^o long at the exact centre of the tuning band.

θ_o	$F(\theta_o)$
20^o	0.167
30^o	0.237
40^o	0.288
50^o	0.314
60^o	0.306
70^o	0.254

With the filter designed in this manner, octave tuning around $\theta_o = 52.885^o$ will cause less than a 20% change in absolute bandwidth.

The scaling of the network admittance performed previously resulted in frequency dependent terminating resistors of conductance

$$GL = GS = \tan(a\omega)/\tan(a\omega_o) \qquad (4.2.32)$$

Tuning the filter over an octave with $\theta_o = 52.9^o$ at midband will change the terminating resistors by a factor of 3.92:1. Such a variation is unacceptable because it would result in a very poor filter response at tuned frequencies away from the optimum value. In order to maintain a good response over broad tuning bandwidths this frequency variation must be removed. Redundant, non-resonated transformer stubs are introduced at the input and output of the filter to achieve this objective [Fig. 4.2.5]. It is proven in Appendix 4.1 that the values of the admittances of the transformer stubs must satisfy

$$Y_o = 1 - 1/\cos(\theta_o) \qquad (4.2.33)$$

$$Y_{o1} = 1/\cos(\theta_o) \qquad (4.2.34)$$

$$Y_1' = 1 - 1/\cos(\theta_o) \qquad (4.2.35)$$

With these values of transformer elements the admittance of the load seen by the filter looking back into Y_1', and after scaling by $\tan(a\omega)/\tan(a\omega_o)$ is

$$Y_L = \frac{\sin(2\theta)}{\sin(2\theta_o)} + j\,\frac{(\cos(2\theta) - \cos(2\theta_o))}{\sin(2\theta_o)} \qquad (4.2.36)$$

Y_L is resonant at θ_o and the required minimum variation in the real part of Y_L is achieved. With $\theta_o = 45^o$ at the middle of the tuning band, then octave tuning from 30^o to 60^o changes the load admittance from 0.866 to 1, thus only a very small

deterioration in filter response will be noticed.

To achieve realisable element values, the admittance level of the filter must be scaled at each node in order that the high admittances of the shunt resonators can be absorbed into the coupling elements. Scaling also allows the lumped capacitors to have any desired equal value which is important for the realisation of practical varactor tuned filters. After scaling the rth node in the filter by a factor n_r^2 the typical coupling network between nodes r and r+1 will be as shown in Fig. 4.2.6. After absorbing the ideal transformers in the coupling network into the inverters, we obtain

$$K_{r,r+1} = n_r . n_{r+1} \, Y_{r,r+1} / \tan(\theta_o) \qquad (4.2.37)$$

The scaling constant α becomes

$$\alpha = \frac{n_r^2 [Y_r + Y_{r-1,r} + Y_{r,r+1}]}{CL_r \tan(\theta_o)} \qquad (4.2.38)$$

The ideal transformers which remain at the input and output of the filter [Fig. 4.2.7] cannot be absorbed into the inverters and must be absorbed into the redundant transformer stubs. It can be shown by a procedure similar to that in Appendix 4.1 that the values of the transformer elements will be modified as below

$$Y_o = 1 - 1/n_1 \cos(\theta_o) \qquad (4.2.39)$$

$$Y_{O1} = 1 / n_1 \cos(\theta_o) \qquad (4.2.40)$$

$$Y_1' = 1/n_1^2 - 1/n_1 \cos(\theta_o) \qquad (4.2.41)$$

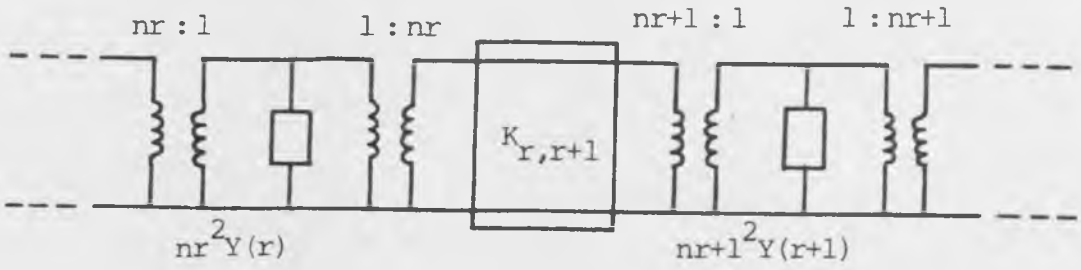

Fig. 4.2.6 Scaling procedure on internal nodes of the combline filter

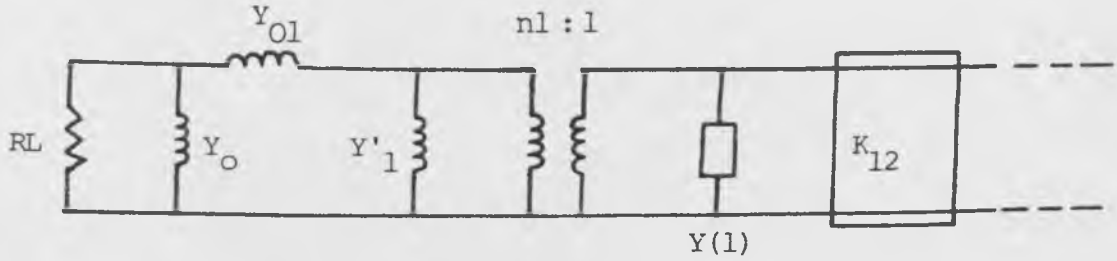

Fig. 4.2.7 The input (output) of the combline filter after scaling of the internal nodes

These values will yield the required load frequency variation given in 4.2.36 and the condition for realisability is now that Y_o is positive. This will be true if $n_1 \geq 1/\cos(\theta_o)$. Typically, passband bandwidths of less than 30% will allow this condition to be satisfied.

Examining 4.2.36 we see that the load admittance has a resonant imaginary part, when the filter is tuned to frequencies at which this is not zero this admittance will affect the first and last resonators. To compensate for this the first and last resonators will be scaled as follows.

From 4.2.7 and 4.2.36 the admittance of the first (and last) resonator is

$$Y(1) = CL_1\alpha(\beta\omega \tan(a\omega)-1) + \frac{\cos(2a\omega) - \cos(2a\omega_o)}{\sin(2a\omega_o)} \qquad (4.2.42)$$

The required value of this resonator admittance is

$$Y(1) = CL_1\alpha[\beta\omega \tan(a\omega)-1] \qquad (4.2.43)$$

The value of α in 4.2.42 will now be modified so that 4.2.42 will posess the same susceptance slope parameter as 4.2.43 at ω_o. Thus, differentiating 4.2.30 and 4.2.31 and equating at ω_o with the modified value of α in 4.2.42 being α' we obtain

$$2a = CL_1(\alpha' - \alpha)[\beta \tan(\theta_o) + \beta\theta_o[1+\tan^2(\theta_o)]] \qquad (4.2.44)$$

Rearranging we obtain

$$\alpha' = \alpha + \frac{2a}{CL_1\beta[\tan(\theta_o) + \theta_o(1 + \tan^2(\theta_o))]} \qquad (4.2.45)$$

From 4.2.45 and 4.2.21

$$\alpha' = \alpha[1 + \frac{a\Delta\omega}{CL_1}] \qquad (4.2.46)$$

which is the required scaling factor for r=1 and r=n.

The design equations for the tunable combline filter can now be evaluated.

From 4.2.9 and 4.2.13 we obtain

$$[Y_r + Y_{r-r,r} + Y_{r,r+1}] = C\omega_o \tan(\theta_o) \qquad (4.2.47)$$

where C is the value of the lumped tuning capacitor at band centre.

From 4.2.22 and 4.2.46

$$\alpha = \frac{2\omega_o \tan(\theta_o)}{\Delta\omega[(\theta_o) + \theta_o(1+\tan^2(\theta_o))]} \qquad (4.2.48)$$

[for r = 2 to n - 1]

and

$$\alpha = \alpha[1 + \frac{a\Delta\omega}{CL_1}] \qquad (4.2.49)$$

[for r = 1 and r = n]

From 4.2.38

$$n_r = [CL_r \tan(\theta_o)]^{\frac{1}{2}}/[Y_r + Y_{r-1,r} + Y_{r,r+1}]^{\frac{1}{2}} \qquad (4.2.50)$$

From 4.2.37

$$Y_{r,r+1} = \frac{K_{r,r+1} \tan(\theta_o)}{n_r . n_{r+1}} \qquad (4.2.51)$$

Finally from 4.2.47 and 4.2.51 Y_r can be obtained.

Thus in summary, we initially obtain the values C_{LR} and $K_{r,r+1}$ for the lowpass prototype filter, this would normally be the Chebyshev prototype filter [4.3]. Next the value of θ_o at the middle of the tuning band must be chosen, for optimum passband return loss across the tuning band θ_o should be 45^o, if constant bandwidth is required θ_o should be 52.9^o. The value of the lumped tuning capacitor should then be chosen and the admittance of the combline filter can then be derived by applying equations 4.2.47 to 4.2.51 and 4.2.39 to 4.2.41. For a Chebyshev prototype filter only the first half of the element values need to be evaluated since the network will be symmetrical.

4.2.2 Theory of Tunable Open-Circuited Combline Filters

Lossy short circuits can become a problem in the practical realisation of S.S.S combline filters with narrow passband bandwidths. Also in the case of varactor tuned combline filters, since the varactors are heavily coupled into the resonators, certain requirements may not be met because of energy dissipation in the varactors.

An alternative to the tunable combline filter is the tunable open-circuited combline filter in which the resonators are between one quarter and one half wavelength long at bandcentre, and no short circuits are required. The varactors are not as heavily coupled into the resonators of this filter, since, because the resonators are longer, they contain more stored energy than the normal combline filter. Consequently for a given resonant frequency and passband bandwidth this filter will have a lower dissipation loss than the tunable combline filter. In Appendix 4.2 it is shown that the Q factor of this filter will be approximately twice that of the tunable combline filter. Unfortunately, the inevitable trade off is that of tuning bandwidth. The tunable combline filter will tune from 30^{o} to 60^{o} with a 6:1 capacitance variation, the open-circuited combline filter will only tune from 120^{o} to 150^{o} with the same capacitance ratio.

The basic physical structure of this filter is shown in Fig. 4.2.8. The structure is essentially the same as the normal combline filter except that the short circuits have been removed and replaced by open circuits. The equivalent circuit of the filter is identical to that shown in Fig. 4.2.2 except that the inductor symbols now represent open circuited stubs with electrical length of between one quarter and one half wavelength at band centre.

The admittance of the rth resonator in the open circuited combline filter is

$$Y(r) = \omega C + jY_r \tan(a\omega) \qquad 4.2.52$$

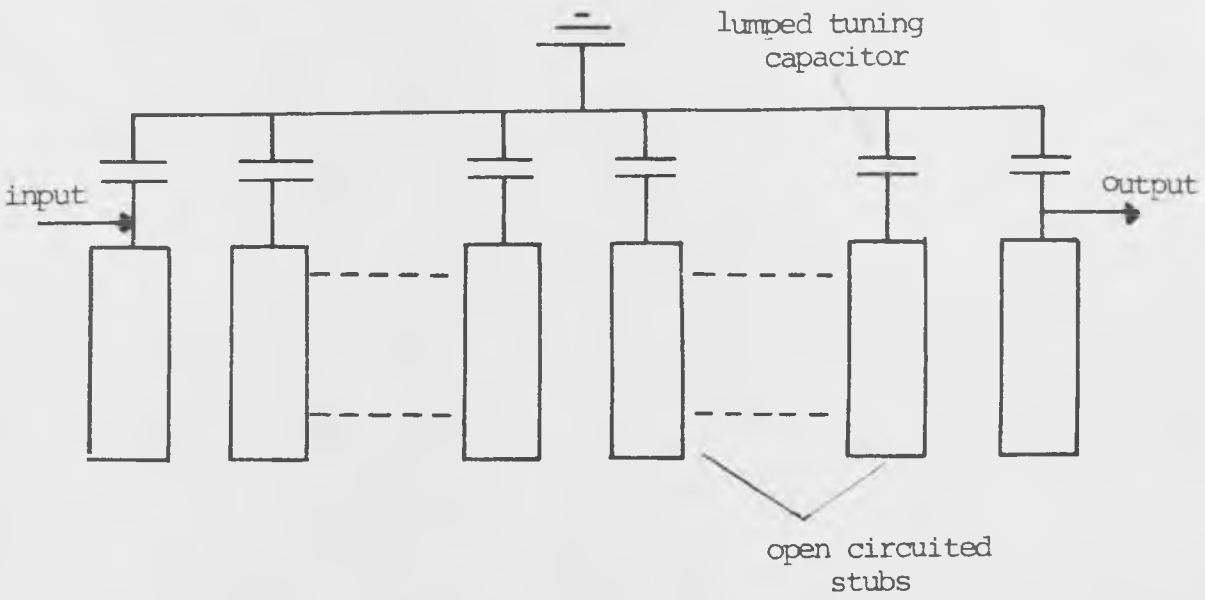

Fig. 4.2.8 The Open Circuited Combline Filter

Comparing this admittance with the admittance of the comb-line resonator it can be seen that it is identical except that $\tan(a\omega)$ has been replaced by $-1/\tan(a\omega)$. Using this substitution throughout section 3.2.1 results in the design equations for this filter. For this reason the proof of the design is not presented here, the equations are merely stated below.

The Design Process

Firstly compute the element values CL_r and $K_{r,r+1}$ in the lowpass prototype filter.

Choose C, the lumped tuning capacitor at band centre.

Choose the midband phase lengths of the resonators, this should be 135^o if optimum return loss is required and 136.26^o if constant bandwidth is required, there is however no significant difference between these two values.

Next calculate the admittance to ground at each node in the filter from

$$(Y_r + Y_{r-1,r} + Y_{r,r+1}) = -C\omega_o/\tan(\theta_o) \qquad (4.2.53)$$

Calculate the scaling factor of each resonator from

$$\alpha = \frac{2\omega_o}{\tan(\theta_o)\Delta\omega[\tan(\theta_o)-\theta_o(1+\tan^2(\theta_o))]} \qquad (4.2.54)$$

[for r = 2 to n - 1]

And

$$\alpha' = \alpha[1 + \frac{a\Delta\omega}{CL_1}] \qquad (4.2.55)$$

[for r = 1 and r = n]

Calculate the scaling factor at each node from

$$n_r = \left[\frac{CL_r^{\alpha}}{(Y_r + Y_{r-1,r} + Y_{r,r+1})\tan(\theta_o)} \right] \qquad (4.2.56)$$

Calculate the coupling admittance between the stubs from

$$Y_{r,r+1} = -K_{r,r+1}/[n_r.n_{r+1}\tan(\theta_o)] \qquad (4.2.57)$$

Calculate the admittance to ground of the rth stub from

$$Y_r = -C\omega_o/\tan(\theta_o) - Y_{r-1,r} - Y_{r,r+1} \qquad (4.2.58)$$

Finally calculate the admittances of the transformer elements from

$$Y_o = 1 - 1/n_1\sin(\theta_o) \qquad (4.2.59)$$

$$Y_{o1} = 1/n_1 \sin(\theta_o) \qquad (4.2.60)$$

$$Y_1' = 1/n_1^2 - 1/n_1 \sin(\theta_o) \qquad (4.2.61)$$

4.2.3 Theory of the Distributed Combline Filter

The theory of tunable combline filters is now extended to the design of a distributed combline filter suitable for S.S.S realisation of narrow band fixed frequency bandpass filters. Although either of the previous two filters can be used as fixed frequency filters they both require lumped capacitors in order for them to operate. This would not at first seem a problem since the capacitors could be realised using tuning screws. However, low loss filters require large

ground plane spacings and the screws must then penetrate deep into the cavity. The inductance of the screws can then seriously deteriorate the filter performance. It would thus be desirable if a design procedure could be developed for fixed frequency filters requiring no lumped capacitors.

The advantages of using a design technique based on the tunable combline filter are two fold. Firstly the redundant transformer elements cancel the frequency variation of the coupling between the resonators, thus low V.S.W.R. passbands of up to 30% can be achieved. Secondly, because the filter will inevitably require fine tuning, the advantage of having approximately constant bandwidth independent of tuned frequency is obvious.

The S.S.S circuit configuration of the distributed combline filter is shown in Fig. 4.2.9. This filter is relatively easy to analyse if the input and output feed terminals are located along the dotted lines in Fig. 4.2.9. In that case, the equivalent circuit of the filter is as shown in Fig. 4.2.10. The inductor symbols in Fig. 4.2.10 represent the long sections shown in Fig. 4.2.9, these being open circuited stubs of between one quarter and one half wavelength long at band centre. The capacitors represent the short sections, these being open circuited stubs which are less than one quarter wavelength long. With coupling allowed only between adjacent short sections it is obvious that the equivalent circuit of the filter is similar to that of a combline filter

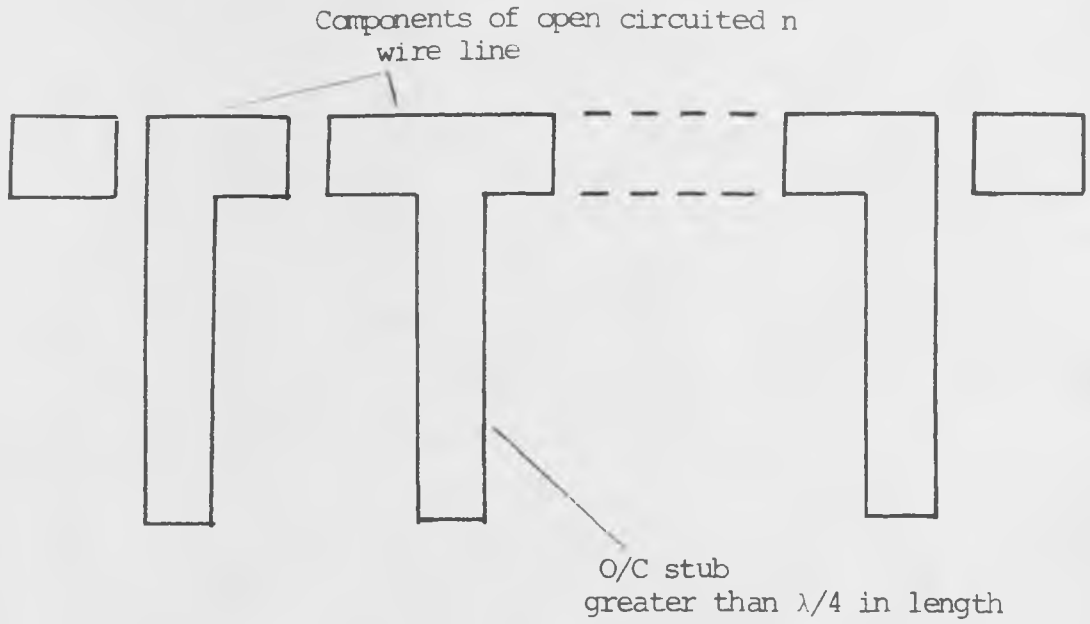

Fig. 4.2.9 The distributed combline filter structure

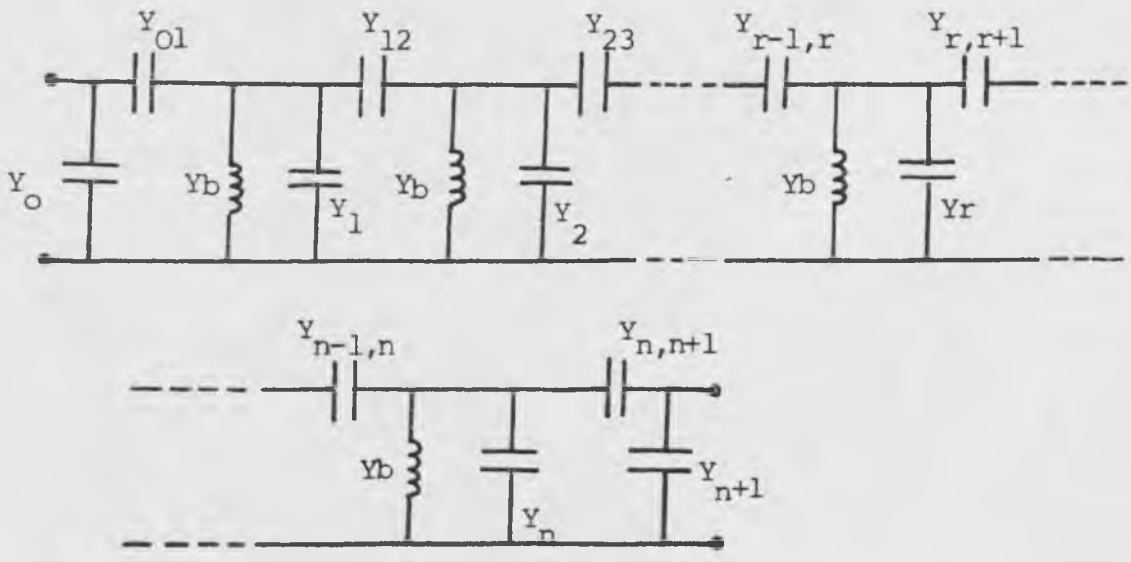

Fig. 4.2.10 Equivalent circuit of the distributed combline filter

with the n wire line composed of the short stubs and the resonating elements being the distributed inductive open-circuited stubs.

In Fig. 4.2.10 Yb represents the admittance of the inductive stubs, these all being identical. The propogation constants of the short and long stubs are denoted 'a' and 'b' respectively.

The process of obtaining a set of design equations for this filter is very similar to that for the previous two filters. Firstly, admittance inverters are formed, then the frequency dependence of the inverters is scaled into the terminating resistors and the network is scaled at each node to obtain realisable element values. The frequency transformation is

$$\omega \rightarrow \alpha[\beta \tan(b\omega)/\tan(a\omega) + 1] \qquad (4.2.62)$$

where

$$\alpha = \frac{n_r^2 \tan(a\omega_o)[Y_r + Y_{r-1,r} + Y_{r,r+1}]}{CL_r} \qquad (4.2.63)$$

And

$$\beta = Yb/[Y_r + Y_{r-1,r} + Y_{r,r+1}] \qquad (4.2.64)$$

$$= -\frac{\tan(a\omega_o)}{\tan(b\omega_o)}$$

For narrow bandwidths the passband bandwidth of the filter is approximated by

$$\Delta\omega = \frac{\sin(2a\omega_o)\sin(2b\omega_o)}{\alpha[a\sin(2b\omega_o) - b\sin(2a\omega_o)]} \qquad (4.2.65)$$

We require a turning point of 4.2.65, thus

$$\frac{\partial(\Delta\omega)}{\partial\omega} = 0 \Big|_{\omega=\omega_o} \qquad (4.2.66)$$

or

$$\frac{a^2\cos(2a\omega_o)}{\sin^2(2a\omega_o)} = \frac{b^2\cos(2b\omega_o)}{\sin^2(2b\omega_o)} \qquad (4.2.67)$$

The most obvious solution of 4.2.67 is that $a\omega_o = 45^o$ and $b\omega_o = 135^o$. Unfortunately, with this solution, from 4.2.64 we obtain

$$Yb = [Y_r + Y_{r-1,r} + Y_{r,r+1}] \qquad (4.2.68)$$

This is an unacceptable solution because for a finite physical separation between the long stubs we require Y_r greater than Yb. Solutions of 4.2.67 must thus be constrained to the following set

$$\begin{aligned} a\omega_o &< 45^o \\ b\omega_o &> 135^o \end{aligned} \qquad (4.2.69)$$

For example $a\omega_o = 30^o$ and $b\omega_o = 136^o$ are solutions of 4.2.67 and from 4.2.64 we then have

$$Yb = 0.57[Y_r + Y_{r-1,r} + Y_{r,r+1}] \qquad (4.2.70)$$

For narrow bandwidths $Y_{r-1,r}$ and $Y_{r,r+1}$ will be small and we thus have

$$Yb \simeq 0.57\, Y_r \qquad (4.2.71)$$

This implies a finite physical separation between the long stubs.

The Design Process for the Distributed Combline Filter

As stated, the design process of this filter is very similar to that for the tunable combline filter. The design process is not derived in detail, merely summarised below.

Firstly obtain the lowpass prototype element values $K_{r,r+1}$ and CL_r.

Choose $a\omega_o$ and $b\omega_o$ to satisfy 4.2.67 under the constraint of 4.2.69

Choose Yb

Calculate the admittance to ground at each node in the filter from

$$[Y_r + Y_{r-1,r} + Y_{r,r+1}] = \frac{-Yb \tan(b\omega_o)}{\tan(a\omega_o)} \qquad (4.2.72)$$

Calculate the resonator scaling factor α from

$$\alpha = \frac{\sin(2a\omega_o)\sin(2b\omega_o)}{\Delta\omega[a\sin(2b\omega_o) - b\sin(2a\omega_o)]} \qquad (4.2.73)$$

[for r = 2 to n - 1]

and

$$\alpha' = \alpha\left[1 + \frac{a\Delta\omega}{CL_1}\right] \qquad (4.2.74)$$

[for r = 1 and r = n]

Calculate the scaling factor at each node in the filter from

$$n_r = [CL_r\alpha/[\tan(a\omega_o)(Y_r + Y_{r-1,r} + Y_{r,r+1})]]^{\frac{1}{2}} \qquad (4.2.75)$$

Calculate the coupling admittance between each stub from

$$Y_{r,r+1} = \frac{K_{r,r+1}}{n_r n_{r+1} \tan(a\omega_o)} \qquad (4.2.76)$$

Calculate the admittance to ground of each stub from

$$Y_r = \frac{-Yb \tan(b\omega_o)}{\tan(a\omega_o)} - Y_{r-1,r} - Y_{r,r+1} \qquad (4.2.77)$$

Finally the admittances of the transformer elements (of electrical length aω) are calculated from

$$Y_o = 1 - 1/n_1 \sin(a\omega_o) \qquad (4.2.78)$$

$$Y_{01} = 1/n_1 \sin(a\omega_o) \qquad (4.2.79)$$

$$Y_1' = 1/n_1^2 - 1/n_1 \sin(a\omega_o) \qquad (4.2.80)$$

4.3 Design of Tunable Bandpass Filters

4.3.1 Computer Analysis of Tunable Bandpass Filters

In order to predict the performance of varactor tuned and fixed frequency filters computer analysis programs were

developed. The varactor equivalent circuit model and the S.S.S. losses were included in the programs as described in chapter three.

Figures 4.3.1 - 4.3.3 show the computed midband dissipation loss of varactor tuned combline filters as a function of the passband bandwidth, the degree of the filter, and bias voltage. The results were obtained from the analysis of filters with a centre frequency of 4GHz, a passband return loss of 15dB and with the MA46620G varactor as the tuning element. The S.S.S loss was not included in this analysis as it is primarily caused by lossy short circuits which are not ammenable to analysis.

In order to use the data presented in Figs. 4.3.1 to 4.3.3 to predict the insertion loss of a filter with a midband frequency other than 4GHz the bandwidth of the filter must be scaled by a factor 4/fo where fo is the centre frequency of the filter in GHz.

Computer analysis of the tunable open circuited combline filter is not presented. This is because in Appendix 4.2 it is shown that the Q factor of this filter is approximately double that of the tunable combline filter. Thus, the loss of this filter will be the same as that for a combline filter with double the bandwidth.

The computed midband dissipation loss of the distributed combline filter is shown in Fig. 4.3.4. The data presented in Fig. 4.3.4 is for 4GHz filters with 0.3" ground plane spacings. The analysis of filters with other centre frequencies and ground plane spacings is easily accomplished since the

Bandwidth	Bias 0V	Bias 4V	Bias 30V
0.5%	19.7dB	14.7dB	9.98dB
1%	11.9dB	8.4dB	5.5dB
2%	6.5dB	4.4dB	3.1dB
5%	2.65dB	1.8dB	1.5dB
10%	1.4dB	0.97dB	0.7dB

Fig. 4.3.1 Computed Mid-Band Loss of Varactor tuned Combline Filters of degree two as a function of passband bandwidth and bias voltage

Bandwidth	Bias 0V	Bias 4V	Bias 30V
0.5%	37.5dB	29dB	23.1dB
1%	23.0dB	17.2dB	12.9dB
2%	13.4dB	9.2	7.1
5%	9.3dB	6.1dB	4.9dB
10%	5.7	3.7dB	3.1dB

Fig. 4.3.2 Computed Mid-Band Loss of Varactor tuned Combline Filters of degree three

Bandwidth	Bias 0V	Bias 4V	Bias 30V
0.5	55	44	34
1	36.2	26.8	20
2	20.9	14.5	10.8
5	9	5.9	4.4
10	4.65	3.2	2.5

Fig. 4.3.3 Computed Mid-Band Loss of Varactor tuned Combline Filters of degree 4

Bandwidth	Degree 3	Degree 5	Degree 7	Degree 9	Degree 11
0.5%	1.8dB	11 dB	19.9dB	33.6dB	49.7dB
1%	0.6dB	3.5dB	7.7dB	14.9dB	23.3dB
2%	0.26dB	1.66dB	3.85dB	6.9dB	11.1dB
5%	0.17dB	0.6dB	1.42dB	2.59dB	4.1dB
10%	0.09dB	0.3dB	0.65dB	1.18dB	1.86dB

Fig. 4.3.4 Computed Mid-Band Loss of 4 GHz distributed combline filters as a function of bandwidth and degree. These results are for a ground plane spacing of 0.3"

filter Q factor is proportional to the ground plane spacing and proportional to the square root of frequency.

4.3.2. Design of a Varactor Tuned Combline Filter

The initial aim in varactor tuned bandpass filter design was to achieve octave tuning. This requires a 6:1 capacitance ratio to tune from $\theta = 30^{o}$ to $\theta = 60^{o}$. Varactors with chip capacitance ratios of 8:1 are available but these capacitance ratios are severely degraded when the chip is enclosed in a microwave package. For example, the MA 46620G varactor has Cj(o) = 0.8pF and Cj(-60) = 0.1pF. This varactor is enclosed in a stripline package with a capacitance of 0.18pF. The terminal capacitance ratio of the packaged varactor is thus reduced to 3.5:1. This capacitance ratio will provide tuning from $\theta = 35^{o}$ to $\theta = 55^{o}$ which is considerably less than an octave range. Attempts to remove package effects by bonding varactor chips directly onto the S.S.S circuit board have proved unsuccessful because of poor contacts and the long highly inductive bandwire required. Octave tuning would thus seem to be restricted to lower frequencies where higher capacitance varactors can be used. For example, hyperabrupt varactors with zero bias capacitances of 4pF and chip capacitance ratios of 10:1 are commercially available. Even when packaged, these devices will exhibit terminal capacitance ratios of 7:1. Unfortunately, the Q factors of these varactors are too low for the application of broadband tuning of microwave filters above frequencies of 1GHz.

The design objective was thus to realise a tunable combline filter capable of tuning from $\theta = 35^{o}$ to $\theta = 55^{o}$. The centre frequency of this filter was to be 4GHz and the midband dissipation loss was to be less than 6dB. The loss specification which seems somewhat arbitrary, was chosen because it is similar to specifications offered by manufacturers of U.H.F. varactor tuned filters. Examining Fig. 4.3.1 we see that a two resonator filter with a 5% passband bandwidth tunable about 4GHz, will have a maximum midband loss of 3dB. This is the computed loss contributed by the varactors. Further loss will be contributed by the short circuits of the S.S.S resonators and by the varactor contact resistance. The total extra loss will probably be less than 2dB, thus this specification will satisfy the loss requirement of 6dB maximum.

The design process in section 4.2.1 was used to design the filter to the following specifications

Centre frequency	4GHz
Passband bandwidth	200 MHz
Passband return loss	15dB
Varactor capacitance	0.6pF
Length of resonators at mid-band	45^{o}
Number of resonators	2

The varactor capacitance used in the design process was 10% less than the geometric mean of the zero bias and 60V varactor capacitances. This value was used to compensate for the varactor bondwire inductance which tends to tune the filter down in frequency.

The admittances of the stubs in the combline filter were calculated to be as follows (for a 1Ω system):

$Y_o = 0.6607$

$Y_{o1} = 0.3393$

$Y_1 = Y_2 = 0.4517$

$Y_{12} = 0.0668$

Calculations of the Dimensions of the Combline Filter

The procedure for calculating the physical dimensions of the combline filter is somewhat different to previously presented methods because the lines are coupled, this procedure is now presented in detail.

Firstly, the static capacitances of the stubs (per unit length) are calculated using

$$C/\varepsilon = 7.54\ Y \qquad (4.3.1)$$

Thus

$C_o/\varepsilon = 4.982$

$C_{o1}/\varepsilon = 2.558$

$C_1/\varepsilon = C_2/\varepsilon = 3.4058$

$C_{12}/\varepsilon = 0.5037$

Next the normalised coupling gaps between the stubs can be obtained by using the values of C_{o1} and C_{12} in the graph of $\Delta C/\varepsilon$ as a function of s/b in Appendix 2.1. These values are

$$\frac{S01}{b} = 0.015$$

$$\frac{S12}{b} = 0.305$$

A ground plane spacing of 0.3" was to be used, thus

$$S01 = 0.0045"$$

$$S12 = 0.0915"$$

Next, the widths of the bars must be evaluated. The capacitance to ground of an S.S.S bar is affected by its proximity to neighbouring bars. The total capacitance per unit length to ground of such a bar is expressed by

$$\frac{C}{\varepsilon} = \frac{4w}{b} + 2Cf'e_1 + 2Cf'e_2 \qquad (4.3.2)$$

where $Cf'e_1$ and $Cf'e_2$ are the fringing capacitances from one corner and half the associated vertical side wall of an S.S.S bar to ground when an open circuit is placed along the line midway between a bar and its nearbouring bar. These fringing capacitances are known as the even mode fringing capacitances. The even mode fringing capacitances are presented as a function of the separation between the bars in Appendix 2.1.

For the transformer stubs at the input and output of the filter we have

$$Cf'e_1 \text{ and } Cf' = 0.45$$

From Appendix 2.1

$$Cf'e_2 = 0.014$$

Rearranging 4.3.2 we obtain

$$\frac{w}{} = \frac{b}{4}\left[\frac{c}{\varepsilon} - 2Cf'e_1 - 2Cf'e_2\right] \qquad (4.3.3)$$

Thus for the transformer stubs

$$w_o = \frac{0.3}{4}[4.982 - 0.9 - 0.028]$$

$$w_o = 0.304"$$

For the resonators the even mode fringing capacitances are

$$Cf'e_1 = 0.014$$

$$Cf'e_2 = 0.23$$

Thus, from 4.3.2

$$w_1 = w_2 = 0.218"$$

The calculation of the lengths of the resonators was relatively simple. These were designed to be 45^o long at 4GHz which is a length of 0.369". The lengths were then modified to account for fringing from the ends using equation 2.1.13 as follows

$$L \rightarrow L - 0.23b \qquad (4.3.4)$$

With b = 0.3" we obtain

$$L = 0.3"$$

Design of bias chokes

The combline resonators are short circuited at one end by clamping them into the side walls of the S.S.S housing. Thus a d.c. short circuit exists at one end of the resonator. Consequently, the r.f short circuit needed by the varactors cannot be realised by a d.c. short circuit, otherwise both terminals of the varactor would be short circuited to d.c. The r.f. short circuit to the varactors was provided by connecting a 10pF chip capacitor in series with the varactors to ground. The bias filter was then connected at the junction of the chip capacitor and the varactor. The bias filter design was otherwise similar to that described in section 4.3.2. The layout of the printed circuit board of the filter is shown in Fig. 4.3.6.

The design of the S.S.S housing was essentially similar to that for the bandstop filters. The housing was gold plated to provide good ohmic connections for the short circuits. The assembled filter with the top half removed is shown in photograph no. 3.

Measured Performance of the Varactor Tuned Combline Filter:

The frequency response of this filter is shown in Figs. 4.3.7 - 4.3.9 for bias voltages of 0V, 4V and 30V. The performance of this device is summarised below

Bias Voltages = OV, OV

Passband

Centre Frequency	3.2 GHz
Passband Bandwidth	186 MHz
Passband Insertion Loss	5.4 dB
Passband Return Loss	8.1 dB

Stopband

Fo ± 400 MHz	24 dB
Fo ± 1000 MHz	38 dB

Bias Voltages = 4V, 3.8V

Passband

Centre Frequency	4.16 GHz
Passband Bandwidth	209 MHz
Passband Insertion Loss	4.1 dB
Passband Return Loss	10.5 dB

Stopband

Fo ± 400 MHz	26 dB
Fo ± 1000 MHz	39 dB

Bias Voltages = 30V, 25.6V

Passband

Centre Frequency	4.8 GHz
Passband Bandwidth	189 MHz
Passband Insertion Loss	4.2 dB
Passband Return Loss	9.1 dB

Stopband

Fo ± 400 MHz	26 dB
Fo ± 1000 MHz	37 dB

The tuning bandwidth of the combline filter was slightly less than expected. This was a result of the fringing capacitance from the ends of the combline resonators to ground. This capacitance appears in parallel with the varactor thus effectively increasing the parasitic package capacitance. The value of the fringing capacitance was calculated to be 0.045 pF which is 20% of the varactor package capacitance. Experiments involving rounding the corners of the combline resonators to minimise this capacitance have proved unsuccessful and it would thus appear that the fringing must be accepted.

Large Signal Effects

Second harmonic distortion was measured using the same techniques as in section 3.5. The 2nd ordered intercept point was + 7 dBm at 1 volt bias and +31 dBm at 10 volts bias. This is approximately 6 dBm lower than that of the bandstop filter and is explained by the fact that the varactors are more strongly coupled into the bandpass filter than the bandstop filter. Again, no third harmonic distortion was observed.

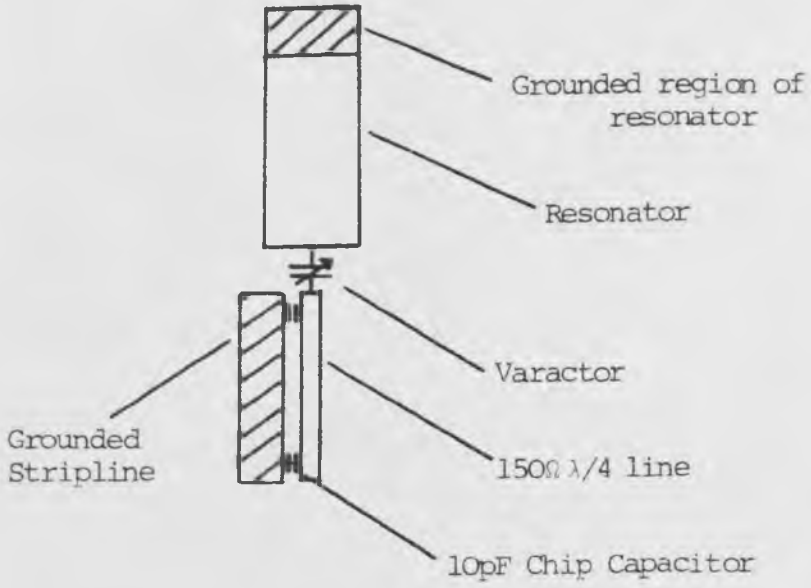

Fig. 4.3.5 Realisation of bias filter

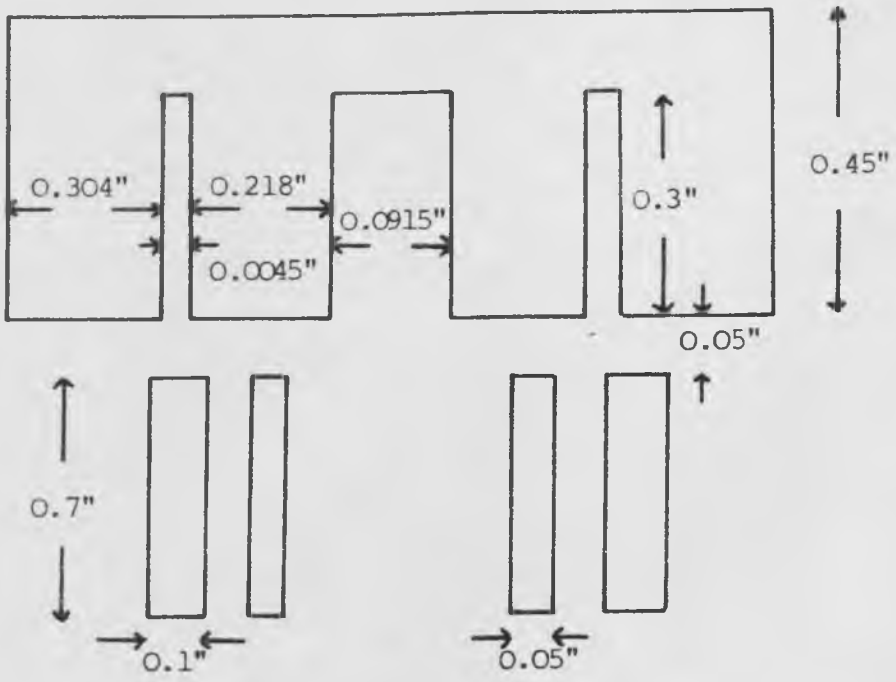

Fig. 4.3.6 The dimensions of the Printed Circuit of the varactor tuned Combline Filter

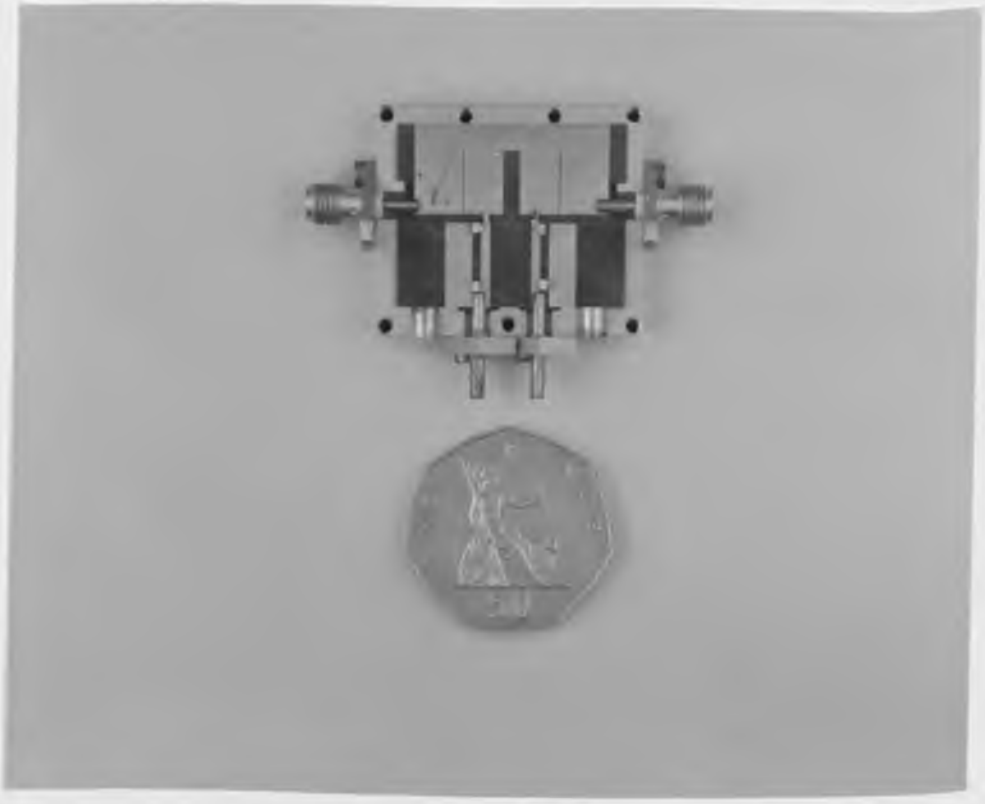

Photograph no. 3

The Varactor tuned Combline Filter

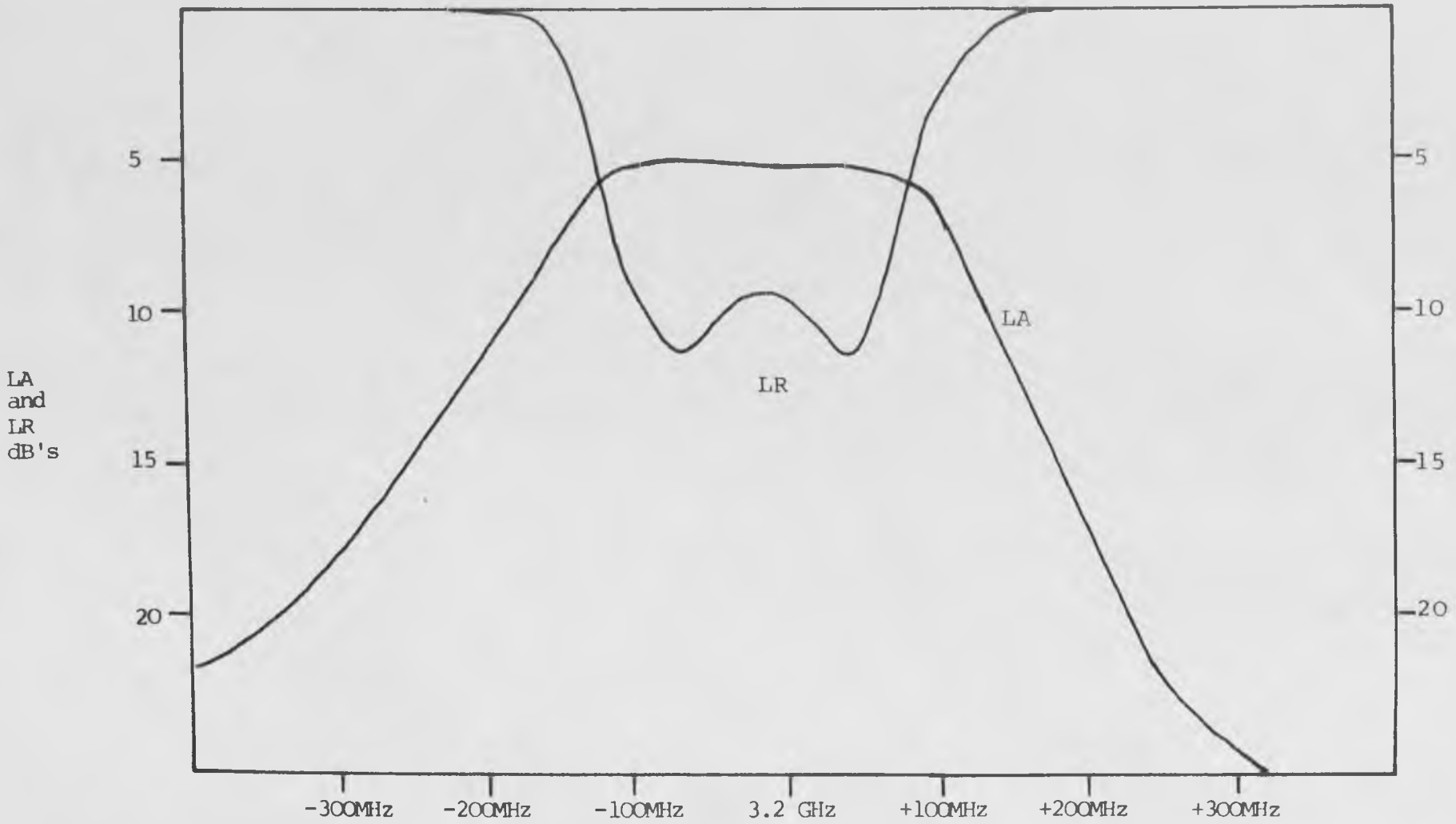

Fig. 4.3.7 Frequency Response of Varactor tuned Combline Filter at zero bias

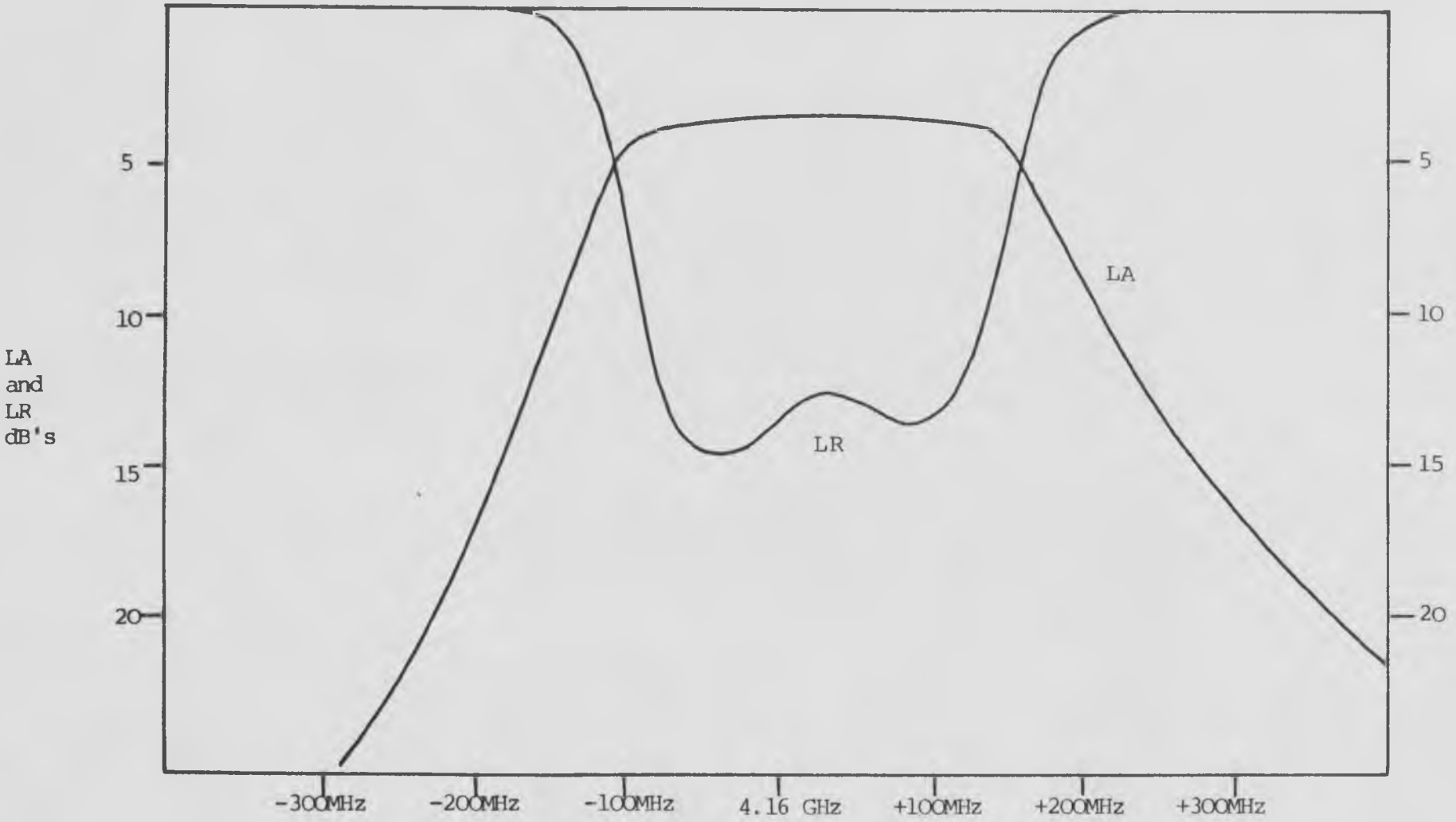

Fig. 4.3.8 Frequency Response of varactor tuned Combline Filter with approximately 4V bias

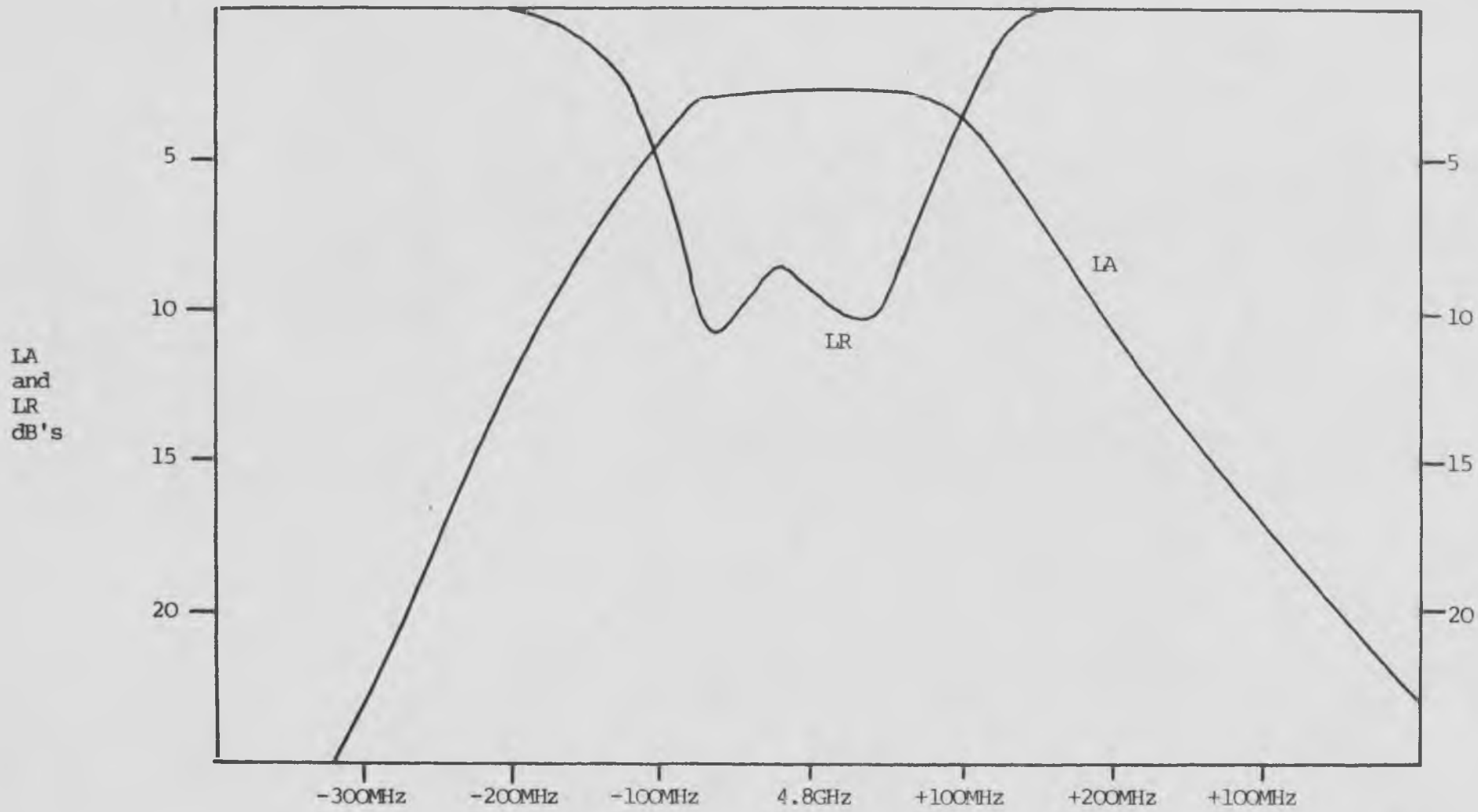

Fig. 4.3.9 Frequency Response of Varactor Tuned Combline Filter with 30V bias

4.3.3 Design of a Varactor Tuned Open Circuited Combline Filter

A varactor tuned open circuited combline filter was designed and constructed to the following specifications.

Centre frequency	4GHz
Tuning bandwidth	1GHz
Passband bandwidth	120MHz
Passband return loss	15dB
Number of resonators	3
Passband insertion loss	< 7dB

The computed midband insertion loss of this filter was less than 5dB at any tuned frequency. The element values of the combline array were evaluated using the technique described in section 4.2.2. The element values were

Y_O	=	0.683
Y_{O1}	=	0.3108
$Y_1 = Y_3$	=	0.3328
Y_{12}	=	0.0494
Y_2	=	0.5518

The physical design and construction of this filter was essentially the same as the method described in section 4.3.1. The layout of the S.S.S circuit board of this filter is shown in Fig. 4.3.10 and a picture of the assembled device is shown in photograph no. 4.

The measured performance of this filter is summarised below.

Bias Voltages = 0V, 0.01V, 0V

Passband

Centre Frequency	31.51 GHz
Passband Bandwidth	108 MHz
Passband Insertion Loss	6.1 dB
Passband Return Loss	9.1 dB

Stopband

Fo ± 200 MHz	35 dB
Fo ± 500 MHz	57 dB

Bias Voltages = 4V, 4.61V, 4.2V

Passband

Centre Frequency	3.9 GHz
Passband Bandwidth	118 MHz
Passband Insertion Loss	5.2 dB
Passband Return Loss	11 dB

Stopband

Fo ± 200 MHz	37 dB
Fo ± 500 MHz	59 dB

Bias Voltages 30 V, 38.7V, 32V

Passband

Centre Frequency	4.43 GHz
Passband Bandwidth	112 MHz
Passband Insertion Loss	4.3 dB
Passband Return Loss	10.1 dB

Stopband

Fo ± 200 MHz	36 dB
Fo ± 500 MHz	54 dB

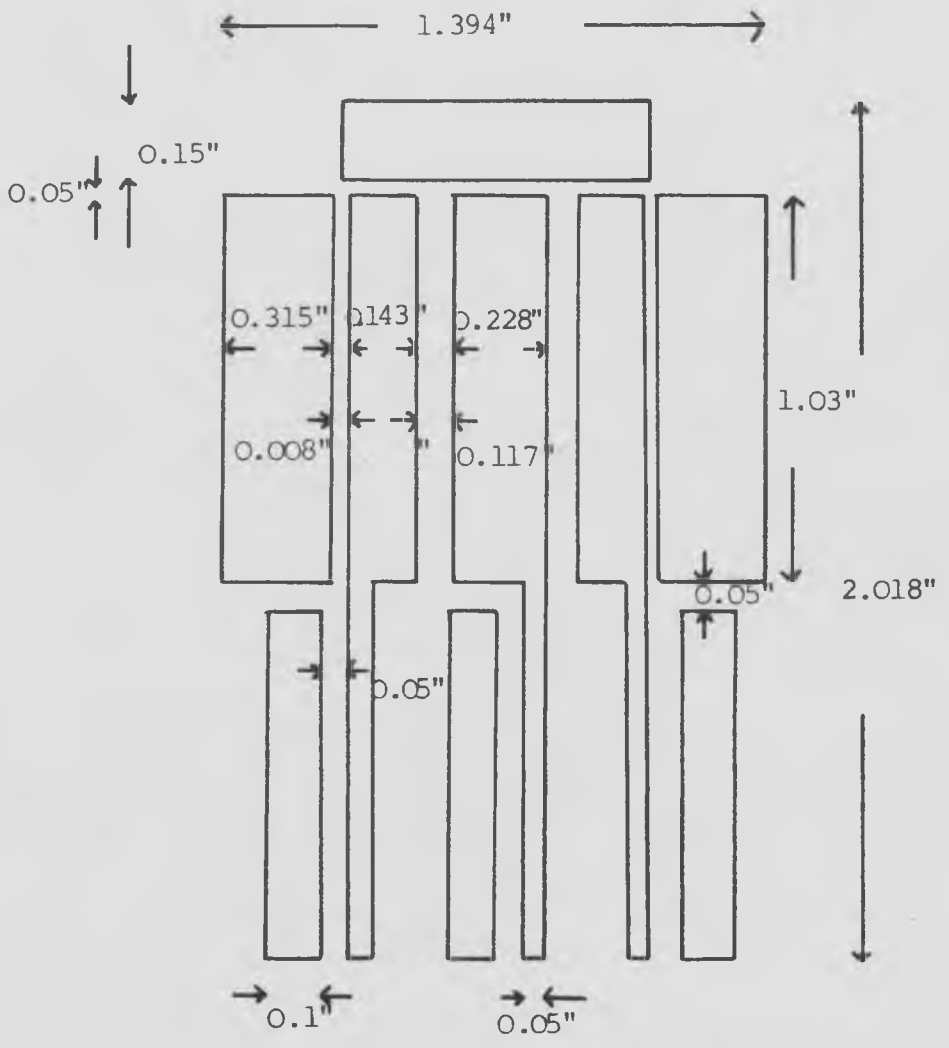

Fig. 4.3.10 Dimensions of the circuit board of the open circuited combline varactor tuned filter

Photograph no. 4

The Varactor tuned Open Circuited Combline Filter

4.3.4 Design of Fixed Frequency Distributed Combline Filters

Two distributed combline filters were designed to the following specifications

Design 1

Centre frequency	4 GHz
Passband bandwidth	50 MHz
Passband return loss	15 dB
Number of resonators	3

Design 2

Centre frequency	4 GHz
Passband bandwidth	200 MHz
Passband return loss	15 dB
Number of resonators	3

Design 1

The element values for the distributed combline filter were computed using the procedure in section 4.2.3. The admittances of the long resonators, of electrical length 136^{o} were chosen to be 0.5 The admittances of the array of stubs of length 36^{o} were

$$Y_{o} = 0.746$$
$$Y_{o1} = 0.232$$
$$Y_{1} = Y_{3} = 0.572$$
$$Y_{12} = Y_{23} = 0.026$$
$$Y_{2} = 0.781$$

A ground plane spacing of 0.3" was chosen and the physical dimensions of the filter were calculated using the same procedure as for the tunable combline filter.

Correction for Coupling Between Resonators

In the design process, the 136^{o} long stubs were assumed to be isolated from each other. In practice this is not the case and they were 0.387" apart. This corresponds to a coupling admittance (normalised to 1Ω) of 0.0027 The unwanted coupling will alter the response of the filter. The coupling can be removed by inserting walls in the S.S.S housing between the stubs. This is, of course, a complicated mechanical procedure and it is simpler to alter the coupling between the 36^{o} long stubs to compensate for the unwanted coupling. The coupling admittance between the 36^{o} long stubs was 0.026 and thus the total coupling admittance between the resonators at 4GHz was

$$Y = 0.025 \tan(36) + 0.0027 \tan(136) \qquad (4.3.5)$$

$$= 0.0188 - 0.0026$$

The admittance between the 36^{o} stubs should thus be increased by 0.0026 at 4GHz.

Thus $Y_{12} \tan(36) = 0.0214$

or $Y_{12} = 0.295$

The modified circuit board dimensions of this filter are shown in Fig. 4.3.11. A picture of the assembled filter is shown in photograph no. 5.

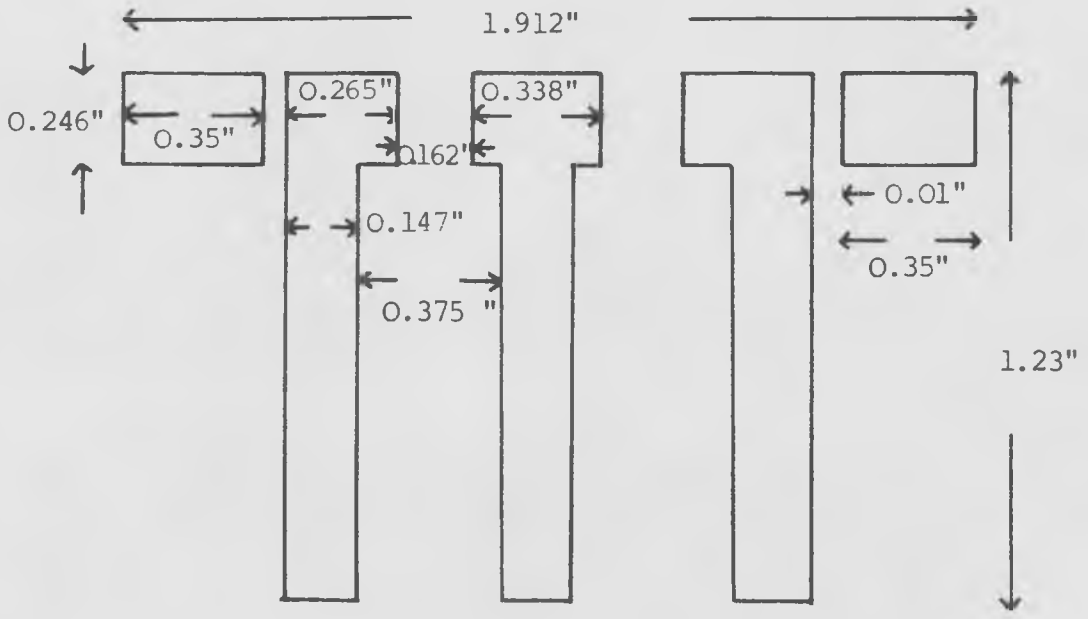

Fig. 4.3.11 Dimensions of the Narrow Band Distributed Combline Filter

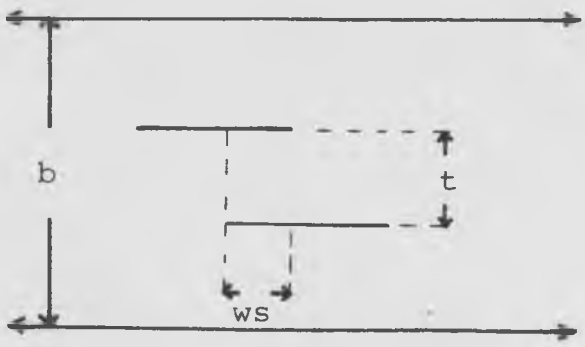

Fig. 4.3.12 Broadside Coupled Strips used for realising high values of coupling admittance

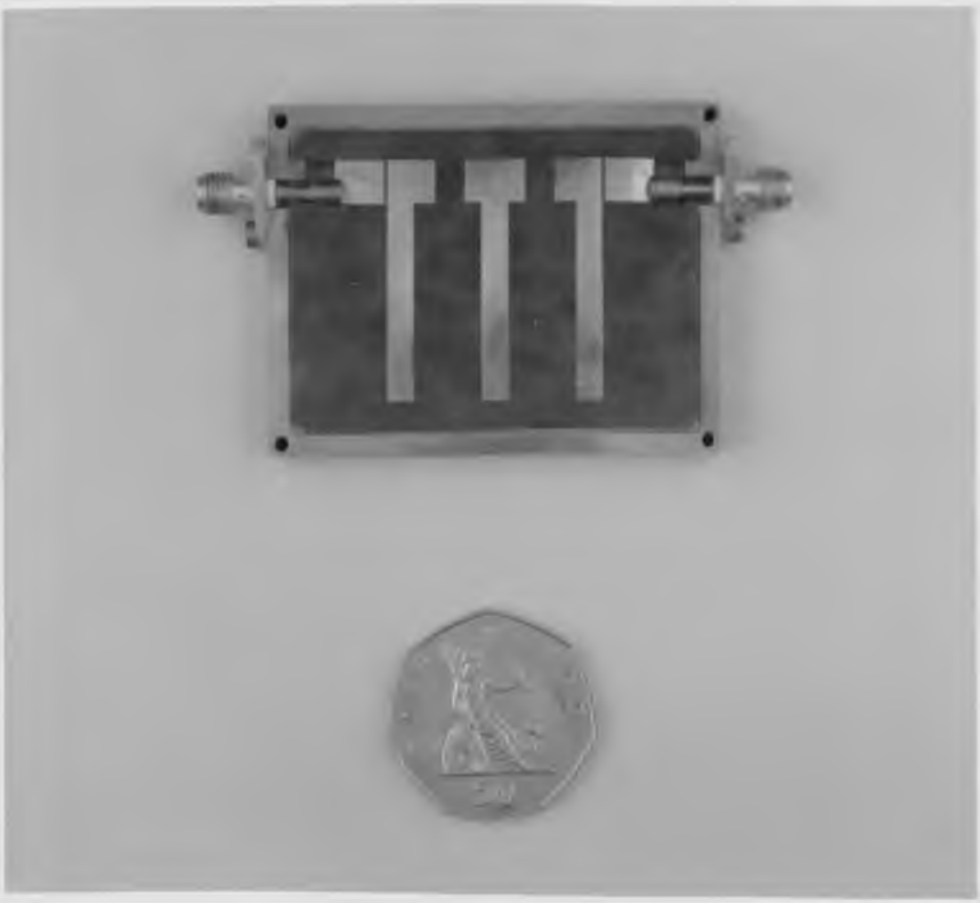

Photograph no. 5

The 4GHz Distributed Combline Filter

Design 2

The element values of this filter were calculated using the procedure described in section 4.2.3. The lengths of the short resonators were 20° at 4GHz and the long resonators were 137° long. The long resonators were chosen to have a characteristic admittance of Yb = 0.45 and the admittances of the remaining elements (normalised to a 1Ω system) are shown below.

$$Y_o = 0.273$$
$$Y_{01} = 0.72$$
$$Y_1 = Y_3 = 0.493$$
$$Y_{12} = Y_{23} = 0.167$$
$$Y_2 = 0.991$$

The design of the physical dimensions of the S.S.S circuit board were similar to that for design 1 with one exception. The value of Y_{01} of 0.72 was relatively high and could not be realised by side coupled strips. This coupling was achieved by overlapping strips on opposite sides of the dielectric circuit board [Fig.4.3.12]. An approximate design procedure for calculating the overlap w_s for a given coupling capacitance ΔC is presented in ref 4.4. This procedure assumes zero thickness conductors and a homogeneous dielectric medium. In practice, the coupled lines operate in an inhomogeneous dielectric medium, but since the dominant coupling fields occur mainly in the dielectric circuit board, this will not be a serious problem. The overlap distance w_s is calculated as follows

$$\frac{ws}{b} = \frac{1}{\pi}\left[\frac{t}{b}\log_e\left(\frac{q}{a}\right) + (1-t/b)\log_e\left(\frac{1-q}{1+a}\right)\right] \qquad (4.3.6)$$

where

$$q = K/a \qquad (4.3.7)$$

$$K = \left[\exp\left(\frac{\pi\Delta C}{2}\right) - 1\right] \qquad (4.3.8)$$

$$a = \sqrt{\left(\frac{t/b-K}{t/b+1}\right)^2 + K} - \left(\frac{t/b-K}{t/b+1}\right) \qquad (4.3.9)$$

In these equations ΔC is the required coupling capacitance defined by

$$\Delta C = \frac{7.54\ Y_{01}}{\sqrt{\varepsilon_r}} \qquad (4.3.10)$$

However, the effective electrical length of a transmission line in a dielectric is increased by a factor $\sqrt{\varepsilon_r}$, thus in order to preserve the correct coupling admittance at the mid-band frequency of the filter ΔC must be modified as below

$$\Delta C = \frac{7.54\ Y_{01}}{\varepsilon_r} \qquad (4.3.11)$$

Note that 4.3.11 is only valid for short electrical lengths of transmission line ($\theta < 45^{\circ}$) when the tangential frequency behaviour is not significant. In this particular example this condition is satisfied.

For $Y_{01} = 0.72$ then

$$\Delta C = 2.467$$

Using this value of ΔC and applying 4.3.6 - 4.3.10 we obtain

$$\underline{ws = -0.027"}$$

Where the negative sign indicates that the lines are offset rather than overlapping.

The remainder of the design of this filter was similar to that for design 1. The final dimensions of the circuit board are shown in Fig. 4.3.13.

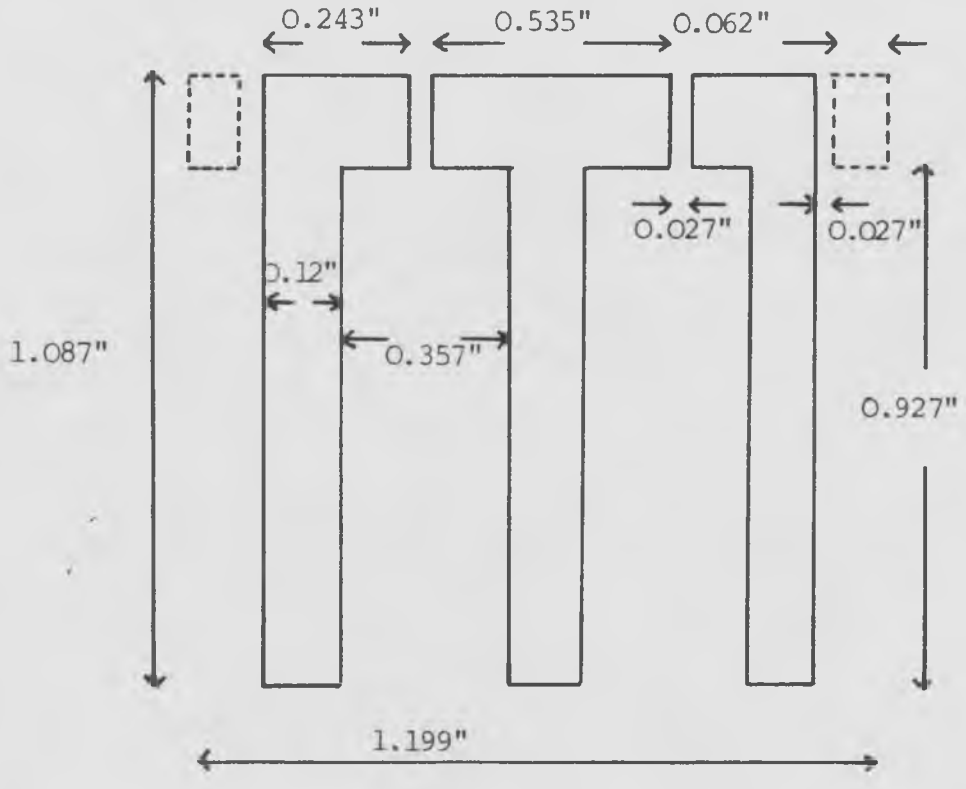

Fig. 4.3.13 Dimensions of the 5% Bandwidth Distributed Combline Filter

Measured Performances of the Fixed Frequency Bandpass Filters

Design 1

Initially, this filter exhibited an undercoupled response. This was caused by fringing capacitance between the ends of the transformer elements and the first and last stubs which increased the effective value of Y_{01}. To compensate for this fringing the coupling gaps at the input and output of the filter were increased until an equiripple response was observed. This occurred when the coupling gaps were 0.021", i.e. approximately double their designed value. The response of this filter is shown in Fig. 4.3.14 and is summarised below.

Passband

Centre frequency	4 GHz
Bandwidth	45MHz
Return loss	15 dB
Insertion loss	2 dB

Stopband

Fo $\pm$ 100MHz	35 dB
Fo $\pm$ 200 MHz	50 dB

Design 2

This filter performed according to the specification at the first attempt. The response, shown in Fig. 4.3.15 is summarised below

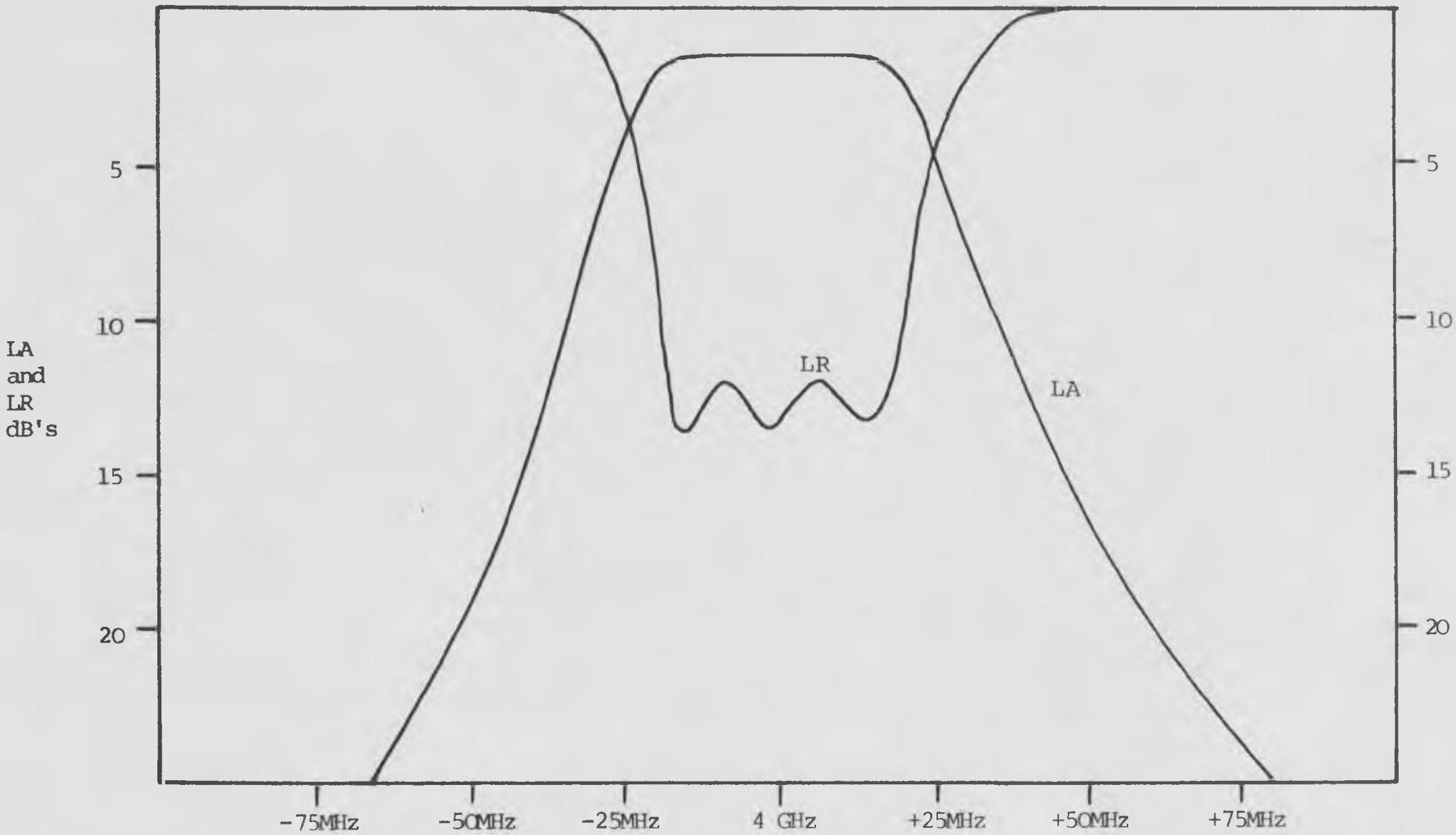

Fig. 4.3.14 Frequency Response of the 1% Bandwidth Distributed Filter

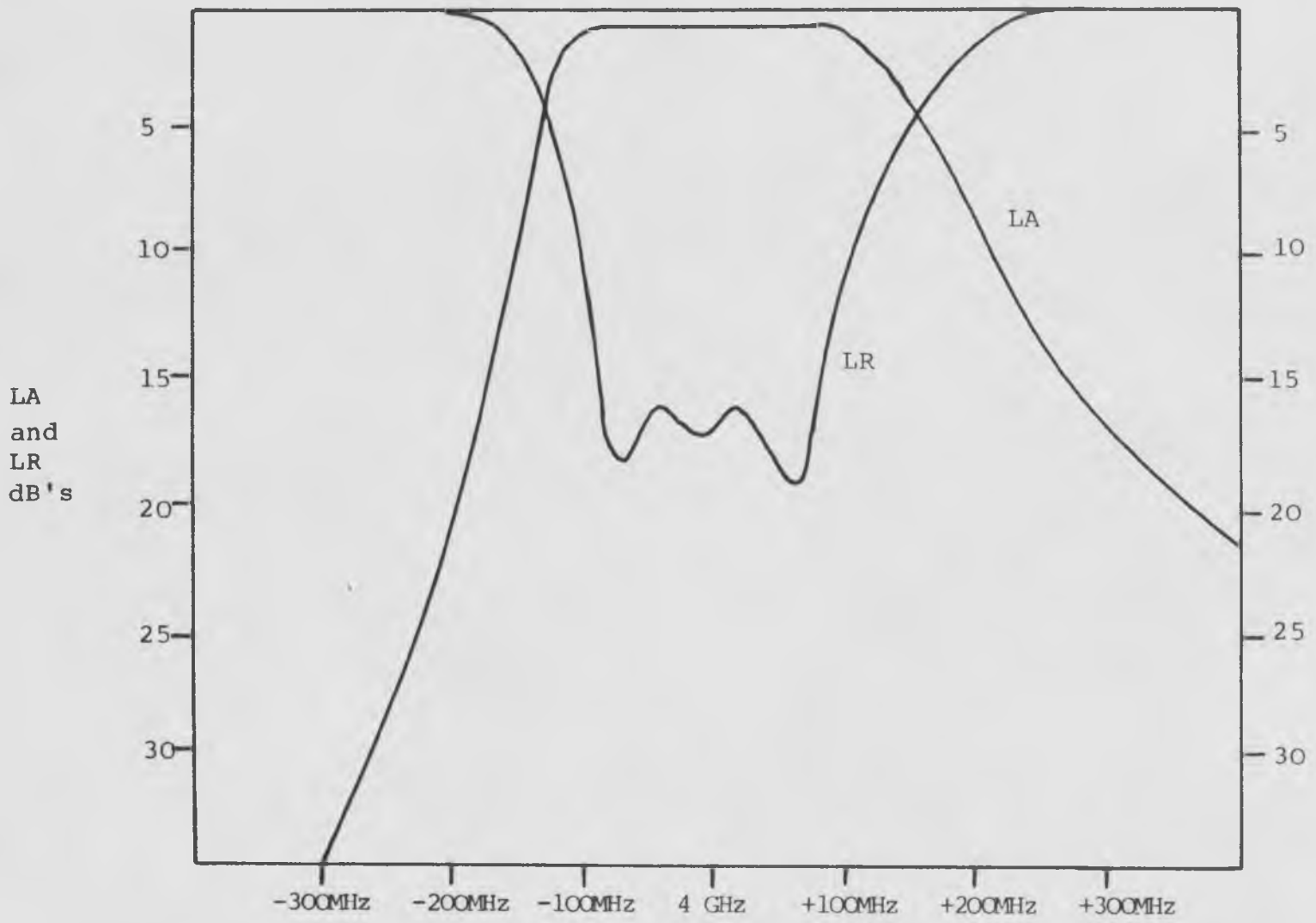

Fig. 4.3.15 Frequency Response of the 5% Bandwidth Distributed Filter

Passband	
Centre frequency	4 GHz
Bandwidth	200MHz
Return loss	17 dB
Insertion loss	0.4 dB
Stopband	
Fo $\pm$ 400 MHz	28 dB
Fo $\pm$ 800 MHz	45 dB

4.4 Conclusions

A novel design theory has been developed for tunable combline filters capable of octave tuning with approximately constant response shape. Explicit design formulae are presented. Computer analysis of varactor tuned combline filters is presented enabling the performance of any device to be predicted. Experimental devices have been constructed and the results exhibit close agreement with theory.

The basic tunable combline filter theory is extended to the design of open circuited combline and distributed combline filters. Computer analysis and experimental performances of these devices are also presented.

References

4.1 "Theory of Microwave Coupled Line Networks"
J.O. Scanlan
I.E.E.E. Proceedings Vol 68 No 2 FEB 1980

4.2 'Combline Filters of Narrow or Moderate Bandwidth'
G.L. Matthaei
Microwave Journal, Vol 6 pp82-91 (AUG 1963)

4.3 'Theory of Electrical Filters'
pp 48-49
J.D. Rhodes
Wiley

4.4 'Impedance of Offset Parallel Coupled Strip Transmission Lines'
J.P. Shelton Jr.
I.E.E.E. Trans MTT VOL MTT-14 No 1 JAN 1966

Appendix 4.1

Derivation of the values of the transformer elements in the combline filter.

The input/output coupling network is shown in Fig. 4.2.5. It is assumed, for simplicity, that the network is symmetrical, i.e. $Y_o = Y'_1$. Evaluating the input admittance of this network, looking back into the load via Y'_1, and after scaling by the factor $\tan(a\omega)/\tan(a\omega_o)$ we obtain the real and imaginary parts below.

$$|\text{Re } Yin(j\omega) = \frac{\tan(a\omega)}{\tan(a\omega_o)[(1+Y_o/Y_{o1})^2 + \tan^2(a\omega)/Y_{o1}^2]} \qquad (A.4.1)$$

$$|\text{Im } Yin(j\omega) =$$

$$\frac{-[(1+Y_o/Y_{o1})\,Y_o\,(2 + Y_o/Y_{o1}) + \tan^2(a\omega)(1 + Y_o/Y_{o1})/Y_{o1}]}{\tan(a\omega_o)[(1 + Y_o/Y_{o1})^2 + \frac{\tan^2(a\omega)}{Y_{o1}^2}]} \qquad (A.4.2)$$

For a perfect match at $\omega = \omega_o$ we require

$$|\text{Re}Yin(j\omega_o) \equiv 1 \qquad (A.4.3)$$

$$|\text{Im } Yin(j\omega_o) \equiv 0 \qquad (A.4.4)$$

From A.4.3, A.4.4 and A.4.1 we obtain

$$(1 + Y_o/Y_{o1})^2 + \tan^2(a\omega_o)/Y_{o1}^2 = 1 \qquad (A.4.5)$$

or

$$Y_o^2 + 2\,Y_o\,Y_{o1} + \tan^2(a\omega_o) = 0 \qquad (A.4.6)$$

Substituting A.4.6 into A.4.1 we obtain

$$|\mathrm{Re}\,Yin(j\omega) = \frac{\tan(a\omega)}{\tan(a\omega_o)\left[1 - \frac{\tan^2(a\omega)}{Y_{01}^2} + \tan^2\frac{(a\omega_o)}{Y_{01}^2}\right]} \qquad (A.4.7)$$

With $a\omega = \theta$ and after some manipulation we obtain

$$|\mathrm{Re}Yin(j\omega) = \frac{Y_{01}^2 \sin(\theta)\cos(\theta)\cos^3(\theta_o)}{\sin(\theta_o)\left[Y_{01}^2\cos^2(\theta)\cos^2(\theta_o) + \cos^2(\theta_o) - \cos^2(\theta)\right]} \qquad (A.4.8)$$

Examining A.4.8 we see that if the denominator were made frequency invarient we would obtain the required slow frequency variation of $\sin(\theta)\cos(\theta) = \sin(2\theta)/2$. To remove the frequency dependence of the denominator we have

$$Y_{01} = 1/\cos(\theta_o) \qquad (A.4.9)$$

Thus

$$|\mathrm{Re}Yin(j\omega) = \frac{\sin(2\theta)}{\sin(2\theta_o)} \qquad (A.4.10)$$

Substituting A.4.9 into A.4.6 we obtain

$$Y_o = 1 - 1/\cos(\theta_o) \qquad (A.4.11)$$

Appendix 4.2

A Comparison of the Q Factors of Varactor Tuned Combline and Open Circuited Combline Filters

The Q factor of a shunt resonator composed of a conductance G in parallel with a susceptance $B(\omega)$ can be expressed as follows.

$$Q = \frac{\omega_o}{2G} \frac{\partial}{\partial \omega} (B(\omega)) \Big|_{\omega = \omega_o} \qquad (A.4.12)$$

where ω_o is the resonant frequency of the circuit.

The basic resonators of the combline and open circuited combline filters are shown in Figs. A.4.1 and A.4.2. In order to evaluate the Q factors of these resonators it is necessary to have a shunt model for the varactor.

The admittance of the varactor is

$$Y = \frac{1}{R - j/\omega C} \qquad (A.4.13)$$

$$= G + j\beta \qquad (A.4.14)$$

where

$$G = \frac{R(\omega C)^2}{(1 + (R\omega C)^2} \qquad (A.4.15)$$

$$X = \frac{j\omega C}{(1 + (R\omega C)^2)} \qquad (A.4.16)$$

Now $$R\omega C = 1/Q \qquad (A.4.17)$$

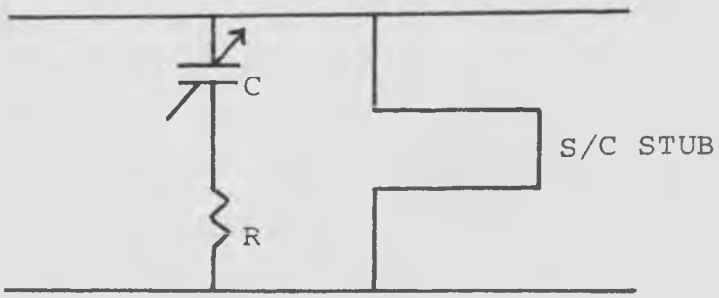

Fig. A.4.1 The Combline Varactor Tuned Resonator

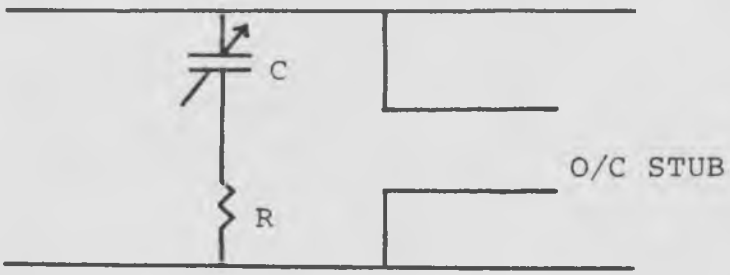

Fig. A.4.2 The Open Circuited Combline Varactor Tuned Resonator

where Q is the varactor Q factor. Normally Q >> 1

Thus $G \simeq R(\omega C)^2$ (A.4.18)

$$jB \simeq j\omega C \tag{A.4.19}$$

Using the shunt varactor model in the combline filter we obtain

$$B(\omega) = j\omega C - jY/\tan(a\omega) \tag{A.4.20}$$

Thus

$$\frac{\partial B(\omega)}{\partial \omega} = C + \frac{Ya}{\sin^2(a\omega)} \tag{A.4.21}$$

Now $Y = \omega_o C \tan(a\omega_o)$ (A.4.22)

Letting $\theta c = a\omega$, from A.4.21 and A.4.22 we obtain

$$\frac{\partial B(\omega)}{\partial \omega}\Big|_{\omega=\omega_o} = C[1 + \frac{2\theta_c}{\sin(2\theta_c)}] \tag{A.4.23}$$

Similarly, for the open circuited combline filter, with $\theta oc = \mathring{a}\omega$, we obtain

$$\frac{\partial B(\omega)}{\partial \omega}\Big|_{\omega=\omega_o} = C[1 - \frac{2\theta oc}{\sin(2\theta oc)}] \tag{A.4.24}$$

Thus, for similar varactors, the ratio of the Q factors of the two filters is given by

$$\frac{Qc}{Qoc} = \frac{\left[1 + \frac{2\theta c}{\sin(2\theta c)}\right]}{\left[1 - \frac{2\theta oc}{\sin(2\theta oc)}\right]}$$

In particular for $\theta c = 45^{\circ}$ and $\theta oc = 135^{\circ}$ we obtain from A.4.25 that

$$Qoc = 2.22Qc$$

5. GENERAL CONCLUSIONS

This thesis has been devoted to a study of the design and realisation of varactor tuned microwave filters. In particular, both bandpass and bandstop filters, with narrow passband and stopband bandwidths and broad tuning bandwidths are investigated.

In chapter one the advantages of varactor diodes as compared to YIG devices for the tuning of microwave filters are discussed. A brief introduction to varactor physics and an examination of the specifications of commercially available varactor tuned filters shows that with the use of GaAs varactors, the operating frequencies of varactor tuned filters can be considerably extended.

Also in chapter one, various realisation techniques for microwave filters are discussed and it is concluded that varactor tuned filters are best suited to realisation using Suspended Substrate Stripline techniques.

In chapter two initial experimental varactor tuned filters are discussed. Methods of characterisation of varactor diodes are presented, thus enabling correct choice of a varactor for a given requirement.

Initial work concentrated on the relatively simple problem of tuning bandstop resonators. A novel bandstop resonator realised in Suspended Substrate Stripline is presented. Experimental characterisation of this resonator is presented thus enabling exact design to be performed. Several varactor tuned resonators have been constructed and the experimental performances of these devices show the various trade offs between insertion loss, stopband bandwidth and tuning bandwidth. The design of varactor bias filters is also discussed in this section.

Next in chapter two, the design of varactor tuned bandstop filters is discussed. These filters were composed of the basic bandstop resonators separated at intervals along a uniform impedance main line. These Filters exhibited a frequency response which was symmetrical only at a single tuned frequency, and was skewed at frequencies above and below that frequency. Network Analyser measurements showed that the phase angle between the resonators of the filter at that particular frequency was not 90^0 as would normally be expected. This was a consequence of the fact that each single resonator possessed a skewed frequency response and a phase shift between the resonators not equal to 90^0 was required to compensate for the individual resonators and thus produce a symmetrical filter response. It thus became obvious that a design technique for calculation of the correct phase shift between the bandstop resonators was required.

Finally in chapter two, the design of varactor tuned bandpass filters is discussed. In particular the experimental performance of a two cavity filter is presented. This filter exhibited an equiripple response at a single frequency, however, tuning the filter only 5% away from that frequency produced a drastic deterioration in passband response. This phenomenon was a result of the tangential frequency variation of the coupling between the filters resonators. Thus, if broadband tuning were to be achieved, a technique for externally compensating for the distributed coupling between the resonators would be required.

In chapter three the design and physical realisation of varactor tuned bandstop filters is described. Firstly, a novel technique for evaluating the correct phase shift between bandstop resonators in order to achieve the optimum symmetrical response is presented. This method results in simple recurrance formulae, which are easy to evaluate using a calculator. The design and experimental performance of two fixed frequency bandstop filters designed using this technique is presented. Computer loss analysis of these filters is presented, enabling the simple evaluation of the selectivity of these filters. Next in chapter three the design of a three cavity varactor tuned bandstop filter tunable from 3.5 GHz to 4.5 GHz is presented. This device performed in very close agreement with computer predictions.

In Chapter four, the design of varactor tuned bandpass filters is presented. Firstly a novel technique for the design of combline filters is presented. This technique uses input and output coupling mechanisms to the filter which compensate for the frequency variation of the coupling between its resonators, thus enabling broadband tuning to be achieved with minimum degradation in passband performance. In addition this filter possesses the important property of retaining almost constant passband bandwidth across very broad tuning bandwidths. An experimental two cavity device of this type achieved 1600 MHz tuning around 4 GHz with a constant return loss and almost constant passband bandwidth across the entire tuning bandwidth. Computer analysis of this varactor tuned bandpass filter is presented enabling determination of the passband loss as a function of centre frequency, degree and passband bandwidth.

The design theory of tunable combline filters is also extended to include two other types of filter in chapter four. These are a tunable combline filter with open circuited resonators and a distributed fixed frequency combline. The former type of device possesses a higher Q factor than the normal combline filter allbeit with a loss of tuning bandwidth. The distributed combline filter design is a useful technique for realising a narrow band fixed frequency bandpass response. This type of filter is relatively insensitive to manufacturing tolerances. Several experimental fixed frequency and varactor tuned open circuited combline filters have been constructed and their performances are presented along with computer predictions of passband insertion loss.

In summary, the design and construction techniques for varactor tuned microwave bandpass and bandstop filters have been presented. Experimental devices have been constructed and these exhibit low loss and broad tuning bandwidths.

FUTURE WORK

In order to achieve octave tuning of microwave varactor tuned filters a terminal varactor capacitance ratio of 6:1 is required. This involves removing the package capacitance from the varactors. To achieve this end chip varactors have been examined. The problem with these devices is a large increase in parasitic inductance due to the long bondwire required to connect the top of the chip to the duroid. A better alternative for future work would be to use beam lead varactors which could be manufactured with very low package capacitance and inductance.